AD-A162 140 A MODEL FOR PREDICTING THERMOMECHANICAL RESPONSE OF LARGE SPACE STRUCTURE (U) TEXAS A AND M UNIV COLLEGE STATION MECHANICS AND MATERIALS RE D H ALLEN ET AL 1/3

UNCLASSIFIED JUN 84 MM-4875-84-16 AFOSR-TR-85-1080 F/G 11/4 NL

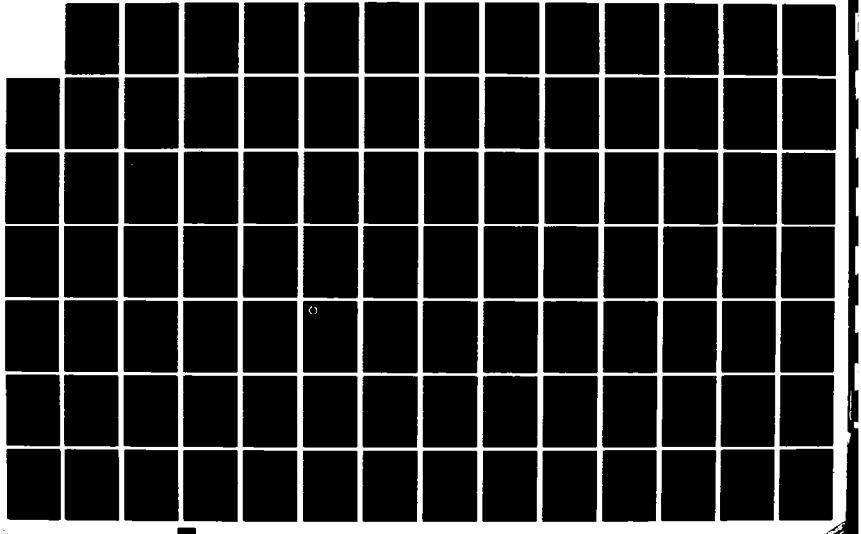

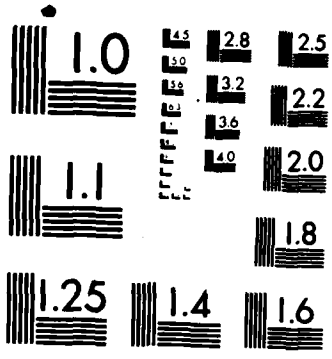

(2)

Mechanics and Materials Center
TEXAS A&M UNIVERSITY
College Station, Texas

A MODEL FOR PREDICTING THERMOMECHANICAL RESPONSE OF LARGE SPACE STRUCTURES

ANNUAL TECHNICAL REPORT

D. H. ALLEN
AND
W. E. HAISLER

AIR FORCE OFFICE OF SCIENTIFIC RESEARCH
OFFICE OF AEROSPACE RESEARCH
UNITED STATES AIR FORCE
CONTRACT NO. F49620-83-C-0067

MM 4875-84-16

JUNE 1984

SECURITY CLASSIFICATION OF THIS PAGE UNCLASSIFIED

REPORT DOCUMENTATION PAGE

1a. REPORT SECURITY CLASSIFICATION: Unclassified	1b. RESTRICTIVE MARKINGS
2a. SECURITY CLASSIFICATION AUTHORITY	3. DISTRIBUTION/AVAILABILITY OF REPORT: Unlimited Approved for public release; distribution unlimited.
2b. DECLASSIFICATION/DOWNGRADING SCHEDULE	
4. PERFORMING ORGANIZATION REPORT NUMBER(S)	5. MONITORING ORGANIZATION REPORT NUMBER(S): AFOSR-TR- 85-1080
6a. NAME OF PERFORMING ORGANIZATION: Aerospace Engineering Dept. / 6b. OFFICE SYMBOL (If applicable)	7a. NAME OF MONITORING ORGANIZATION: Air Force Office of Scientific Research
6c. ADDRESS (City, State and ZIP Code): Texas A&M University, College Station, Texas 77843	7b. ADDRESS (City, State and ZIP Code): Bolling AFB, Washington, D.C. 20332
8a. NAME OF FUNDING/SPONSORING ORGANIZATION OFF. OF SCIETIFIC RESEARCH, NA / 8b. OFFICE SYMBOL (If applicable) AFOSR/NA	9. PROCUREMENT INSTRUMENT IDENTIFICATION NUMBER: F49620-83-C-0067
8c. ADDRESS (City, State and ZIP Code): BOLLING AFB DC. 20332-6448	10. SOURCE OF FUNDING NOS. — PROGRAM ELEMENT NO.: 61102F; PROJECT NO.: 2302; TASK NO.: B1; WORK UNIT NO.:
11. TITLE (Include Security Classification): A Model for Predicting Thermomechanical Response of Large Space Structures — Technical Report	
12. PERSONAL AUTHOR(S): D.H. Allen & W. E. Haisler	
13a. TYPE OF REPORT: Interim Annual / 13b. TIME COVERED: FROM March'83 TO April'84	14. DATE OF REPORT (Yr., Mo., Day): June , 1984 / 15. PAGE COUNT: 22 and Appendix
16. SUPPLEMENTARY NOTATION: (keywords:)	

17. COSATI CODES			18. SUBJECT TERMS (Continue on reverse if necessary and identify by block number)
FIELD	GROUP	SUB. GR.	large Space structures, thermal loads, constitutive properties, finite element methods, environmental effects

19. ABSTRACT (Continue on reverse if necessary and identify by block number)

It is known that large space structures will be subjected to thermomechanical loadings and environmental conditions which are likely to degrade the constitutive properties of the structural materials, thus leading to possible failure of these vehicles. Therefore, it is desireable to develop new analytical models which are capable of accounting for these degraded properties seo that design procedures can be improved. There are three important ascpects of such an effort: selection and development oc constitutive models applicable to large space structures, construction of analytical models and experimentation to determine the precise nature of the material parameters to be utilized in the analytical model. These three components of the research must be tied together into a single concise package in order to obtain a useful model.

This research project is a three year effort to develop an analytical model capable of predicting the response of space structures with degrading material properties under quasi-static as well as dynamic cyclic thermomechanical loading conditions. This report details the research completed during the first year of AFSOR contract no. F49620-83-C-0067.

20. DISTRIBUTION/AVAILABILITY OF ABSTRACT: UNCLASSIFIED/UNLIMITED ☒ SAME AS RPT. ☐ DTIC USERS ☐	21. ABSTRACT SECURITY CLASSIFICATION: UNCLASSIFIED
22a. NAME OF RESPONSIBLE INDIVIDUAL: Dr. Tony Amos	22b TELEPHONE NUMBER (Include Area Code): (202)767-4937 / 22c OFFICE SYMBOL: AFOSR/NA

DD FORM 1473, 83 APR EDITION OF 1 JAN 73 IS OBSOLETE.

SECURITY CLASSIFICATION OF THIS PAGE

A MODEL FOR PREDICTING THERMOMECHANICAL RESPONSE OF LARGE SPACE STRUCTURES

Annual Technical Report

Submitted by

D.H. Allen

and

W.E. Haisler

AEROSPACE ENGINEERING DEPARTMENT

TEXAS A&M UNIVERSITY

to the

Air Force Office of Scientific Research
Office of Aerospace Research
United States Air Force

MM 4875-84-16

Contract No. F49620-83-C-0067
June 1984

TABLE OF CONTENTS

1. INTRODUCTION

1.1 Summary

It is known that large space structures will be subjected to thermomechanical loadings and environmental conditions which are likely to degrade the constitutive properties of the structural materials, thus leading to possible failure of these vehicles. Therefore, it is desirable to develop new analytical models which are capable of accounting for these degraded properties so that design procedures can be improved. There are three important aspects of such an effort: selection and development of constitutive models applicable to large space structures, construction of analytic models, and experimentation to determine the precise nature of the material parameters to be utilized in the analytical model. These three components of the research must be tied together into a single concise package in order to obtain a useful model.

This research project is a three year effort to develop an analytic model capable of predicting the response of space structures with degrading material properties under quasi-static as well as dynamic cyclic thermomechanical loading conditions. This report details the research completed during the first year of AFOSR contract no. F49620-83-C-0067.

1.2 Statement of Work

A model is being developed for predicting the thermomechanical response of large space structures to cyclic transient temperature loading conditions. The research is being conducted in the following stages:

1) selection and specialization of thermomechanical constitutive equations to be utilized in the analysis of large space structures;
2) construction (where necesssary) of coupled energy balance equations (modified Fourier heat conduction equations) applicable to the constitutive models selected in item 1);

3) casting (where necessary) the resulting field laws into coupled and uncoupled variational principles suitable for use with the finite element method;

4) finite element discretization of the variational principles for several element types;

5) experimentation to determine material properties to be utilized in the constitutive models; and

6) parametric studies of the quasi-static and dynamic response of large space structures undergoing thermomechanically and environmentally degraded material properties.

The experimental effort (discussed in 5) is being supported in part by DOD equipment grant no. 841542 with equipment on-line capability expected by December 31, 1984. The total research effort outlined above spans a period of three years. The following section details results obtained during the first year.

2. RESEARCH COMPLETED TO DATE

2.1 Summary of Completed Research

The following tasks have been completed during the first year of research:

1) literature survey;
2) selection of constitutive equations for thermoviscoplastic metals at elevated temperatures and polymeric composites with thermomechanical load induced damage at temperatures below the glass transition temperature;
3) construction of a coupled energy balance equation for thermoviscoplastic metals;
4) casting of field laws for the materials discussed in 2) into one-dimensional (truss and beam) finite element computer codes with one- and two-way thermomechanical coupling; and
5) initial parametric studies using the models developed in 4) to determine the thermomechanical response of representative space structures with degraded material properties.

The work statement for the second year is as follows:

1) refinement of constitutive equations for polymeric composites based on currently available research;
2) selection and development, to include experimental characterization, of metal matrix composite constitutive equations appropriate for large space structures;
3) construction of coupled energy balance equations for metal matrix composites and application of the resulting field laws to truss finite element codes;
4) further development of beam finite element codes for viscoplastic metals, polymeric composites, and metal matrix composites to include one- and

two-way thermomechanical coupling;

5) determination of the effect of inelastic heat generation on the thermo-vibratory response of representative space structures; and

6) completion of further parametric studies using the models developed in step 4).

In addition, a DEC 11/23 (LSI 11/23 Plus) has been purchased with internal university funding and is now being utilized to generate many of the numerical results obtained on the contract.

Additional experimental equipment is also being purchased under DOD equipment grant no. 841542. This equipment will support item 2) of the second year work statement listed above. At this time the equipment has been ordered and is expected to be on-line by December 31, 1984.

In addition to the funding supplied by AFOSR, the Texas Engineering Experiment Station, a branch of the Texas A&M University System, has provided substantial internal support for the research detailed herein. This support has been utilized to support additional graduate students and for travel. In addition, Dr. Michael S. Pilant of the Mathematics Department at TAMU is being supported for one-half month per year to study computational algorithms for solving thermoviscoplastic field problems.

Finally, it should be pointed out that a material property degradation experiment is currently underway on the NASA LDEF under the direction of Dr. Allen. Effects of long term space exposure on material properties of polyethylene will become available during the second contract year.

The following sections detail the results obtained during the first contractual year.

2.2 Literature Survey

A detailed literature survey has been completed as part of the first year effort. This report, entitled "Large Space Structures Technology: A Literature Survey", is included as Appendix 6.3. Briefly, the report details recent advances in the areas of materials, structural solution techniques, damping, and preliminary design and experiment. The results of this survey indicate that very little research is available on the effect of material property degradation on large space structural response.

2.3 Selection of Constitutive Equations

Candidate material models have been selected for metals at elevated temperatures and polymeric composites below the glass transition temperature. These are detailed below.

2.3.1 Metals at elevated temperatures are currently modeled using continuum mechanics with internal state variables (ISV's) [1-5], wherein the stress-strain relation is of the form (for infinitesimal strains):

$$\sigma_{ij} = D_{ijk\ell}(\varepsilon_{k\ell} - \varepsilon^{I}_{k\ell} - \varepsilon^{T}_{k\ell}) \quad , \tag{1}$$

where σ_{ij} is the stress tensor, $\varepsilon_{k\ell}$ is the strain tensor, $D_{ijk\ell}$ is the linear elastic modulus tensor, $\varepsilon^{I}_{k\ell}$ is the inelastic strain tensor, and $\varepsilon^{T}_{k\ell}$ is the thermal strain tensor. In addition,

$$\dot{\varepsilon}^{I}_{ij} = f_1(\varepsilon_{k\ell}, T, \alpha^{p}_{k\ell}) \quad , \tag{2}$$

and

$$\dot{\alpha}^{q}_{ij} = f^{q}_{ij}(\varepsilon_{k\ell}, T, \alpha^{p}_{k\ell}) \quad , \tag{3}$$

where f_1 and f^{q}_{ij} are appropriate functions of state, T is the temperature, and $\alpha^{p}_{k\ell}$ are a set of second order tensor valued internal state variables modeling dislocation arrangement, dislocation density, intergranular damage, etc.

Although it has been demonstrated that numerous models fall within the above framework [5], the special cases of equations (1) through (3) utilized thus far are a classical plasticity model developed by Allen and Haisler [6, 7] (see Appendix 6.2), a single internal state variable viscoplastic model developed by Cernocky and Krempl [8, 9] (see Appendix 6.1), and a two internal state variable viscoplastic model developed by Bodner, et al. [10-13] (see Appendices 6.1 and 6.5). It is emphasized, however, that the algorithms developed under this contract can be utilized with any model capable of formulation according to equations (1) through (3).

2.3.2 Polymeric composites are modeled using internal state variable theory as well. However, in this case the ISV's are assumed to be vector-valued and to enter only through the modulus tensor, that is:

$$\sigma_{ij} = C'_{ijk\ell}(\varepsilon_{ij} - \varepsilon^T_{ij}) \quad , \tag{4}$$

where $C'_{ijk\ell}$, the effective modulus tensor, is given by

$$C'_{ijk\ell} \equiv C_{ijk\ell} - P^{pq}_{mnk\ell ij}\,\alpha^p_m\,\alpha^q_n \quad , \tag{5}$$

where α^p_m are a set of vector-valued internal state variables [14] describing transverse cracking, interlaminar delamination, fiber breakage, etc., and modeled by

$$\dot{\alpha}^j_i = \Omega^j_i(\varepsilon_{k\ell},\ T,\ \alpha^p_m) \quad . \tag{6}$$

At low homologous temperatures these materials are assumed to rate insensitive so that the above model will result in quasi-elastic equations in which inelasticity is reflected only through the slowly degrading modulus tensor. Experimental evidence [15, 16] indicates that the time scale for degradation of $C'_{ijk\ell}$ is very long compared to the frequencies and mode shapes of representative

structures. It is therefore sufficient for many space structural applications to treat equations (4) in the degraded state only. This approach is further detailed in Appendix 6.4.

2.3.3 Metal matrix composites are currently being purchased from ARCO Metals, Greenville, S.D., and models for these materials will be developed during the second and third years of the contract.

2.4 Coupled Energy Balance Laws

The energy balance law for thermomechanically coupled media of the type described in section 2.3.1 has been constructed [17] (see also Appendix 6.1). This equation can be utilized to predict temperature rise in a thermoviscoplastic medium subjected to cyclic mechanical loading. This equation is in general a statement of conservation of energy and represents a modification of the Fourier heat conduction equation given by

$$D_{ijk\ell}(\varepsilon_{k\ell} - \alpha_{1k\ell} + \bar{\alpha}_{k\ell}T_R)\dot{\alpha}_{1ij} + D_{ijk\ell}\bar{\alpha}_{ij}\bar{\alpha}_{k\ell}T\dot{T} - D_{ijk\ell}\bar{\alpha}_{ij}T\dot{\varepsilon}_{k\ell} - \rho C_v\dot{T} + q_{j,j} = \rho r \quad , \quad (7)$$

where $\alpha_{1k\ell}$ is the internal state variable modeling drag stress, $\bar{\alpha}_{k\ell}$ is the thermal conductivity tensor, ρ is the mass density, C_v is the specific heat, q_i is the heat flux vector, and r is the specific heat supply.

The above result has been utilized to predict the thermomechanical response of a single insulated truss element to cyclic mechanical loading (see Appendix 6.1). As shown in Figs. 1 and 2, substantial temperature rise (approximately 3.7°C) is predicted for each cycle.

It is now thought that in polymeric composites about 95% of the strain energy lost to inelastic deformations is expended in the creation of internal surfaces called damage. It is therefore not necessary to construct two-way coupled energy balance laws for these materials and the classical Fourier heat conduction equation is adequate for modeling the temperature field. Therefore, the models developed herein utilize only one-way coupling for polymeric composite media: that is, the temperature field affects the displacement field but not vice versa.

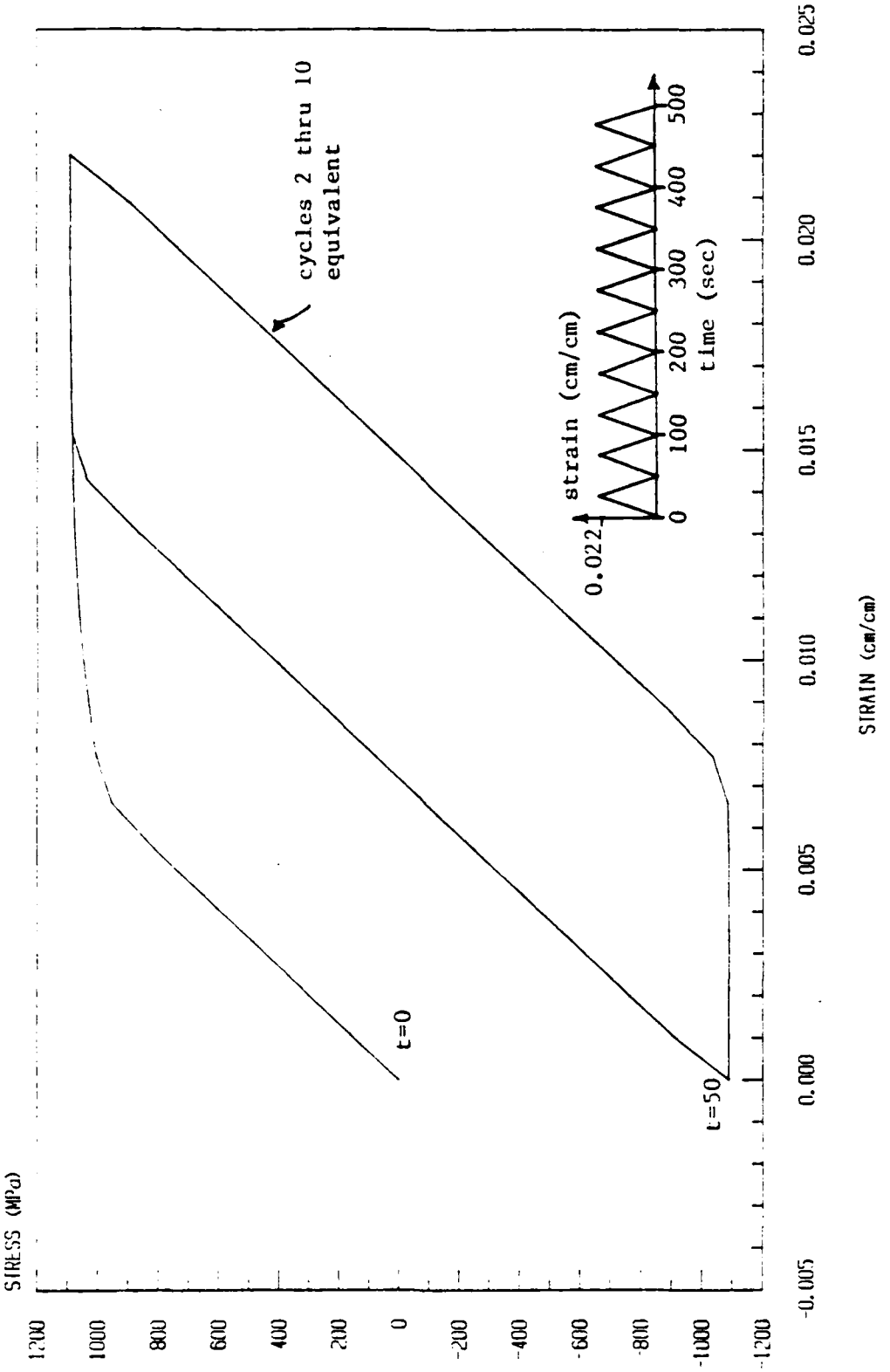

Fig. 1. Predicted Stress-Strain Behavior of IN100 at 1005°K (1350°F) Subjected to Multi-cylic Load

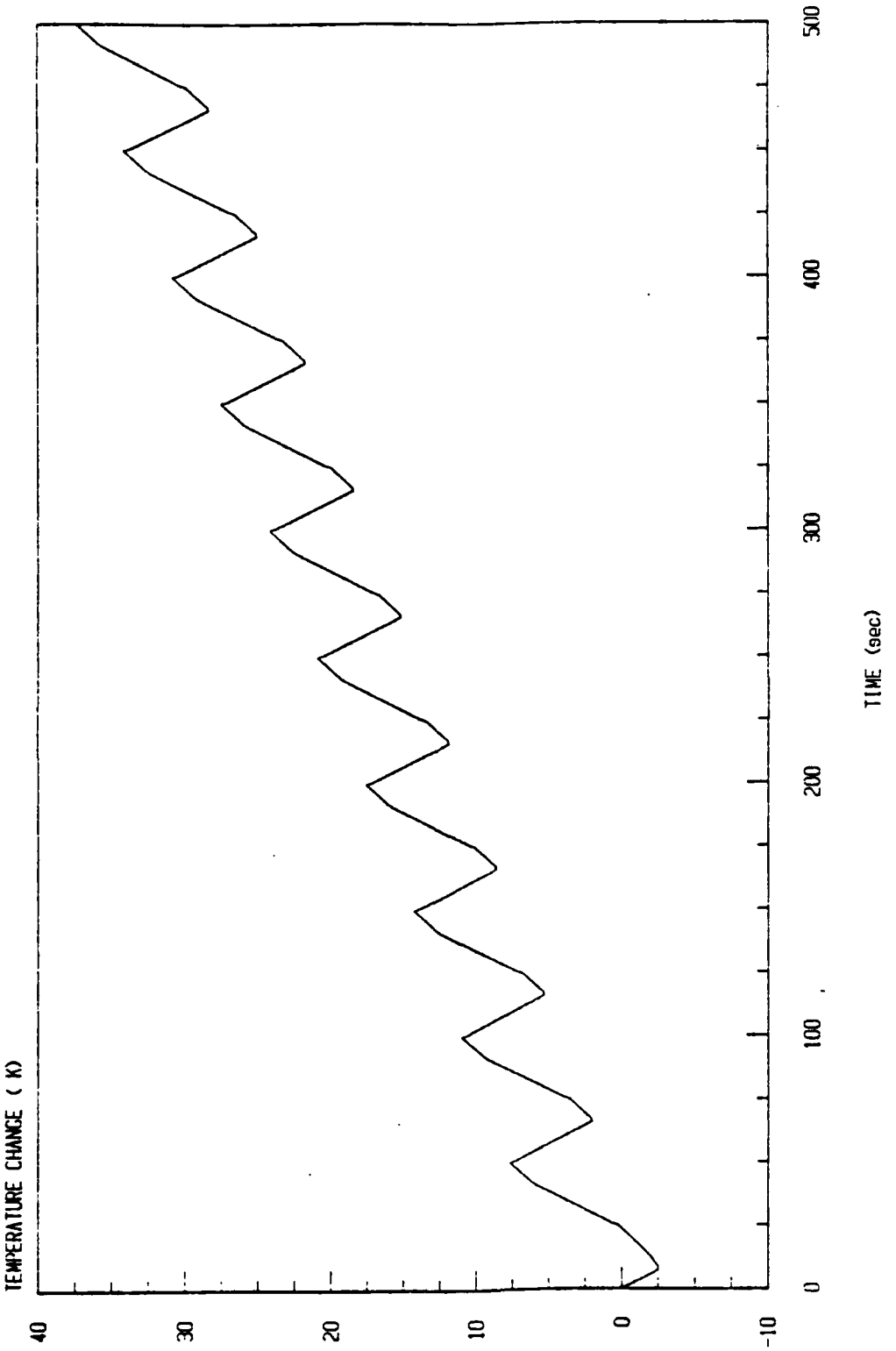

Fig. 2. Predicted Temperature Change for IN100 at 1005°K (1350°F) Subjected to Multi-cyclic Load History Shown in Fig. 10

2.5 Finite Element Computer Codes

Five finite element computer codes have been developed and/or refined during the first year of research. These are:

1) one-dimensional truss type heat conduction code for predicting time-dependent axial temperature variations in truss structures;
2) one-dimensional truss code for predicting dynamic response of truss structures with quasi-elastic materials properties to thermomechanical inputs (see Appendix 6.4);
3) one-dimensional beam code for predicting dynamic response of beam structures with quasi-elastic material properties to thermomechanical inputs (see Appendix 6.4);
4) one-dimensional fully two-way coupled truss code for predicting the quasi-static response of truss structures with thermoviscoplastic material properties to thermomechanical inputs (see Appendix 6.5); and
5) two-dimensional continuum code for predicting quasi-static response of elastic-plastic media to mechanical inputs (see Appendix 6.2).

Algorithms for constructing elastic versions of items 1) through 3) are in the research literature and will not be discussed further herein. Details of the quasi-elastic material properties are discussed in Appendix 6.4. Results of the analytical models are significant in that they show substantial changes can occur in the dynamic response of representative space structures due to small changes in the material properties of the structural elements. A brief review of these results will be given in the following section.

The fully two-way coupled truss code has been constructed at this time, as detailed in Appendix 6.5. However, numerical results have not yet been obtained. These should be forthcoming in the near future.

Finally, the numerical efficiency of a previously developed elasto-plasticity code has been significantly increased, as detailed in Appendix 6.2.

The codes listed above will be utilized and further refined by the inclusion of more advanced material models during the second and third years of the research effort.

2.6 Initial Parametric Studies

For purposes of illustrating the capability of the currently developed models, several sample problems have been provided for space structures with realistic degradation of material properties (see Appendix 6.4). As an example, consider the truss structure shown in Fig. 3. This beam-like structure is cantilevered at one end to simulate an antenna boom. The structure is sixty feet long with bays ten feet long by three feet wide. The structure is constructed from graphite-epoxy composite material with a quasi-isotropic ply layup. Experimental research indicates that the material may undergo up to 15 percent loss in stiffness due to cyclic thermomechanical fatigue which causes a variety of damage modes in the structure. Additional loss of stiffness may be attributed to elevated temperature and chemical changes due to solar radiation and other environmental effects. In this model the properties are degraded spacially on an element by element basis as a function of the stress history in the structure induced by long term thermomechanical cyclic loading. Stress amplitudes were obtained by using displacements corresponding to the first modal shape and the degraded properties were computed by assuming a linear damage law based on peak stress amplitude. Because the boom is fixed on one end, the stresses are highest there and stiffness degrades the most at the fixed end. Modal frequencies and shapes were then computed for the five cases where the maximum degradation within the structure was 5%, 10%, ..., and 25%. Figure 4 indicates the decrease in the fundamental frequencies of the first two resonant modes as a function of

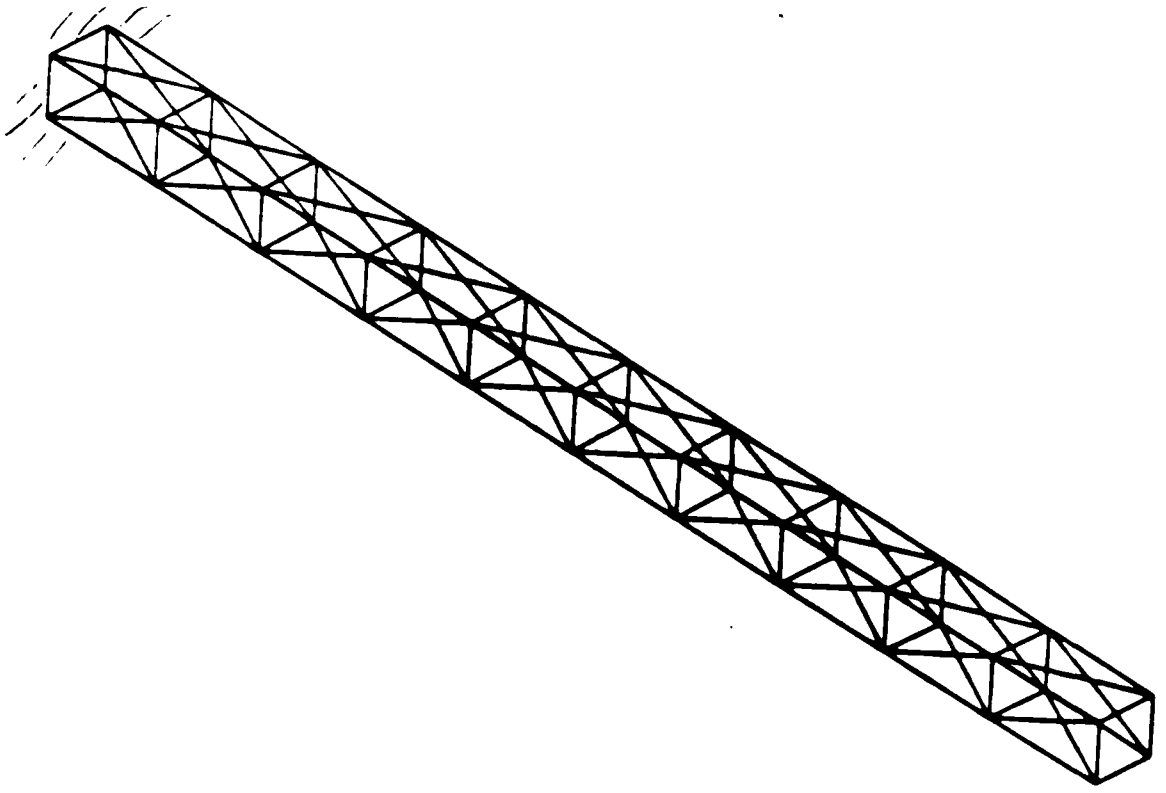

Fig. 3. Typical Space Truss Structure.

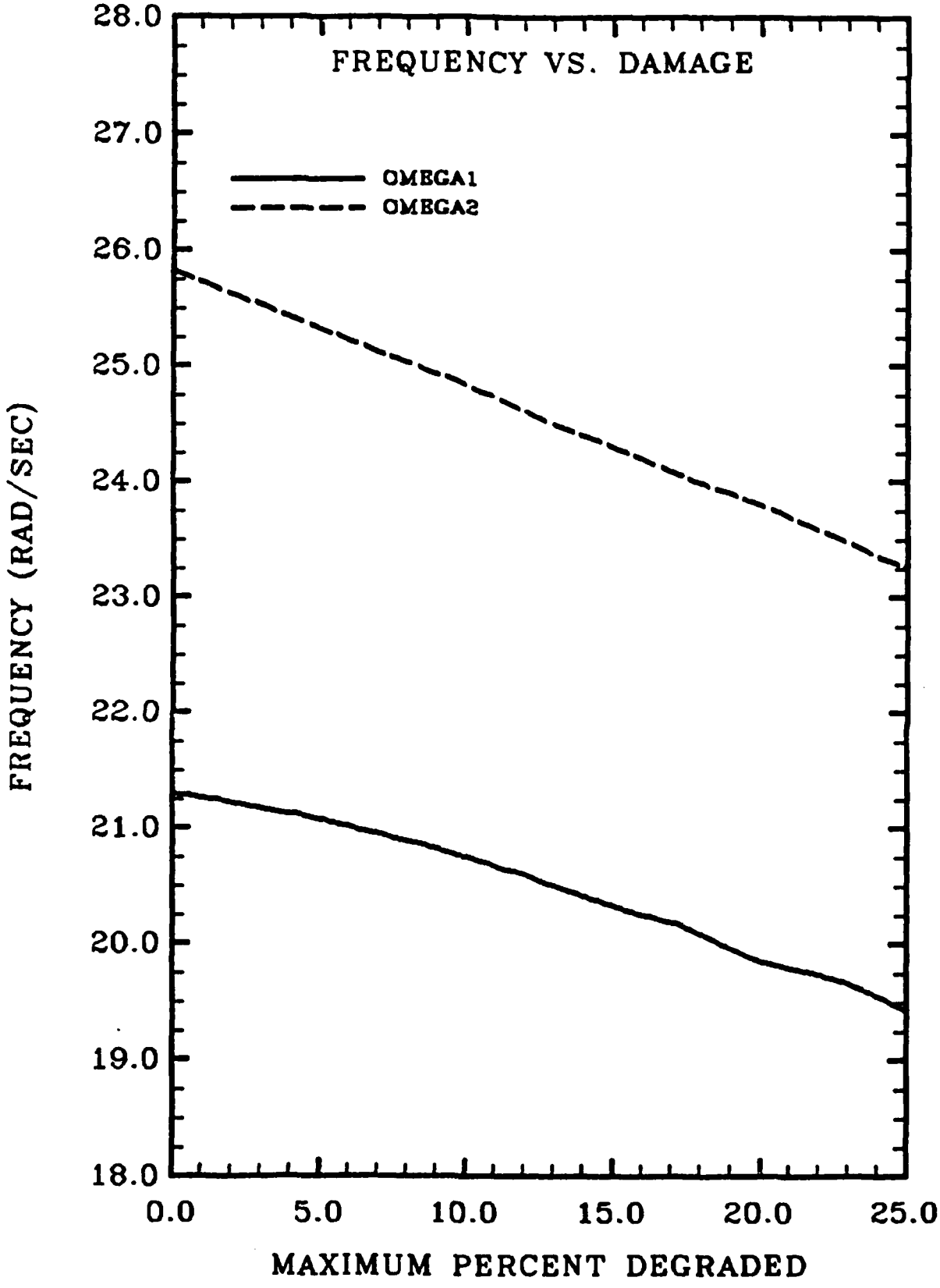

Fig. 4. Frequency Change in First Two Modes of Typical Space Structure Due to Material Property Degradation.

this spacially induced damage. Figure 5 shows that the shape of the first mode undergoes no appreciable change in shape as the damage occurs, which is due to the fact that the first mode is a symmetric mode. The second mode shape, however, shown in Fig. 6, undergoes a substantial change in shape. This result indicates that active control mechanisms which may be placed according to the original undamaged mode shapes may not be capable of controlling all modes as the structure dynamic response changes over long time periods. The control designer must be cognizant of these modal changes if he is to design a workable control system. Adaptive or robust control systems will be required.

Numerous other results are presented in Appendix 6.4. For example, it is shown that if the material properties degrade on only onde side of the structure, as might happen due to solar radiation, the mode shapes are completely changed. Additional results are presented for the transient responses of truss and frame structures subjected to thruster loads and to cyclic solar radiation (heating) loads.

Further refinement of the material models is expected to improve the capability of the analytic model to predict the effects of material inelasticity on dynamic response of large space structures.

In conclusion, these preliminary results seem to indicate that small changes (or errors) in material properties as they change or degrade due to fatigue, damage, etc. may produce significant changes in predicted dynamic, frequency and modal response. Correspondingly, this affects our ability to design effective control systems and places an even greater burden on the control designer to develop systems which account for these structural changes. It is clear that an understanding of material behavior in space environments and its impact on structural response is very important to successful design and development of large space structures.

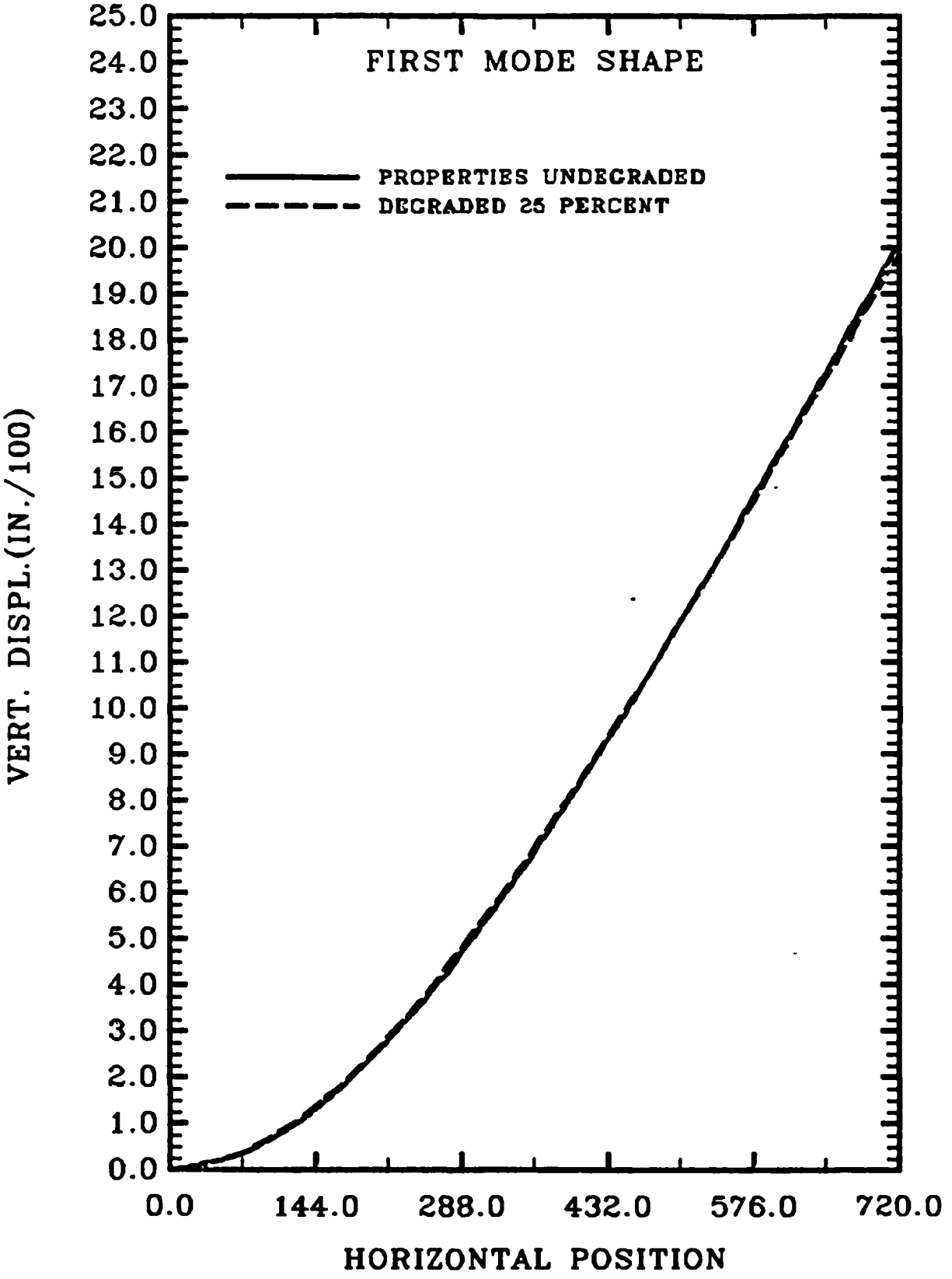

Fig. 5. Change in First Mode Shape of Typical Space Truss Structure Due to Material Property Degradation.

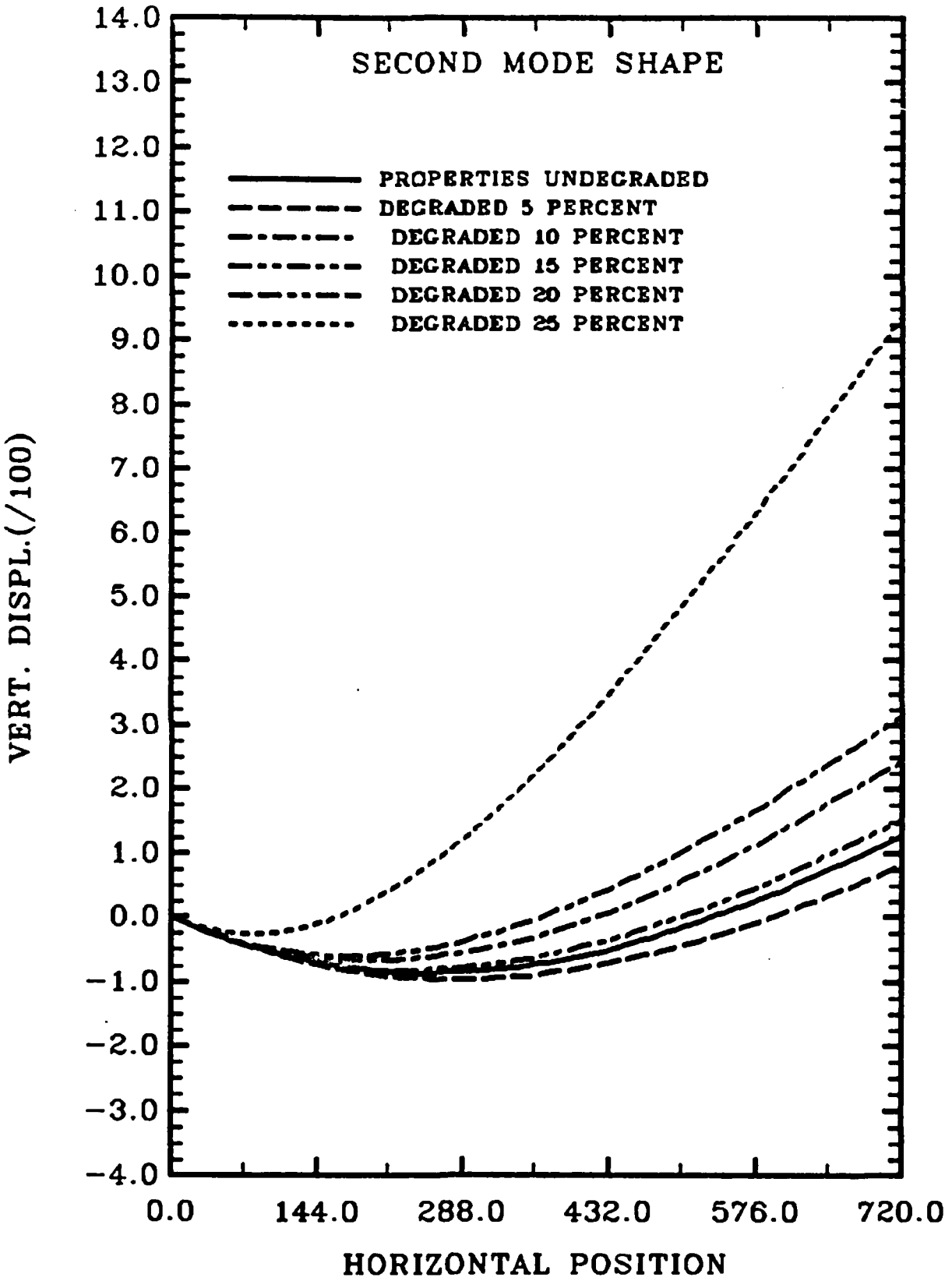

Fig. 6. Change in Second Mode Shape of Typical Space Truss Structure Due to Material Property Degradation.

2.7 References

1. Coleman, B.D. and Gurtin, M.E., "Thermodynamics with Internal State Variables", Journal of Chemical Physics, Vol. 47, pp. 597-613, 1967.

2. Kratochvil, J., and Dillon, O.W., Jr., "Thermodynamics of Crystalline Elastic-Visco-Plastic Materials", Journal of Applied Physics, Vol. 41, pp. 1470-1479, 1979.

3. Kratochvil, J. and Dillon, O.W., Jr., "Thermodynaics of Elastic-Plastic Materials as a Theory with Internal State Variables," Journal of Applied Physics, Vol. 40, pp. 3207-3218, 1969.

4. Allen, D.H., "A Thermodynamic Framework for Comparison of Current Thermoviscoplastic Constitutive Models for Metals at Elevated Temperature", Proceedings International Conference on Constitutive Laws for Engineering Materials: Theory and Application, Tucson, AZ, 1983.

5. Allen, D.H. and Beek, J., "On the Use of Internal State Variables in Thermoviscoplastic Constitutive Equations", Proceedings 2nd Symposium on Nonlinear Constitutive Relations for Elevated Temperature Applications, Cleveland, 1984.

6. Allen, D.H. and Haisler, W.E., "A Theory for Analysis of Thermoplastic Materials", Computers and Structures, Vol. 13, pp. 124-135, 1981.

7. Allen, D.H., "Computational Aspects of the Nonisothermal Classical Plasticity Theory", Computers and Structures, Vol. 15, No. 5, pp. 589-599, 1982.

8. Cernocky, E.P. and Krempl, E., "A Theory of Voscoplasticity Based on Infinitesimal Total Strain", Acta Mechanica, Vol. 36, pp. 263-289, 1980.

9. Cernocky, E.P. and Krempl, E., "A Nonlinear Uniaxial Integral Constitutive Equation Incorporating Rate Effects, Creep and Relaxation", Int. J. Nonlinear Mechanics, Vol. 14, pp. 183-203, 1979.

10. Bodner, S.R. and Partom, Y., "Constitutive Equations for Elastic-Visco-Plastic Strain-Hardening Materials", Journal of Applied Mechanics, Vol. 42, No. 2, pp. 305-389, 1975.

11. Bodner, S.R., "Representation of Time Dependent Mechanical Behavior of Rene 95 by Constitutive Equations", Air Force Materials Laboratory, AFML-TX-79-4116, 1979.

12. Stouffer, D.C. and Bodner, S.R., "A Relationship Between Theory and Experiment for a State Variable Constitutive Equation", Air Force Materials Laboratory, AFWAL-TR-80-4194, 1981.

13. Bodner, S.R., Partom, I. and Partom, Y., "Uniaxial Cyclic Loading of Elastic-Viscoplastic Materials", Journal of Applied Mechanics, 1979

14. Allen, D.H., Groves, S.E. and Schapery, R.A., "A Damage Model for Continuous Fiber Composites", to be presented at the SES Conference, Blacksburg, VA, October 1984.

15. Reifsnider, K.L. and Jamison, K., "Fracture of Fatigue-loaded Composite Laminates". Int. J. Fatigue, pp. 187-197, October 1982.

16. Highsmith, A.L., Stinchcomb, W.W. and Reifsnider, K.L., "Stiffness Reduction Resulting from Transverse Cracking in Fiber-Reinforced Composite Laminates", VPI-E-81.33, Virginia Polytechnic Institute, November 1982.

17. D.H. Allen, "Thermodynamic Constraints on the Constitution of a Class of Thermoviscoplastic Solids", Texas A&M University Mechanics and Materials Center, Report No. MM 12415-82-10, December 1982.

3. PUBLICATIONS LIST

The following research has been accepted for publication:

1. "A Prediction of Heat Generation in a Thermoviscoplastic Uniaxial Bar", by D.H. Allen (Appendix 6.1), accepted by International Journal of Solids and Structures.

2. "An Efficient and Accurate Alternative to Subincrementation for Elastic-Plastic Analysis by the Finite Element Method", by S.E. Groves, D.H. Allen and W.E. Haisler (Appendix 6.2), accepted by Computers and Structures.

The following research is being submitted for publication.

1. "Effect of Degradation of Material Properties on the Dynamic Response of Space Structures", by S. Kalyanasundaram, J.D. Lutz, W.E. Haisler and D.H. Allen (Appendix 6.4), to be submitted to AIAA Journal.

2. "Predicted Axial Temperature Gradient in a Coupled Thermoviscoplastic Uniaxial Bar", by D.H. Allen (Appendix, 6.5), to be submitted to Journal of of Thermal Stresses.

In addition, the following report has been completed during the current contract period:

1. "Large Space Structures Technology: A Literature Survey", by M.A. Zocher, S. Kalyanasundaram, E.W. Nottorf, D.H. Allen and W.E. Haisler (Appendix 6.3).

4. PROFESSIONAL PERSONNEL INFORMATION

4.1 Faculty Research Assignments

1. Dr. Dr. D.H. Allen (Co-principal Investigator) - development of constitutive equations for polymeric composites, metal matrix composites, and high strength metal alloys; development of variational principles and finite element methods for two-way coupled thermoviscoplastic media; experimental methods for material model development.

2. Dr. W.E. Haisler (Co-principal Investigator) - development of finite element algorithms for truss and beam structures with material property degradation; sensitivity studies for large space structures with material prcperty degradation.

3. Dr. M.S. Pilant (Investigator) - development of solution algorithms for coupled thermoviscoplastic media.

4.2 Additional Staff

1. Mr. B. Harbert (Lab Technician) - experimental lab support

2. Mrs. D. Rosenkranz (Secretary) - secretarial support

3. Mr. S. Kalyanasundaram (Ph.D. Research Assistant) - modeling of dynamic response of inelastic structures; expected completed date June 1986.

4. Mr. D. Sanders (Lecturer and Ph.D. Candidate) - creep response of structural members; expected completion date August 1984.

5. Mr. E. Nottorf (M.S. Research Assistant) - development of constitutive models for metal matrix composites; expected completion date May 1985.

6. Mr. J. Lutz (M.S. Research Assistant) - modeling of large space structures with material inelasticity; expected completion date December 1985.

7. Mr. M. Zocher (B.S. Research Assistant) - literature survey; degree completed December 1984.

5. INTERACTIONS

5.1 Papers Presented

Presentations were given at the following conferences:

1. D.H. Allen - 1st AFOSR Forum on Large Space Structures, MIT, September 1983.

2. W.E. Haisler - 2nd AFOSR Forum on Large Space Structures, Washington, D.C., 1984.

Presentations were given on research related topics at the following conferences:

1. D.H. Allen - 2nd Symposium on Nonlinear Constitutive Relations for Elevated Temperature Applications, Cleveland 1984.

2. W.E. Haisler - 2nd Symposium on Nonlinear Constitutive Relations for Elevated Temperature Applications, Cleveland 1984.

The following presentation has been accepted.

1. D.H. Allen - Society of Engineering Science, Blacksburg, VA, 1984.

5.2 Research Related Travel and Consultative Functions

1. D.H. Allen and W.E. Haisler attended the ASME Applied Mechanics Conference, Houston, June 1983.

2. D.H. Allen and W.E. Haisler attended the 1st AFOSR Forum on Large Space Structures, Cambridge, September, 1983.

3. D.H. Allen and E. Nottorf visited Hercules Corp., Magna, UT, to discuss composite materials used in the Shuttle, April 1984.

4. D.H. Allen and E. Nottorf visited Martin-Marietta, Denver, to discuss metal matrix composites in large space structures and to see the PACOSS experiment, April 1984.

5. E. Nottorf visited ARCO Metals, Greenville, S.C., to discuss metal matrix composites, April 1984.

6. D.H. Allen attended NASA Shuttle Launch 41-C to see the launch of LDEF, which contains one of Dr. Allen's experiments, April 1984.

7. W.E. Haisler attended the AFFDL Vibration Damping Conference, Long Beach, CA, April 1984.

8. W.E. Haisler attended the AIAA SDM Conference, Palm Springs, CA, May 1984.

9. D.H. Allen made several trips to Winzen, Intl. in San Antonio, TX to discuss the development of inflatable space structures.

10. D.H. Allen and W.E. Haisler attended the 2nd AFOSR Forum on Large Space Structures, Washington, D.C., June 1984.

11. D.H. Allen and W.E. Haisler attended the 2nd Symposium on Nonlinear Constitutive Equations for Elevated Temperature Applications, Cleveland, June 1984.

6. APPENDIX - INTERIM TECHNICAL REPORTS

Appendix 6.1

Mechanics and Materials Center
TEXAS A&M UNIVERSITY
College Station, Texas

A PREDICTION OF HEAT GENERATION IN A THERMOVISCOPLASTIC UNIAXIAL BAR

D.H. ALLEN

MM 4875-83-10

JULY 1983

SECURITY CLASSIFICATION OF THIS PAGE (When Data Entered)

REPORT DOCUMENTATION PAGE		READ INSTRUCTIONS BEFORE COMPLETING FORM
1. REPORT NUMBER AM 4875-83-10	2. GOVT ACCESSION NO.	3. RECIPIENT'S CATALOG NUMBER
4. TITLE (and Subtitle) A Prediction of Heat Generation in a Thermoviscoplastic Uniaxial Bar		5. TYPE OF REPORT & PERIOD COVERED Interim 6. PERFORMING ORG. REPORT NUMBER
7. AUTHOR(s) David H. Allen		8. CONTRACT OR GRANT NUMBER(s) F49620-83-C-0067
9. PERFORMING ORGANIZATION NAME AND ADDRESS Aerospace Engineering Department Texas A&M University College Station, Texas 77843		10. PROGRAM ELEMENT, PROJECT, TASK AREA & WORK UNIT NUMBERS
11. CONTROLLING OFFICE NAME AND ADDRESS Air Force Office of Scientific Research Bolling AFB Washington, D. C. 20332		12. REPORT DATE July, 1983 13. NUMBER OF PAGES 26
14. MONITORING AGENCY NAME & ADDRESS(if different from Controlling Office)		15. SECURITY CLASS. (of this report) Unclassified 15a. DECLASSIFICATION/DOWNGRADING SCHEDULE
16. DISTRIBUTION STATEMENT (of this Report)		
17. DISTRIBUTION STATEMENT (of the abstract entered in Block 20, if different from Report)		
18. SUPPLEMENTARY NOTES		
19. KEY WORDS (Continue on reverse side if necessary and identify by block number) heat generation heat conduction viscoplasticity thermodynamics internal state variables constitutive equations		

20. ABSTRACT (Continue on reverse side if necessary and identify by block number)

A thermodynamic model is presented for predicting the thermomechanical response, including temperature change, in a uniaxial bar composed of a thermoviscoplastic metallic medium. The model is constructed using the concept of internal state variables, and it is shown that this general framework is capable of encompassing several constitutive models currently used to predict the response of rate sensitive metals in the inelastic range. Results are obtained for monotonic loading which agree with predicted results previously obtained by Cernocky and Krempl for mild steel at room temperature. The model

DD FORM 1473 EDITION OF 1 NOV 65 IS OBSOLETE

Unclassified

SECURITY CLASSIFICATION OF THIS PAGE (When Data Entered)

A PREDICTION OF HEAT GENERATION IN A THERMOVISCOPLASTIC UNIAXIAL BAR

by

David H. Allen

Assistant Professor
Aerospace Engineering Department
Texas A&M University
College Station Texas 77843

July, 1983

Accepted for publication by
International Journal of Solids and Structures
1983

A Prediction of Heat Generation in a Thermoviscoplastic Uniaxial Bar

by

David H. Allen

Abstract

A thermodynamic model is presented for predicting the thermomechanical response, including temperature change, in a uniaxial bar composed of a thermoviscoplastic metallic medium. The model is constructed using the concept of internal state variables, and it is shown that this general framework is capable of encompassing several constitutive models currently used to predict the response of rate sensitive metals in the inelastic range. Results are obtained for monotonic loading which agree with predicted results previously obtained by Cernocky and Krempl for mild steel at room temperature. The model is then utilized in conjunction with Bodner and Partom's constitutive equations to predict temperature change in Inconel (IN) 100 subjected to both monotonic and cyclic loading at 1005°K(1350°F).

Introduction

It has long been known that mechanical and thermodynamic coupling exists in solid bodies [1,2]. However, in elastic bodies this coupling is negligible except when mass inertia is not negligible due to flux of heat generated through the boundary of the body [3]. However, in thermoviscoplastic metals the conversion of mechanical energy to heat may be singificant even under non-inertial conditions, especially since material properties become extremely temperature sensitive in the inelastic range of response [4-11]. Similar research has been performed on non-metallic media [12-15].

General continuum mechanics models have been formulated for broad classes of materials [16-19]. However, to this author's knowledge only recently has attention been paid to the coupled heat conduction equation for thermoviscoplastic metals [11,20]. Recently, Cernocky and Krempl [11] have proposed a model for predicting the temperature rise in a class of thermoviscoplastic metals, with special emphasis on test coupons subjected to either homogeneous uniaxial or torsion loadings. In this paper an alternative approach to that proposed in [11] is discussed. This method uses the thermodynamics with internal state variables originally reported in [17] and discussed elsewhere in detail for metals [18,21,22], with development of the multidimensional coupled heat-conduction equation in [20].

The research herein is presented in three parts: field formulation in one-dimensional form; development of the governing equations from additional constitutive assumptions; and numerical results for selected problems.

Thermodynamics of a Uniaxial Thermoviscoplastic Bar

Consider a slender bar which is subjected to a homogeneously applied deformation field such that the resulting stress field is everywhere uniaxial in the $x_1 \equiv x$ coordinate direction, as shown in Fig. 1. Rigor would require that the possibility of finite deformations be considered. However this condition is covered in detail elsewhere [17,18,20,21,22], and for purposes of simplicity only infinitesimal deformations will be considered herein. For notational simplicity, then, the observable mechanical state variables are

$$u \equiv u_1 = \text{deformation field}, \tag{1}$$

$$\varepsilon \equiv \varepsilon_{11} = \text{infinitesimal strain field, and} \tag{2}$$

$$\sigma \equiv \sigma_{11} = \text{stress field} \tag{3}$$

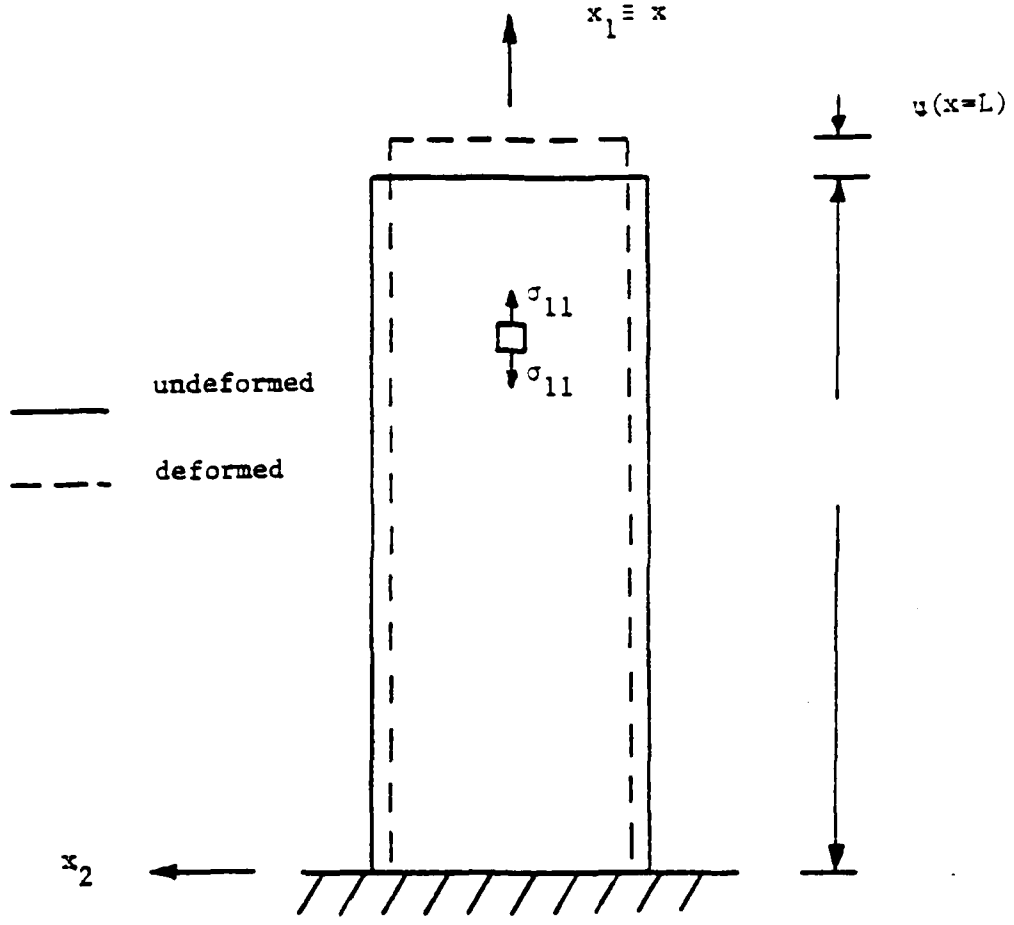

Fig. 1. Geometry and Deformations in a Uniaxial Bar

Although transverse components of deformation and strain may occur, it is assumed that they are not necessary to characterize the uniaxial stress σ.

The mechanical state variables (1) through (3) are adjoined with the thermodynamic state variables:

$e \equiv$ internal energy per unit mass; (4)

$r \equiv$ heat supply per unit mass; (5)

$s \equiv$ entropy per unit mass, (6)

$T \equiv$ absolute temperature; and (7)

$q \equiv q_1 =$ heat flux in the x_1 coordinate direction , (8)

where it is assumed in (8) that the bar is isotropic and long and slender with perfectly longitudinal boundaries so that the heat flux is one-dimensional.

In accordance with the theory of internal state variables [17], observable state variables (1) through (8) are now supplemented with internal state variable growth laws in order to characterize the state of inelastic bodies:

$\alpha_k \equiv$ scalar valued internal state variables, $k = 1, \ldots, n$; (9)

where n is the number of internal state variables required to characterize the state of the body. The precise nature of (9) will be discussed later.

Parameters (1) through (9) are assumed to be functions of space (x) and time (t), and are assumed to be sufficient to describe the uniaxial state of the bar at all times. These parameters are constrained by:

a) the conservation of momentum,

$$\frac{\partial \sigma}{\partial x} = 0 \ , \tag{10}$$

where inertial effects and the body force are assumed to be negligible;

b) the strain-displacement relation,

$$\varepsilon = \frac{\partial u}{\partial x} \ ; \tag{11}$$

c) the balance of energy,

$$\rho\dot{e} - \sigma\dot{\varepsilon} + \frac{\partial q}{\partial x} = \rho r \quad . \tag{12}$$

where ρ represents the mass density; and

d) the second law of thermodynamics,

$$\rho\gamma \equiv \rho\dot{s} - \frac{\rho r}{T} + \frac{\partial}{\partial x}\left(\frac{q}{T}\right) \geq 0 \quad ; \tag{13}$$

where γ is called the internal entropy rate per unit mass.

As detailed by Coleman & Gurtin [17], equations (10) through (13) are now supplemented with the following constitutive assumptions:

$$\sigma = \sigma(\varepsilon, T, \partial T/\partial x, \alpha_k) \quad ; \tag{14}$$

$$e = e(\varepsilon, T, \partial T/\partial x, \alpha_k) \quad ; \tag{15}$$

$$s = s(\varepsilon, T, \partial T/\partial x, \alpha_k) \quad ; \tag{16}$$

$$q = q(\varepsilon, T, \partial T/\partial x, \alpha_k) \quad ; \text{ and} \tag{17}$$

$$\dot{\alpha}_k = \dot{\alpha}_k(\varepsilon, T, \partial T/\partial x, \alpha_k) \quad , \tag{18}$$

where it is obvious that equations (14) through (18) satisfy the principle of equipresence [23]. Equations (10) through (12) and (14) through (18) describe eight +n equations in the eight +n field variables u, ε, σ, e, r, s, T, q, and α_k described in (1) through (9). These are adjoined with boundary conditions on the surfaces x = 0 and x = L to prescribe the one-dimensional field problem.

As detailed elsewhere [17,18,20-22], the second law of thermodynamics [inequality (13)] will constrain constitutive assumptions (14) through (18). This is accomplished by defining the Helmholtz free energy:

$$h \equiv h(\varepsilon, T, \partial T/\partial x, \alpha_k) = e - Ts \Rightarrow e = h + Ts \quad , \tag{19}$$

which together with the Clausuis-Duhem inequality will lead to the conclusions that

$$h = h(\varepsilon, T, \alpha_k) \quad , \tag{20}$$

$$s = \frac{-\partial h}{\partial T} = s(\varepsilon, T, \alpha_k) \quad , \tag{21}$$

$$\sigma = \rho \frac{\partial h}{\partial \varepsilon} \quad , \text{ and} \tag{22}$$

$$q = -k \frac{\partial T}{\partial x_1} + 0 \quad |\frac{\partial T}{\partial x_1}| \quad , \tag{23}$$

where k is the coefficient of heat conduction in the x_1 coordinate direction. Therefore, equations (19) through (23) replace equations (14) through (18) as more concise statements of the constitutive behavior, and it can be seen that specification of the Helmholtz free energy will complete the description of the field problem.

Combination of equations (12) and (19) through (23) will result in the coupled heat conduction equation:

$$\sigma \frac{\partial h}{\partial \alpha_k} \dot{\alpha}_k - \rho T \frac{\partial^2 h}{\partial \alpha_k \partial T} \dot{\alpha}_k - \rho T \frac{\partial^2 h}{\partial \varepsilon \partial T} \dot{\varepsilon} - \sigma T \frac{\partial^2 h}{\partial T^2} \dot{T} + \frac{\partial q}{\partial x} = \rho r \quad , \tag{24}$$

where summation on the range of k is implied.

Henceforth in this investigation it will be assumed that there is no internal heat source (other than material dissipation) so that $r \equiv 0$ in equation (24). In addition, it will be assumed that boundary conditions are applied in such a way that heat flux is negligibly small and $q \cong 0$ in equation (24). This last assumption is not valid under most physical circumstances. However, it can be said that on the basis of heat conduction equation (24) neglecting heat flux will result in an upper bound for the temperature rise during mechanically induced energy dissipation. Inclusion of this term results in a spacially dependent boundary value problem which is beyond the scope of the current research. However, the one-dimensional model proposed herein

does encompass the heat flux phenomenon, and, as such, will be the subject of a future paper by the author.

Development of Governing Equations from Additional Constitutive Assumptions

In order to construct the Helmholtz free energy function the elastic strain is first defined to be

$$\varepsilon^E \equiv \varepsilon - \alpha_1 - \bar{\alpha}\vartheta \quad , \tag{25}$$

where α_1 is the total inelastic strain in the x_1 coordinate system [24], $\bar{\alpha}$ is the coefficient of thermal expansion in the x_1 coordinate direction, and $\vartheta \equiv T - T_R$, where T_R is the initial temperature at which no strain is observed under zero mechanical load. The inelastic strain α_1 will be discussed in greater detail in the next section.

It is now postulated that the Helmholtz free energy may be expanded about the initial configuration in terms of elastic strain and temperature as follows:

$$h = h_R + \frac{E}{2\rho}\varepsilon^{E^2} - \frac{C_v}{2T}\vartheta^2 \quad , \tag{26}$$

where the subscript R denotes the equilibrium value, and

$$h_R \equiv \text{free energy in state R = constant,} \tag{27}$$

$$E \equiv \text{Young's modulus in the } x_1 \text{ coordinate system,} \tag{28}$$

$$C_v \equiv -T(\partial^2 h/\partial T^2) = \text{specific heat at constant volume.} \tag{29}$$

Note that although the first order terms in ε^E and ϑ have been neglected due to symmetry conditions due to the form of equation (25) coupling is retained between total strain, inelastic strain and temperature. Note also that the energy dissipation due to microstructural change has been neglected in free energy equation (26) because this mechanism has been shown to contribute

only a small portion of energy (<10%) to the dissipation process [25]. Further, the fracture energy loss due to microvoid growth, grain boundary sliding, and intergranular macrofracture is neglected due to the small strains considered herein.

Although the second order Taylor series expansion of the Helmholtz free energy given in equation (26) may not be adequate for characterizing the response of many materials, it will be shown in the next section that the above equations are a suitable framework for describing the material behavior of the class of materials considered herein.

Substitution of equation (26) into energy balance law (24) and utilizing equation (25) will result in the coupled heat equation:

$$[(E\varepsilon - E\alpha_1 + E\alpha T_R)\dot{\alpha}_1 + E\bar{\alpha}^2 T\dot{T}] - E\bar{\alpha}T\dot{\varepsilon} - \rho C_v\dot{T} = 0 \ , \tag{30}$$

where the terms in brackets arise due to inelastic response and the following term is the classical elastic coupling term [3]. Equation (30) may be written in the following equivalent form:

$$\dot{T} = \frac{(E\varepsilon - E\alpha_1 + E\bar{\alpha}T_R)\dot{\alpha}_1 - E\bar{\alpha}T\dot{\varepsilon}}{\rho C_v - E\bar{\alpha}^2 T} \ . \tag{31}$$

In order to obtain the stress-strain relation the Helmholtz free energy equation (26) may be substituted into equation (22) to obtain

$$\sigma = E(\varepsilon - \alpha_1 - \bar{\alpha}\theta) \ . \tag{32}$$

Equations (31) and (32) together with internal state variable growth laws (18) will be sufficient to characterize the response of the uniaxial bar subjected to uniaxial homogeneous mechanical loading considered herein.

Selected Problems and Numerical Results

It has been shown that stress-strain relation (32) together with internal state variable growth laws (18) are equivalent to several models

recently proposed for thermoviscoplastic metals [24]. These include Cernocky and Krempl [11,26], Valanis [27], Krieg, et al. [28], and Allen and Haisler [29]. It can also be shown that several others are in accordance with the model developed herein [30-34]. To illustrate this point two models have been selected for further discussion.

Cernocky and Krempl's stress-strain relation may be written in the following uniaxial form:

$$\sigma + K(\sigma, \varepsilon, T)\dot{\sigma} = G(\varepsilon, T) + M(\sigma, \varepsilon, T)[\dot{\varepsilon} - \bar{\alpha}\dot{T}] \quad , \tag{33}$$

where

$$E \equiv M/K \quad , \tag{34}$$

and parentheses imply dependence on the current values of the quantities enclosed. Equations (33) and (34) can be shown to be in agreement with stress-strain equation (32) by defining the inelastic strain α_1 such that

$$\dot{\alpha}_1 = [\sigma - G(\varepsilon, T)]/M(\sigma, \varepsilon, T) \quad , \tag{35}$$

so that

$$\alpha_1(t) = \int_{t_R}^{t} \dot{\alpha}_1(t')dt' \quad , \tag{36}$$

where t_R is the reference time, t' is a dummy variable of integration, and t is the time of interest. Thus, since G, K and M are not history dependent, Cernocky and Krempl's model is a single internal state variable model and equations (31), (32), (35) and (36) describe the uniaxial bar problem using Cernocky and Krempl's model.

To illustrate this point an example problem is now considered. Several uniaxial bars composed of mild steel are subjected to constant strain rates at room temperature with material properties as described in Table 2 of reference [11]. Stress-strain behavior and resulting temperature

rise are shown in Figs. 2 and 3. These results were obtained by integrating equations (31) and (35) with a stable and accurate Euler forward integration scheme. Due to the rate insensitive nature of mild steel at room temperature, the predicted results are identical for strain rates ranging from 0.001 sec^{-1} to 1.0 sec^{-1}. The negligence of heat flux over such a wide range of strain rates is valid only under adiabatic conditions.

It is significant to note that the results obtained in Figs. 2 and 3 are identical to those obtained by Cernocky and Krempl [11]. This is due to the fact that the assumed internal energy rate described by equation (14) in reference [11] can be obtained in the uniaxial form by utilizing equations (19), (21) and (26) in this paper. Further, energy balance equation (55) in reference [11] can be shown to be identical to equation (26) derived herein by substituting equation (32) in this paper. Finally, it should be pointed out that under non-adiabatic conditions neglecting the heat flux in the results obtained herein causes increasing overestimation of the temperatures shown in Fig. 3 as the input strain rate decreases.

Bodner and Partom's model [35,36] may also be written in the uniaxial form described by equation (32), where

$$\dot{\alpha}_1 = \frac{2}{\sqrt{3}} D_o \frac{\sigma}{|\sigma|} \exp\left[-\left(\frac{n+1}{2n}\right)\left(\frac{\alpha_2^2}{\sigma^2}\right)\right]^n , \tag{37}$$

where D_o and n are experimentally obtained material constants and

$$\dot{\alpha}_2 = m(Z_1 - \alpha_2)\sigma\,\dot{\alpha}_1 - AZ_1\left(\frac{\alpha_2 - Z_I}{Z_1}\right)^r , \tag{38}$$

where α_2 is an internal state variable representing drag stress and m, Z_I, Z_1, A, and r are experimentally determined material constants. Although equation (38) contains stress σ, it can be written in the form described

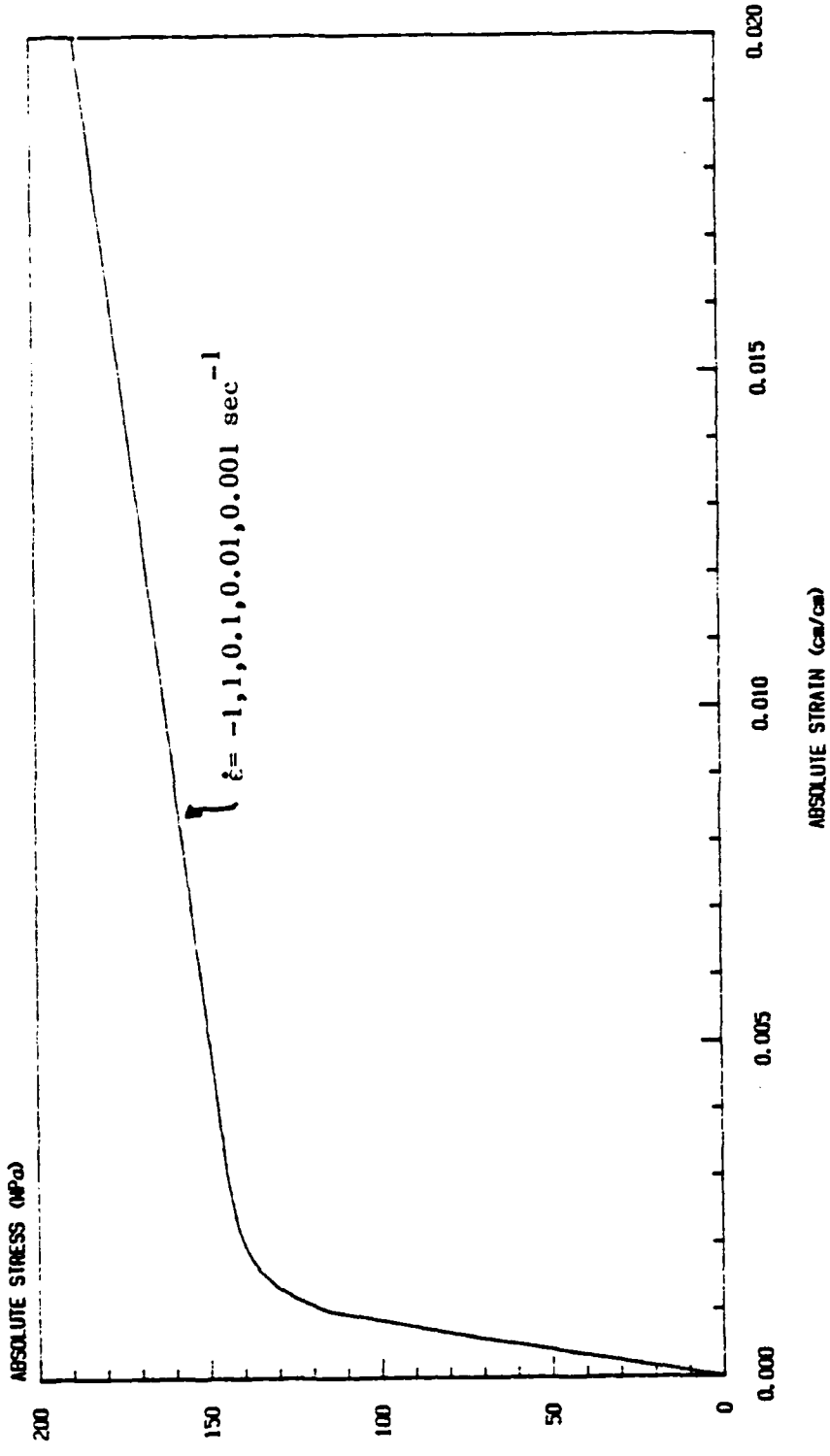

Fig. 2. Predicted Stress-Strain Behavior for Mild Steel at Room Temperature Subjected to Constant Strain Rate in Tension and Compression

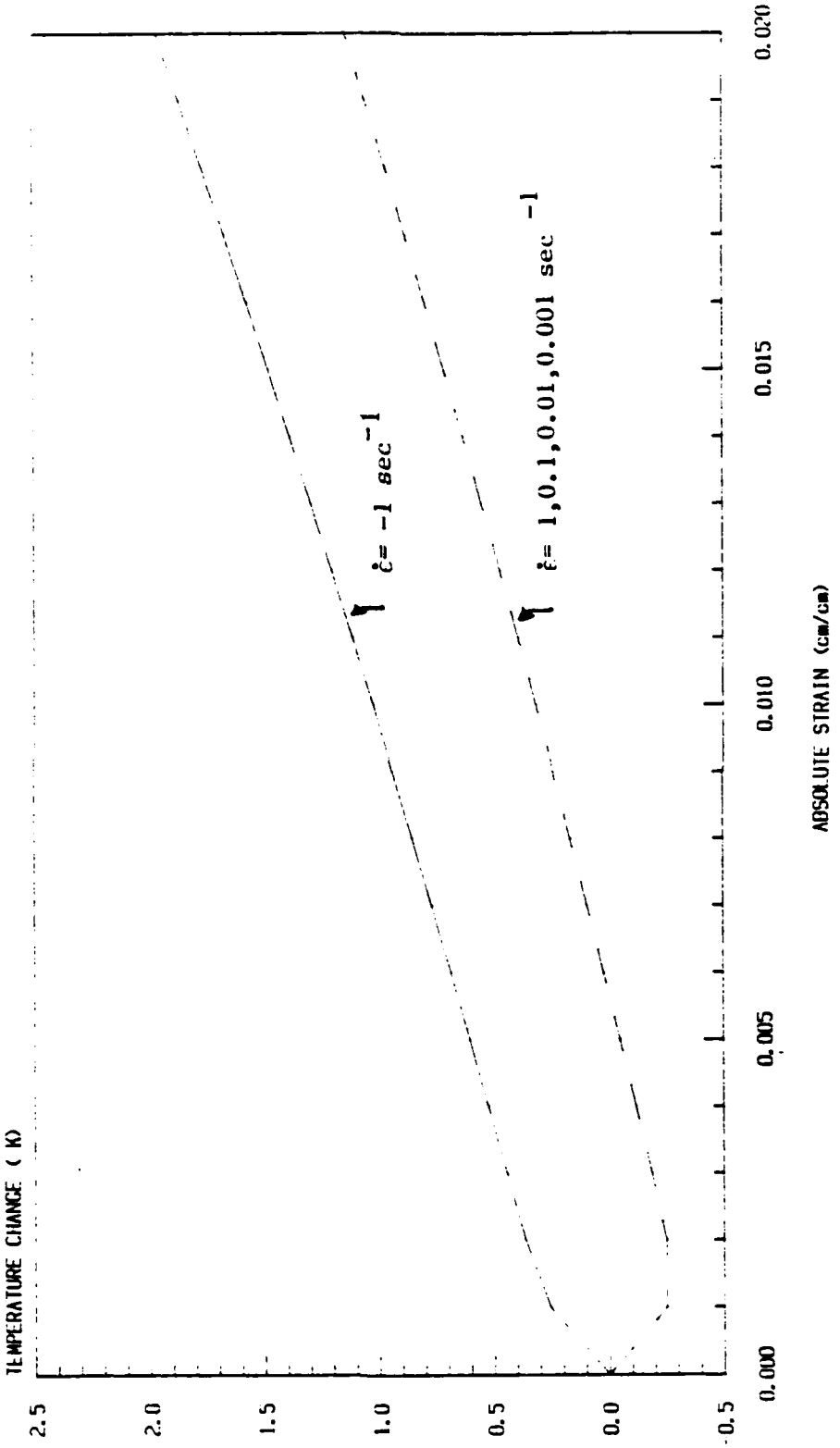

Fig. 3. Predicted Temperature Change for Mild Steel at Room Temperature Subjected to Load Histories Shown in Fig. 2

by equation (18) by direct substitution of equation (32). Thus, Bodner and Partom's model contains two internal state variables in the form described above.

Results are shown in Figs. 4 through 7 for uniaxial bars of IN 100 pulled at various constant strain rates at an initial temperature of 1005°K (1350°F). Experimental data were obtained from Reference [37], and the material constants described above are tabulated in Reference [38]. The stress-strain curves shown in Fig. 4 are identical to those previously obtained [38].

As a second example using Bodner and Partom's model a uniaxial bar of IN 100 with material parameters as described in Refs. [37] and [38] is subjected to the cyclic strain history shown in Fig. 8 and at initial temperature 1005°K (1350°F). Analytic stress-strain behavior is compared to experiment in Fig. 8 and predicted temperature change is shown in Fig. 9.

Finally, a uniaxial bar is subjected to the multicycle test described in Fig. 10, with resulting temperature rise shown in Fig. 11 It is observed that the model predicts a mean temperature rise of approximately 3.7°K (6.7°F) per cycle. The linear increase in mean temperature with time is predicted due to the cyclic saturation of the material on the second cycle, which is in agreement with experimental observations at elevated temperature.

Conclusion

A model has been presented herein for predicting the temperature rise in uniaxial bars composed of thermoviscoplastic metallic media. The model is also applicable to multiaxial conditions, and this has been reported to some extent in reference [20]. Although the procedure used here differs from that proposed in reference [11], it has been shown that the predicted

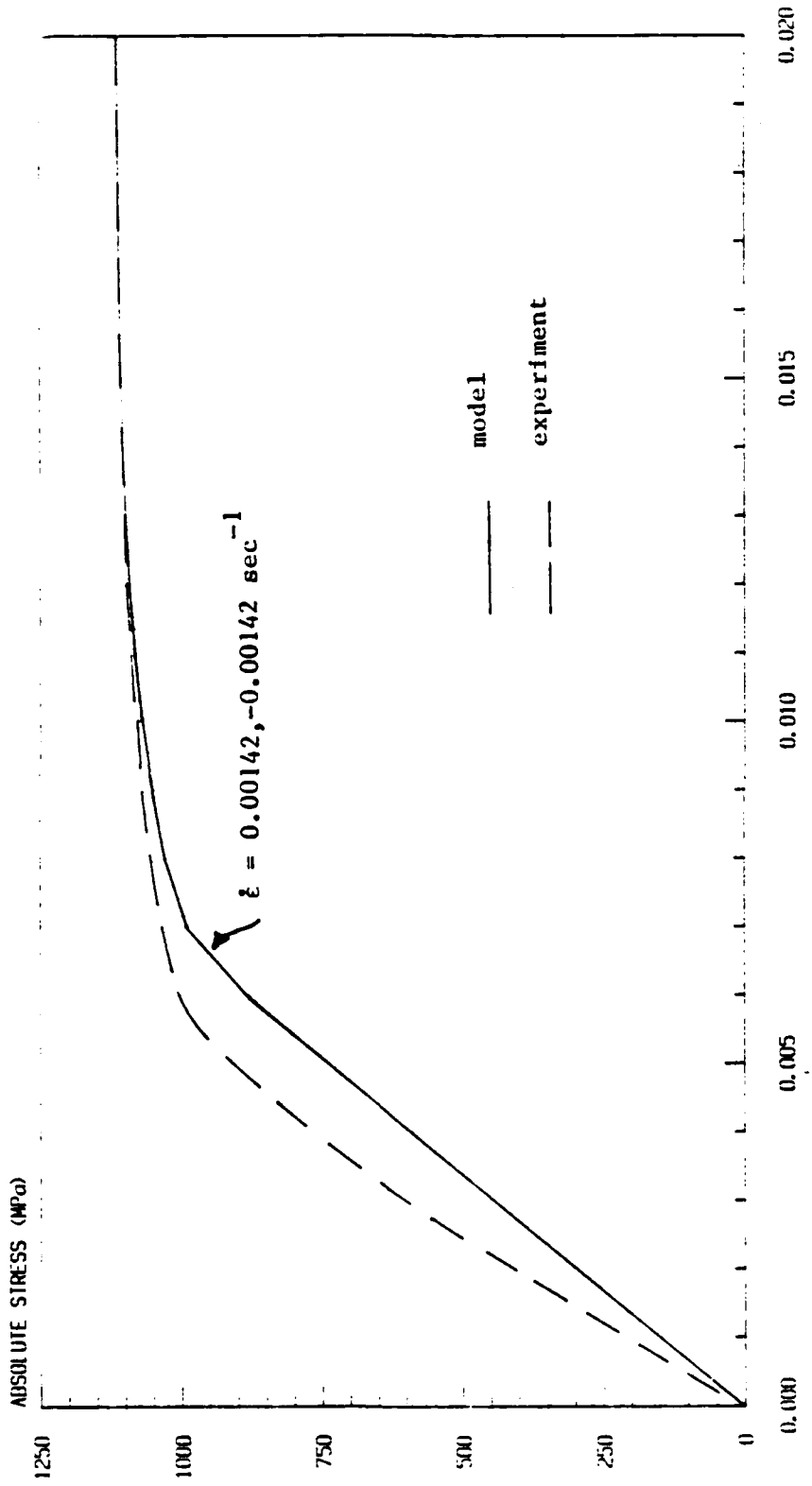

Fig. 4. Stress-Strain Behavior for IN100 at 1005°K (1350°F) Subjected to Constant Strain Rate in Tension and Compression

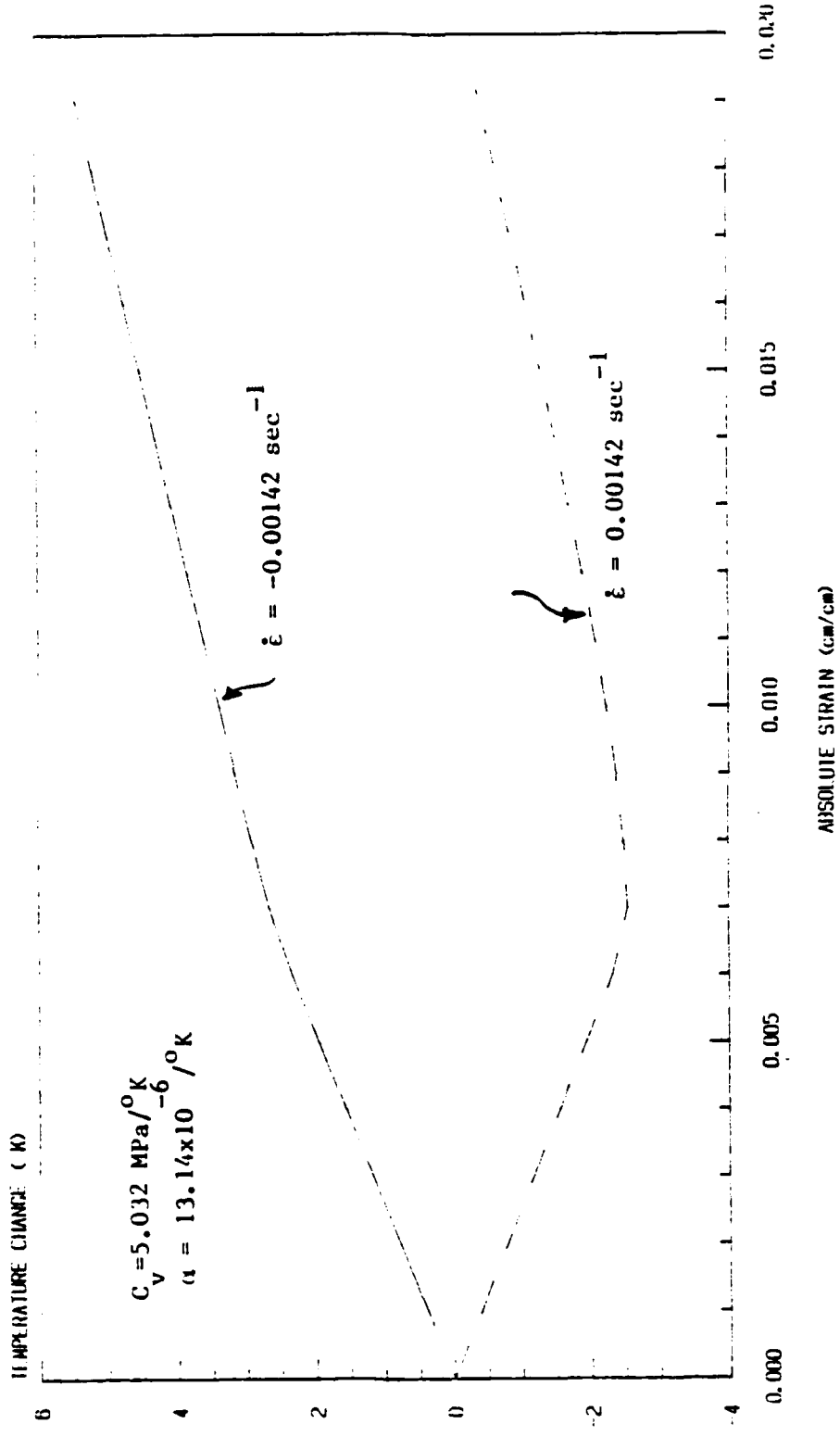

Fig. 5. Predicted Temperature Change for IN100 at 1005°K (1350°F) Subjected to Load Histories Shown In Fig. 4

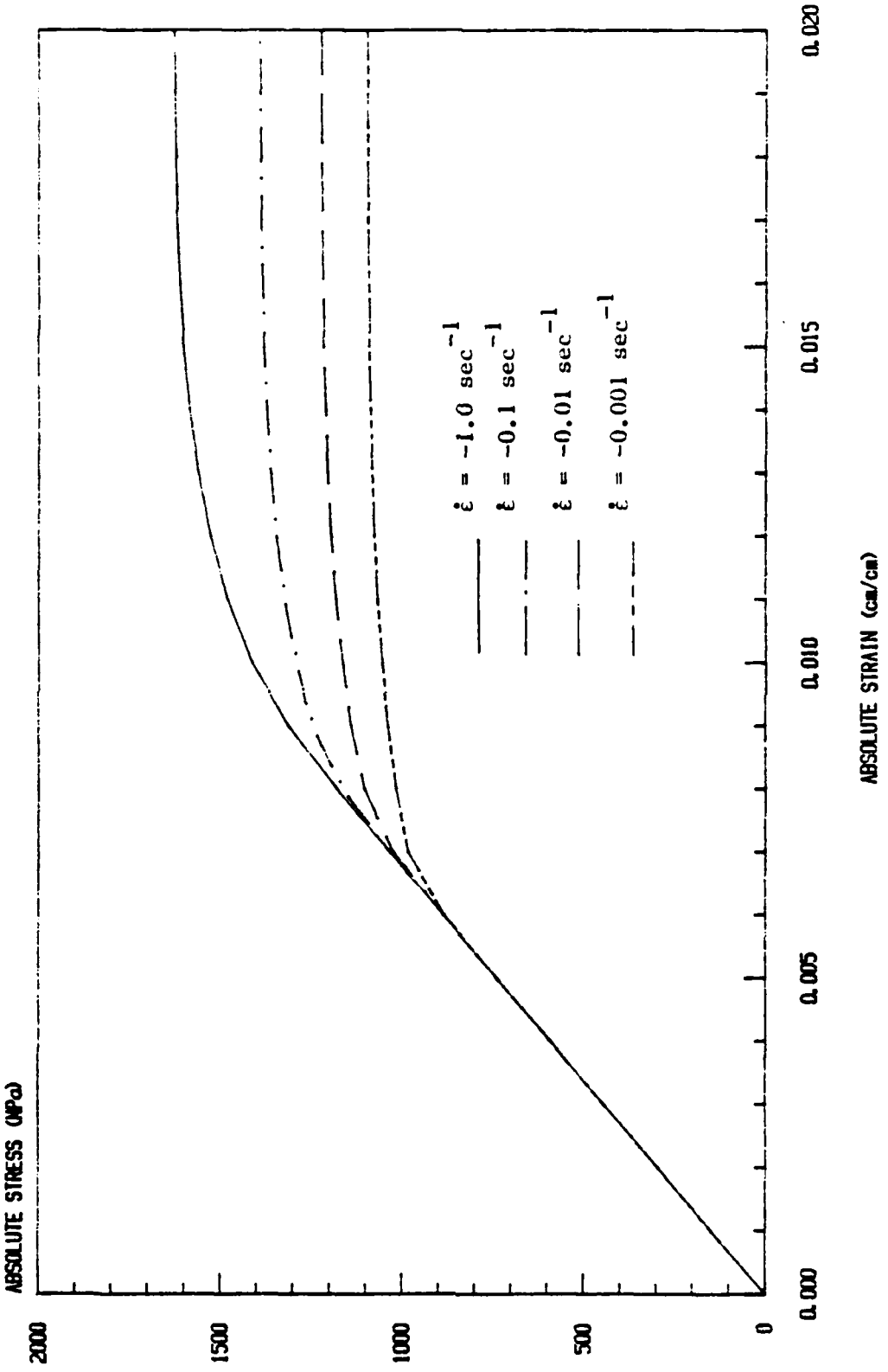

Fig. 6. Predicted Stress-Strain Behavior for IN100 at 1005°K (1350°F) Subjected to Constant Strain Rates in Compression

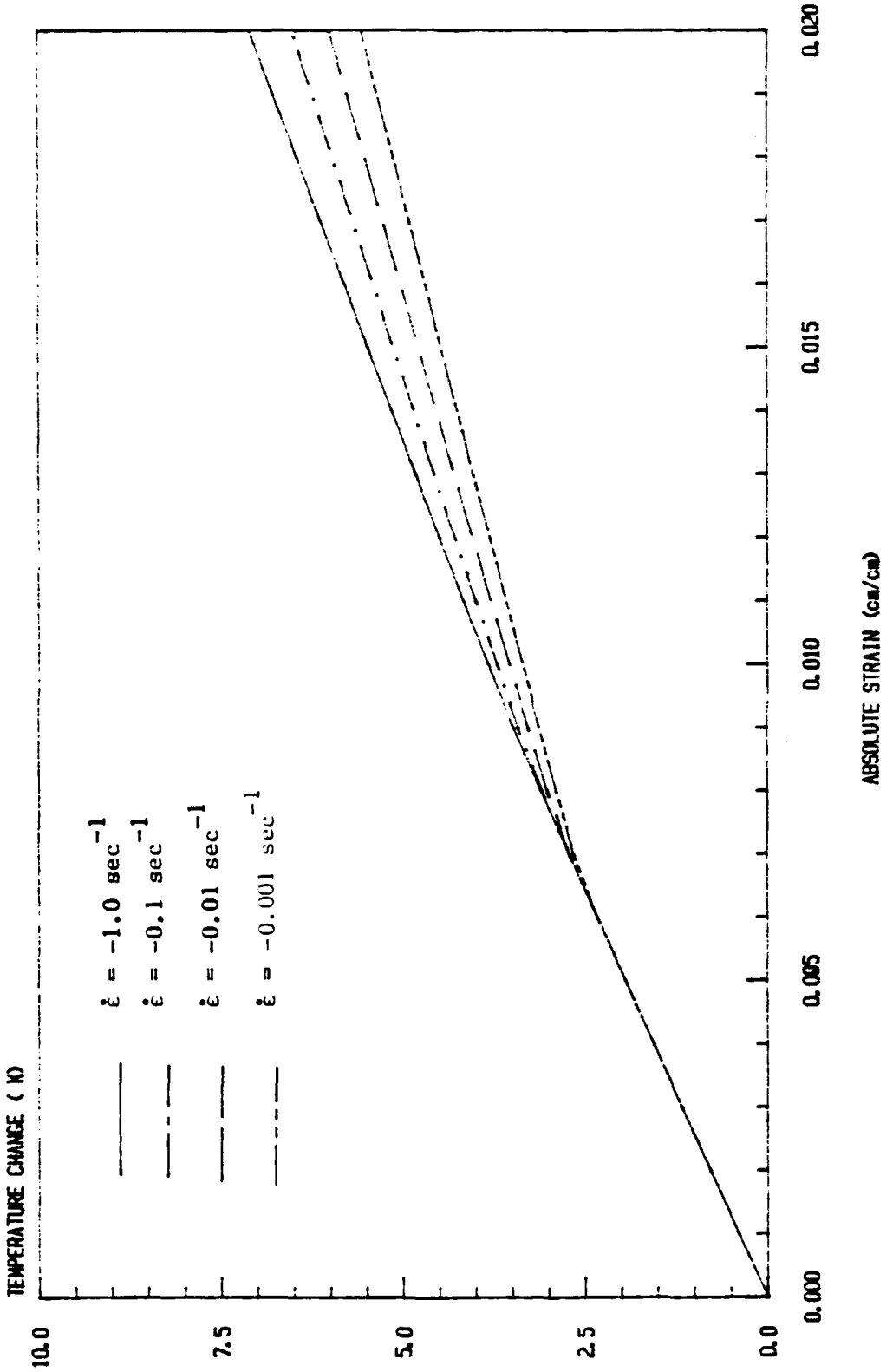

Fig. 7. Predicted Temperature Change for IN100 at 1005°K (1350°F) Subjected to Load Histories Shown in Fig. 6

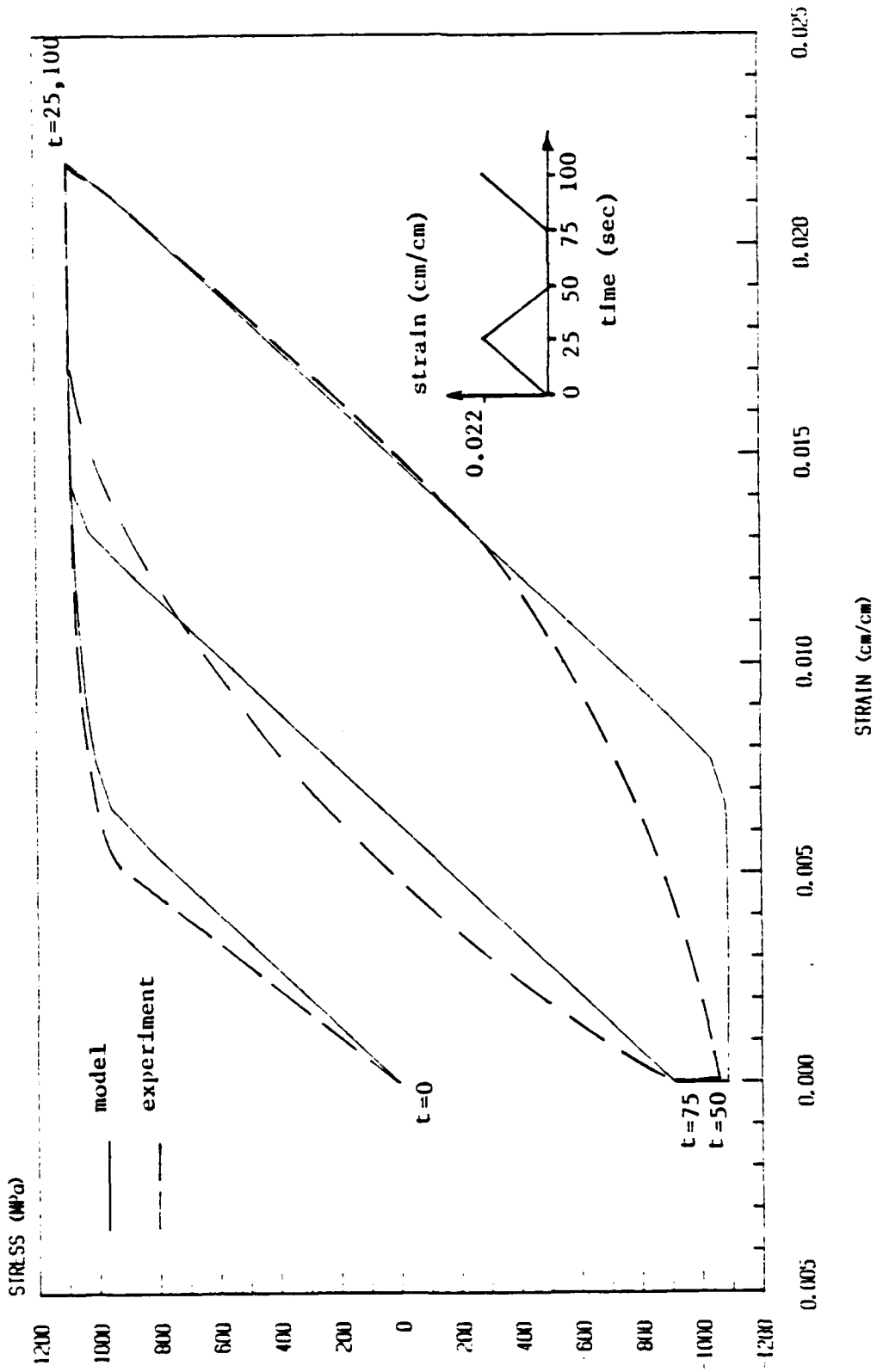

Fig. 8. Stress-Strain Behavior of IN100 at 1005°K (1350°F) Under Cyclic Load with Stress Relaxation

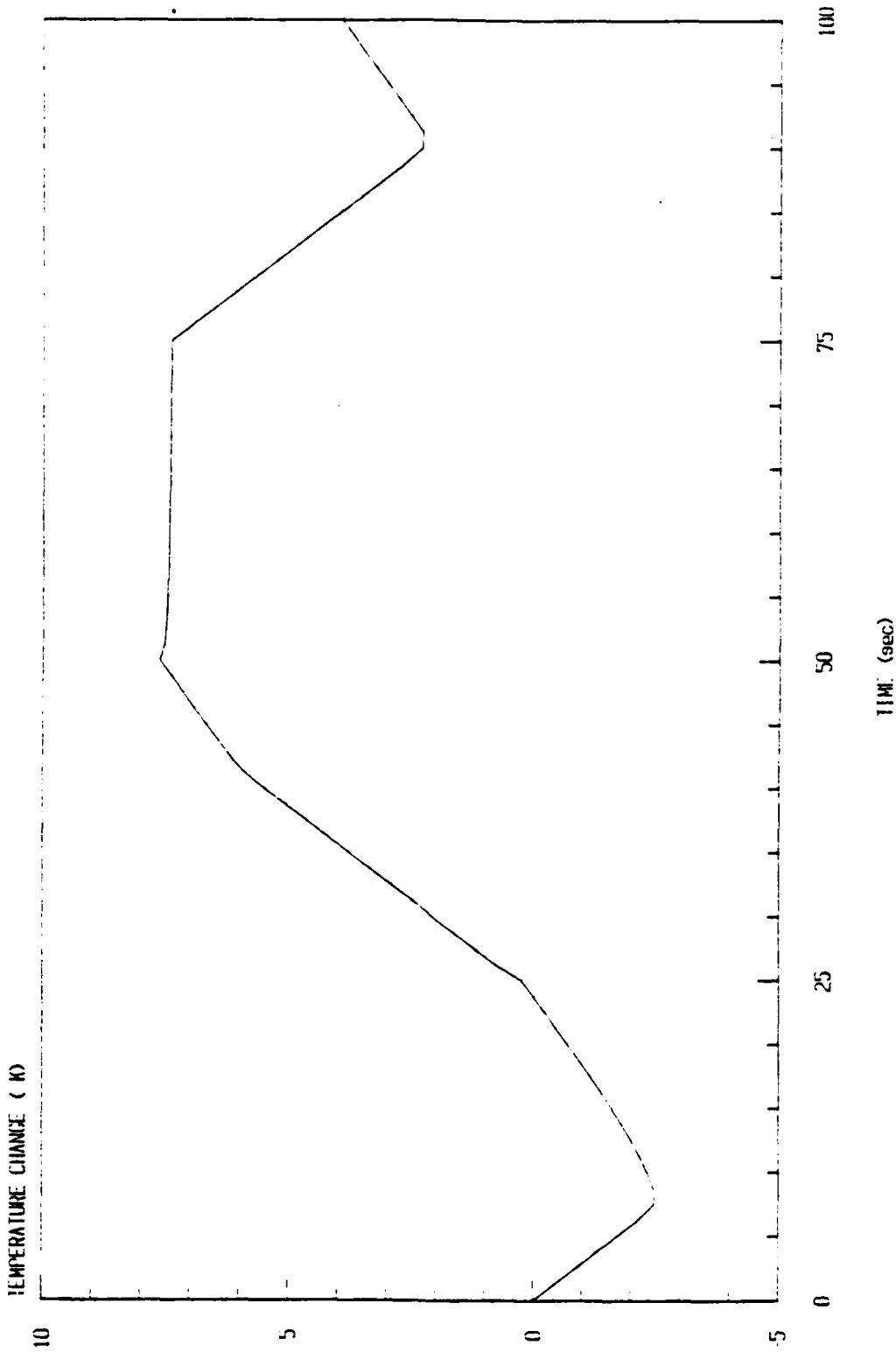

Fig. 9. Predicted Temperature Change for IN100 at 1005°K (1350°F) Subjected to Cyclic Load History Shown in Fig. 8

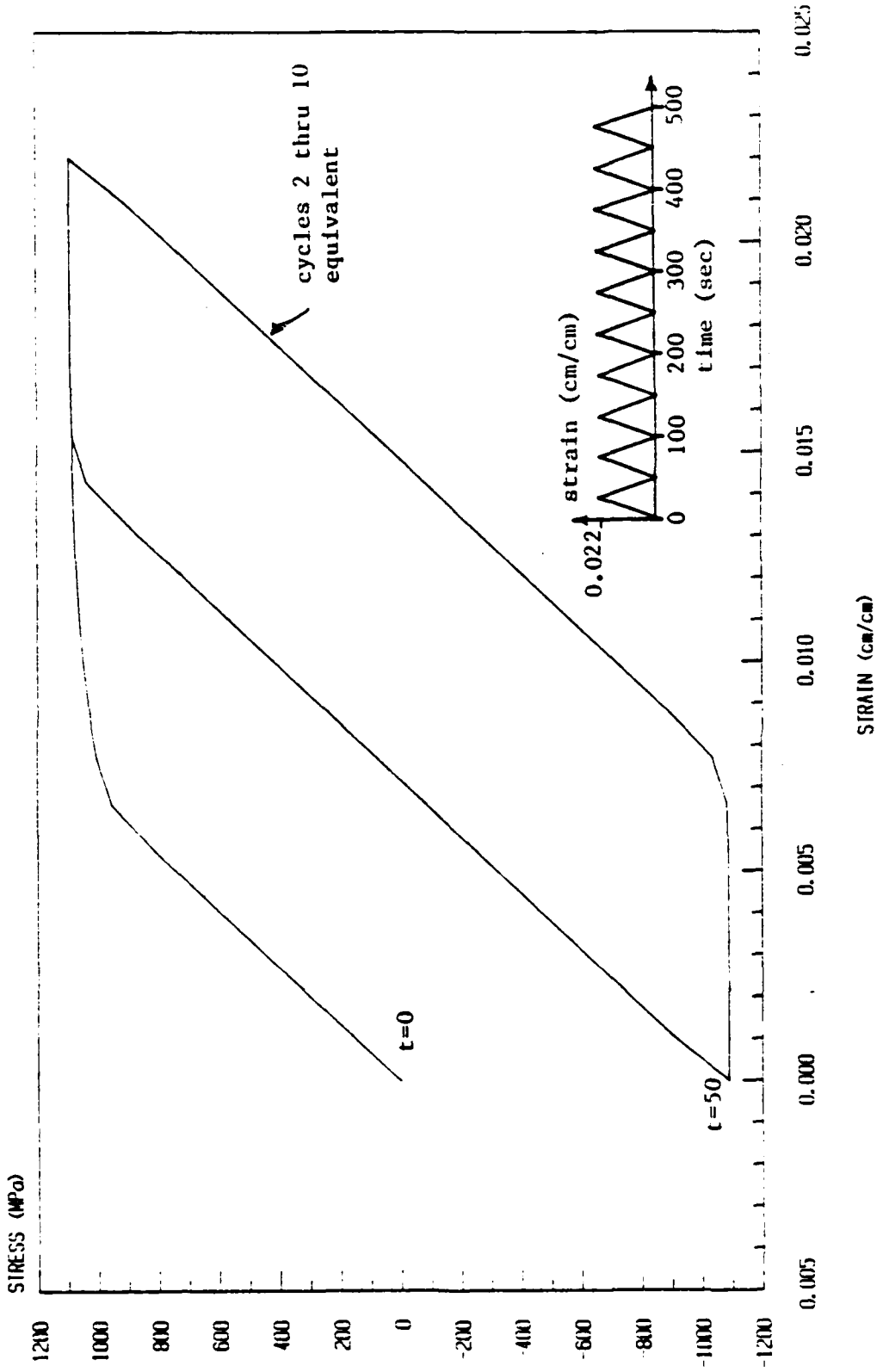

Fig. 10. Predicted Stress-Strain Behavior of IN100 at 1005°K (1350°F) Subjected to Multi-cylic Load

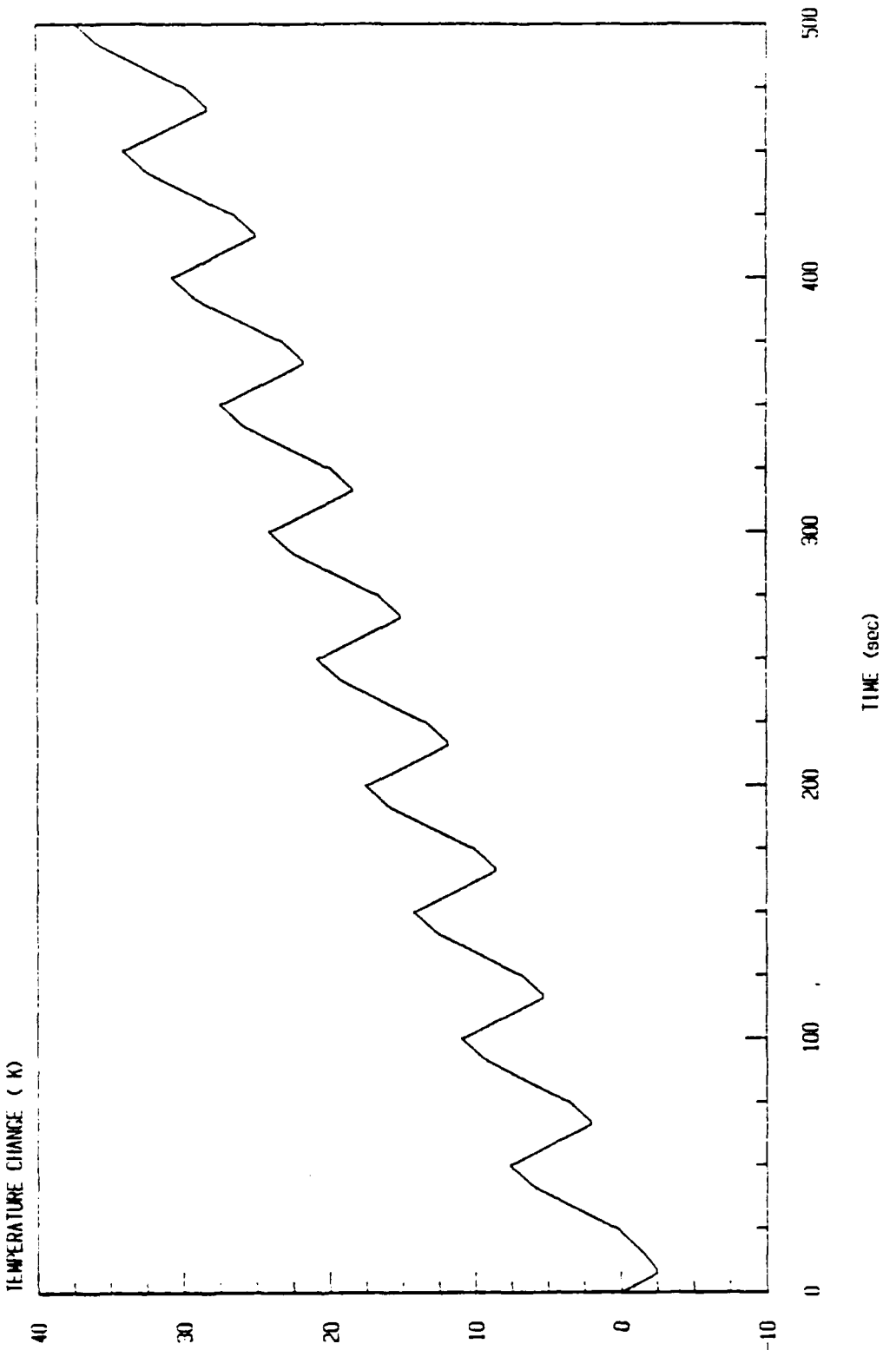

Fig. 11. Predicted Temperature Change for IN100 at 1005°K (1350°F) Subjected to Multi-cyclic Load History Shown in Fig. 10

temperature change is identical to results obtained by Cernocky and Krempl when their mechanical constitutive equations are used. However, it has been shown herein that the introduction of internal state variables leads to a more general model which may be used with virtually any thermoviscoplastic model currently used for metals [24].

It has been found in the current research that significant heating may occur under adiabatic conditions, expecially during cyclic loading, in thermoviscoplastic metallic media. The significance of this heating is compounded by the fact that material properties often become extremely sensitive in the inelastic range of behavior. This issue has not been considered herein, but it certainly warrants study when transient temperature models become available.

Two important questions have not been answered in this research: 1) what effect does the inclusion of the heat flux term have on the predicted results; and 2) what, if anything, does the present model have to do with experimentally observed results? The first question can only be addressed if spacial variation is admitted in the field parameters. The author is currently studying this question and hopes to present results in a future paper. The second question cannot be answered at this time since it requires extremely sophisticated experimentation. Although experimental results have been obtained detailing heat generation in inelastic media, it is not possible to compare the current model since additional complex tests must be performed in order to characterize the thermoviscoplastic material parameters. The author also hopes to address this issue in a future paper.

Acknowledgement

The author gratefully acknowledges support for this research, which was provided by the Air Force Office of Scientific Research under contract no. F49620-83-C-0067.

References

[1] J.M.C. Duhamel, Memoire sur le calcul des actions moleculaires developpees par les changements de temperature dans les corps solides. Memoires par divers savans, vol. 5, pp. 440-498, (1838).

[2] F. Neumann, Vorlesungen uber die theorie der elasticitat der festen Korper und des lichtathers. Leipzig, 107-120, (1885).

[3] B.A. Boley and J.H. Weiner, Theory of Thermal Stresses. Wiley, New York, (1960).

[4] O.W. Dillon, Jr., An experimental study of the heat generated during torsional oscillations. J. Mech. Phys. Solids, vol. 10, 235-224 (1962).

[5] O.W. Dillon, Jr., Temperature generated in aluminum rods undergoing torsional oscillations. J. Appl. Mech. 33, vol. 10, 3100-3105 (1962).

[6] O.W. Dillon, Jr., Coupled thermoplasticity. J. Mech. Phys. Solids, vol. 11, 21-33 (1963).

[7] G.R. Halford, Stored Energy of Cold Work Changes Induced by Cyclic Deformation. Ph.D. Thesis, University of Ilinois, Urbana, Illinois (1966).

[8] O.W. Dillon, Jr., The heat generated during the torsional oscillations of copper tubes. Int. J. Solids Structures, vol. 2, 181-204 (1966).

[9] W. Olszak and P. Perzyna, Thermal Effects in Viscoplasticity. IUTAM Symp., East Kilbride, 206-212, Springer-Verlag, New York (1968).

[10] J. Kratochvil and R.J. DeAngelis, Torsion of a titanium elastic viscoplastic shaft. J. Appl. Mech., vol. 42, 1091-1097 (1971).

[11] E.P. Cernocky and E. Krempl, A theory of thermoviscoplasticity based on infinitesimal total strain. Int. J. Solids Structures, vol. 16, 723-741 (1980).

[12] J.F. Tormey and S.C. Britton, Effect of cyclic loading on solid propellant grain structures. AIAA Journal, vol. 1, 1763-1770 (1963).

[13] R.A. Schapery, Effect of cyclic loading on the temperature in viscoelastic media with variable properties. AIAA Journal, vol. 2, 827-835 (1964).

[14] T.R. Tauchert, The temperature generated during torsional oscillation of polyethylene rods. Int. J. Eng. Sci., vol. 5, 353-365 (1967).

[15] T.R. Tauchert and S.M. Afzal, Heat generated during torsional oscillations of polymethylmethcrylate tubes. J. Appl. Phys., vol. 38, 4568-4572 (1967).

[16] B.D. Coleman, Thermodynamics of materials with memory. Arch. Rational Mech. Anal., vol. 17, 1-46 (1964).

[17] B.D. Coleman and M.E. Gurtin, Thermodynamics with internal state variables. J. Chem. Phys., vol. 47, 597-613 (1967).

[18] A.E. Green and P.M. Naghdi, A general theory of an elastic-plastic continuum. Arch. Rational Mech. Anal., vol. 18, 251-181 (1965).

[19] R.A. Schapery, A theory of nonlinear thermoviscoelasticity based on irreversible thermodynamics. Proc. 5th U.S. Nat. Cong. Appl. Mech. ASME, 511 (1966).

[20] D.H. Allen, Thermodynamic constraints on the constitution of a class of thermoviscoplastic solids. Texas A&M University Mechanics and Materials Research Center, MM 12415-82-10 (1982).

[21] J. Kratochvil and O.W. Dillon, Jr., Thermodynamics of elastic-plastic materials as a theory with internal state variables. J. Appl. Phys., vol. 40, 3207-3218 (1969).

[22] J. Kratochvil and O.W. Dillon, Jr., Thermodynamics of crystalline elastic-visco-plastic materials. J. Appl. Phys., vol. 41, 1470-1479 (1970).

[23] C.A. Truesdell and R.A. Toupin, The classical field theories. Handbuch der Physik, vol. III/1, Springer, Berlin (1960).

[24] D.H. Allen, Some comments on inelastic strain in thermoviscoplastic metals. Texas A&M University Mechanics and Materials Research Center, MM NAG 3-31-83-8 (1983).

[25] G.I. Taylor and H. Quinney, The latent energy remaining in a metal after cold working. Proc. Roy. Soc. A., vol. 143, 307-326 (1934).

[26] E.P. Cernocky and E. Krempl, A theory of viscoplasticity based on infinitesimal total strain. Acta Mechanica, vol. 36, 263-289 (1980).

[27] K.C. Valanis, A theory of viscoplasticity without a field surface part I. general theory. Archives of Mechanics, vol. 2z, 517-533 (1971).

[28] R.D. Krieg, J.C. Swearengen, and R.W. Rohds, A physically-based internal variable model for rate-dependent plasticity. Proceedings ASME/CSME PVP Conference, 15-27 (1978).

[29] D.H. Allen and W.E. Haisler, A theory for analysis of thermoplastic materials. Computers & Structures, vol. 13, 129-135 (1981).

[30] A.K. Miller, An inelastic constitutive model for monotonic cyclic, and creep deformation: part I--equations development and analytical procedures and part II--application to type 304 stainless steel. J. Eng. Mat. & Tech., vol. 98-H, 97 (1976).

[31] K.P. Walker, Representation of hastelloy-x behavior at elevated temperature with a functional theory of viscoplasticity . presented at ASME Pressure Vessels Conference, San Francisco (1980).

[32] E.W. Hart, Constitutive relations for the nonelastic deformation of metals. J. Eng. Mat. & Tech., vol. 98-H, 193 (1976).

[33] U.F. Kocks, Laws for work-hardening and low-temperature creep. J. Eng. Mat. & Tech., vol. 98-H, 76-85 (1976).

[34] D.N. Robinson, A unified creep-plasticity model for structural metals at high temperatures. ORNL TM-5969 (1978).

[35] S.R. Bodner and Y. Partom, Constitutive equations for elastic-viscoplastic strain-hardening materials. J. Appl. Mech., vol. 42, 385-389 (1975).

[36] S.R. Bodner, I. Partom and Y. Partom, Uniaxial cyclic loading of elastic-viscoplastic materials. J. Appl. Mech., No. 79-WA/APM-30 (1979)

[37] D.C. Stouffer, A constitutive representation for IN 100. Air Force Materials Laboratory, AFWAL-TR-81-4039 (1981).

[38] T.M. Milly and D.H. Allen, A comparative study of nonlinear rate-dependent mechanical constitutive theories for crystalline solids at elevated temperatures. Virginia Polytechnic Institute and State University, VPI-E-82-5 (1982).

[31] K.P. Walker, Representation of hastelloy-x behavior at elevated temperature with a functional theory of viscoplasticity . presented at ASME Pressure Vessels Conference, San Francisco (1980).

[32] E.W. Hart, Constitutive relations for the nonelastic deformation of metals. J. Eng. Mat. & Tech., vol. 98-H, 193 (1976).

[33] U.F. Kocks, Laws for work-hardening and low-temperature creep. J. Eng. Mat. & Tech., vol. 98-H, 76-85 (1976).

[34] D.N. Robinson, A unified creep-plasticity model for structural metals at high temperatures. ORNL TM-5969 (1978).

[35] S.R. Bodner and Y. Partom, Constitutive equations for elastic-viscoplastic strain-hardening materials. J. Appl. Mech., vol. 42, 385-389 (1975).

[36] S.R. Bodner, I. Partom and Y. Partom, Uniaxial cyclic loading of elastic-viscoplastic materials. J. Appl. Mech., No. 79-WA/APM-30 (1979)

[37] D.C. Stouffer, A constitutive representation for IN 100. Air Force Materials Laboratory, AFWAL-TR-81-4039 (1981).

[38] T.M. Milly and D.H. Allen, A comparative study of nonlinear rate-dependent mechanical constitutive theories for crystalline solids at elevated temperatures. Virginia Polytechnic Institute and State University, VPI-E-82-5 (1982).

Appendix 6.2

Mechanics and Materials Center
TEXAS A&M UNIVERSITY
College Station, Texas

AN EFFICIENT AND ACCURATE ALTERNATIVE TO SUBINCREMENTATION FOR ELASTIC-PLASTIC ANALYSIS BY THE FINITE ELEMENT METHOD

BY

S.E. GROVES

Lecturer

D.H. ALLEN

Assistant Professor

W.E. Haisler

Professor

MM 4875-83-13

September 1983

SECURITY CLASSIFICATION OF THIS PAGE (When Data Entered)

REPORT DOCUMENTATION PAGE

READ INSTRUCTIONS BEFORE COMPLETING FORM

1. REPORT NUMBER: MM-4875-83-13	2. GOVT ACCESSION NO.
3. RECIPIENT'S CATALOG NUMBER	
4. TITLE (and Subtitle): An Efficient and Accurate Alternative to Subincrementation for Elastic-Plastic Analysis by the Finite Element Method	5. TYPE OF REPORT & PERIOD COVERED: Interim
6. PERFORMING ORG. REPORT NUMBER	
7. AUTHOR(s): Scott E. Groves, David H. Allen, Walter E. Haisler	8. CONTRACT OR GRANT NUMBER(s): F49620-83-C-0067
9. PERFORMING ORGANIZATION NAME AND ADDRESS: Aerospace Engineering Department, Texas A&M University, College Station, TX 77843	10. PROGRAM ELEMENT, PROJECT, TASK AREA & WORK UNIT NUMBERS
11. CONTROLLING OFFICE NAME AND ADDRESS: Air Force Office of Scientific Research, Bolling AFB, Washington, D.C. 20332	12. REPORT DATE: September, 1983
	13. NUMBER OF PAGES: 35
14. MONITORING AGENCY NAME & ADDRESS(if different from Controlling Office)	15. SECURITY CLASS. (of this report): Unclassified
	15a. DECLASSIFICATION/DOWNGRADING SCHEDULE
16. DISTRIBUTION STATEMENT (of this Report): -	
17. DISTRIBUTION STATEMENT (of the abstract entered in Block 20, if different from Report)	
18. SUPPLEMENTARY NOTES	
19. KEY WORDS (Continue on reverse side if necessary and identify by block number): constitutive equations, elastic-plastic, zeta, subincrementation, finite elements	

20. ABSTRACT (Continue on reverse side if necessary and identify by block number)

In this paper a new and efficient alternative to subincrementation is developed for analysis of solid media with rate independent elastic-plastic material behavior. This alternative method is not unlike the subincrementation procedure in that it represents an Euler integration of the nonlinear constitutive equations. However, it takes advantage of the fact that the Euler integration procedure assumes proportional loading steps so that when the uniaxial stress-strain curve is idealized as a piecewise linear relation very large forward integration steps give accurate results. The new procedure, which we call

DD FORM 1 JAN 73 1473 EDITION OF 1 NOV 55 IS OBSOLETE

SECURITY CLASSIFICATION OF THIS PAGE (When Data Entered)

AN EFFICIENT AND ACCURATE ALTERNATIVE TO SUBINCREMENTATION FOR ELASTIC-PLASTIC ANALYSIS BY THE FINITE ELEMENT METHOD

BY

S.E. Groves
Lecturer

D.H. Allen
Assistant Professor

W.E. Haisler
Professor

AEROSPACE ENGINEERING DEPARTMENT
TEXAS A&M UNIVERSITY
College Station, Texas 77843

September 1983

Accepted for publication by
Computers & Structures
1984

ABSTRACT

In this paper a new and efficient alternative to subincrementation is developed for analysis of solid media with rate independent elastic-plastic material behavior. This alternative method is not unlike the subincrementation procedure in that it represents an Euler integration of the nonlinear constitutive equations. However, it takes advantage of the fact that the Euler integration procedure assumes proportional loading steps so that when the uniaxial stress-strain curve is idealized as a piecewise linear relation very large forward integration steps give accurate results. The new procedure, which we call the zeta method, is equally appropriate for cyclic loading with combined isotropic and kinematic hardening. However, due to the nonuniqueness of the monotonic uniaxial stress-strain relation in rate dependent media, the method is not appropriate for use in viscoplastic media.

Although the algorithm deals only with the evaluation of a classical plasticity based constitutive law, numerical results are reported herein for an assortment of problems by the finite element method. It is shown via these results that the zeta method discussed herein provides not only accuracy which is superior to the subincrementation method, but the resulting algorithm also shows improved numerical efficiency.

INTRODUCTION

In recent years the analysis of elastic-plastic solids which behave according to classical rate-independent incremental plasticity constitutive models has become quite commonplace. By far the most often used method for nonhomogeneous boundary value problem solutions is the finite element method. By the nature of the kinematics and material behavior this is a nonlinear field problem, and a considerable body of research has been generated dealing with efficient numerical solution of the nonlinear boundary value problem. One efficiency measure adopted solely to improve material models and independent of large deformation behavior is the subincrementation method [1-3].

In this paper the subincrementation method will be briefly reviewed and an alternative procedure will be proposed. It will be shown that this new method gives both improved accuracy and efficiency over the subincrementation method, and this contention will be supported via several numerical results.

REVIEW OF THE ELASTIC-PLASTIC FIELD PROBLEM

An elastic-plastic medium subjected to an isothermal loading must in general satisfy the following conditions at all points in its interior V and on its surface B: (1) conservation of linear and angular momentum, (2) conservation of mass; (3) strain-displacement relations; (4) the first and second laws of thermodynamics; and (5) stress-strain relations (constitution). Of course, there are additional constitutive relations [4], but these need not be considered in order to characterize the mechanical response when internal heat generation is negligible. It will

be assumed that the above restriction holds for the media considered herein, although the method to be considered here applies equally to transient temperature phenomena.

Condition (5) is the main topic of the discussion herein. In this paper we consider only elastic-plastic media: that class of materials for which the stress (or strain) tensor can be considered to be a time independent functional of the strain (or stress) tensor, that is, stress is dependent on the entire history of strain but independent of the time scale. It has been shown that this functional form can often be written in an equivalent differential equation form [5]. One common strain formulation is of the general type [6]

$$d\sigma_{ij} = C_{ijkl} d\varepsilon_{kl} \quad , \tag{1}$$

where for small deformation σ_{ij} and ε_{ij} represent infinitesimal stress and strain tensors, respectively, and C_{ijkl}, called the effective modulus tensor, is the repository for history dependence via its dependence on the equivalent uniaxial plastic strain, $\bar{\varepsilon}^P$, which is a metric in the space of plastic strain defined by

$$\bar{\varepsilon}^P(t) \equiv \int_0^{\bar{\varepsilon}^P(t)} d\bar{\varepsilon}^P = \int_0^{\varepsilon_{ij}^P(t)} \sqrt{\frac{2}{3} d\varepsilon_{ij}^P d\varepsilon_{ij}^P} \quad , \tag{2}$$

where t represents time and

$$d\varepsilon_{ij}^P \equiv d\varepsilon_{ij} - D_{ijkl} d\sigma_{kl} \quad , \tag{3}$$

and D_{ijkl} is the elastic modulus tensor, assumed to be independent of deformation. In a uniaxial sense the effective modulus tensor C_{ijkl} may be thought of as a secant modulus.

It should be noted that for finite deformation equations (1) may still be applicable if σ_{ij} and ε_{ij} are replaced by frame indifferent quantities consistent with hypoelasticity [7]. Note also that under certain simplifying assumptions equations (1) reduce to the classical Prandtl- Reuss equations [8,9].

It has been shown that equations (1) are consistent with the first and second laws of thermodynamics [10-12]. Therefore, since the energy balance is trivially satisfied in an isothermal domain with negligible internal heat generation and conservation of mass is satisfied if the density is timewise constant during infinitesimal deformation, we need consider only conditions (1), (3) and (5) here.

In the finite element method conditions (1) and (3) are usually satisfied via an incremental variational principle integrated over the domain of interest. The discretization process then entails reducing the volume integral for the variational principle to some sub-domain aptly called a finite element. The integration over the volume of each element is usually sufficiently difficult to require numerical integration, and for this purpose a quadrature procedure is generally employed. Thus, the integration is reduced to evaluation of the integrand at a finite number of integration points within an element.

The volume integration of each element yields a set of matrix equations which are assembled into a global set of matrix equations. These equations are nonlinear even during infinitesimal deformations due to the nonlinearity of equations (1). Therefore, an iterative technique is generally used to solve the global equations on each load step, and the constitutive equations (1) must be solved several times for all

integration points on each load step until convergence occurs.*

SOLUTION OF THE CONSTITUTIVE EQUATIONS

It has become common practice in the literature to incrementalize equations (1) by simply replacing differentials $d\sigma_{ij}$ and $d\varepsilon_{ij}$ with increments $\Delta\sigma_{ij}$ and $\Delta\varepsilon_{ij}$, respectively. However, since the integrand depends on the strain tensor during the load increment, an important task becomes the integration of equations (1) over some input increment in the strain tensor, viz.:

$$\Delta\sigma_{ij} = \int_{\sigma_{ij}(\varepsilon_{ij}(t))}^{\sigma_{ij}(\varepsilon_{ij}(t+\Delta t))} d\sigma_{ij} = \int_{\varepsilon_{ij}(t)}^{\varepsilon_{ij}(t+\Delta t)} C_{ijkl}(\bar{\varepsilon}^P) d\varepsilon_{kl} \quad , \tag{4}$$

where t represents the time at the start of a load increment, and $t+\Delta t$ is the time at the end of a load increment.

Equations (4) definitely present a uniqueness problem since the strain tensor may be cycled during the time increment Δt. In order to avoid this difficulty a sufficient condition may be adopted which is not unlike the condition required to obtain the Mises-Hencky deformation theory [15] from the Prandtl-Reuss equations. It is assumed that during the time increment Δt all components of the strain tensor increase monotonically via the relation

$$d\varepsilon_{kl} = K_{kl} d\bar{\varepsilon}^P \quad , \quad K_{kl} = \text{constants} \quad , \tag{5}$$

where $d\bar{\varepsilon}^P$ must be a monotonically increasing function of strain during plastic loading over the time increment Δt. Substitution of equations (5) into (4) yields

*For a more complete discussion of the finite element method applied to elastic-plastic media, see references [13] and [14].

$$\Delta\sigma_{ij} = \int_{\bar{\varepsilon}^P(\varepsilon_{ij}^t)}^{\bar{\varepsilon}^P(\varepsilon_{ij}^{t+\Delta t})} C_{ijkl}(\bar{\varepsilon}^P)K_{kl}\,d\bar{\varepsilon}^P \quad , \tag{6}$$

which is obviously a unique relation due to the monotinicity of the plastic strain increment during the time increment Δt. Now define the following fourth order tensor which is constant over the time step Δt:

$$C'_{ijkl} \equiv \frac{1}{\Delta\bar{\varepsilon}^P} \int_{\bar{\varepsilon}^P(t)}^{\bar{\varepsilon}^P(t+\Delta t)} C_{ijkl}(\bar{\varepsilon}^P)\,d\bar{\varepsilon}^P \quad . \tag{7}$$

Then substitution of definitions (7) into equation (6) gives

$$\Delta\sigma_{ij} = C'_{ijkl}K_{kl}\Delta\bar{\varepsilon}^P = C'_{ijkl}\Delta\varepsilon_{kl} \quad , \tag{8}$$

which is the exact incremental relation which should be used with the incremental variational principle. It should be noted that equations (1) and (8) are by no means equivalent since C'_{ijkl} can be seen from definitions (7) to represent an average effective modulus tensor during the time increment Δt. Unfortunately, equations (7) cannot be integrated precisely because the upper limit of integration $\bar{\varepsilon}^P(t+\Delta t)$ cannot be determined until equations (8) have been evaluated.

It will be recalled that the equivalent uniaxial plastic strain can be shown to be equal to the axial plastic strain when a bar is pulled uniaxially [16]. Now define the equivalent uniaxial stress

$$\bar{\sigma} \equiv \left[\frac{3}{2}\left(\sigma_{ij} - \frac{\sigma_{KK}}{3}\delta_{ij}\right)\left(\sigma_{ij} - \frac{\sigma_{KK}}{3}\delta_{ij}\right)\right]^{\frac{1}{2}} \quad , \tag{9}$$

which can also be seen to be equivalent to the axial stress when a bar is pulled uniaxially [16]. Thus, the information required to characterize equations (6) is obtainable from a single monotonically increasing

equivalent uniaxial plastic strain diagram as shown in Fig. 1. Note that the curve shown represents nothing more than a uniaxial stress-strain diagram with abscissa transformed via definition (3). In addition, for combined isotropic-kinematic hardening the ordinate in Fig. 1 should be transformed as well [17].

It is apparent from Fig. 1 that for a continuously work hardening material the relation between the equivalent uniaxial plastic strain $\bar{\varepsilon}^P$ and the slope of the uniaxial stress-plastic diagram is unique, that is,

$$\bar{\varepsilon}^P = F\left(\frac{d\bar{\sigma}}{d\bar{\varepsilon}^P}\right) \quad , \tag{10}$$

where F is a bijective mapping. Therefore, the effective modulus tensor may be written alternatively as

$$\bar{C}_{ijkl}\left(\frac{d\bar{\sigma}}{d\bar{\varepsilon}^P}\right) = C_{ijkl}(\bar{\varepsilon}^P) \quad , \tag{11}$$

Thus, because the effective modulus tensor C_{ijkl} is a nonlinear function of the plastic secant modulus $d\bar{\sigma}/d\bar{\varepsilon}^P$, integration of equations (7) is not a trivial task. In order to avoid this numerical complexity it is not uncommon to simply approximate the effective modulus tensor by

$$C_{ijkl}(\bar{\varepsilon}^P) \cong C_{ijkl}(\bar{\varepsilon}^P(t)) \quad , \tag{12}$$

thus reducing integration of equations (6) to

$$\Delta\sigma_{ij} \cong C_{ijkl}(\bar{\varepsilon}^P(t))K_{kl}\Delta\bar{\varepsilon}^P = C_{ijkl}(\bar{\varepsilon}^P(t))\Delta\varepsilon_{kl} \quad , \tag{13}$$

which is Euler's method of forward integration. Obviously, since this is nothing more than a simple first order Taylor series expansion its accuracy will depend on the relative nonlinearity or curvature of the uniaxial stress-plastic strain curve during a given load increment. This condition is illustrated for the uniaxial case in Fig. 2.

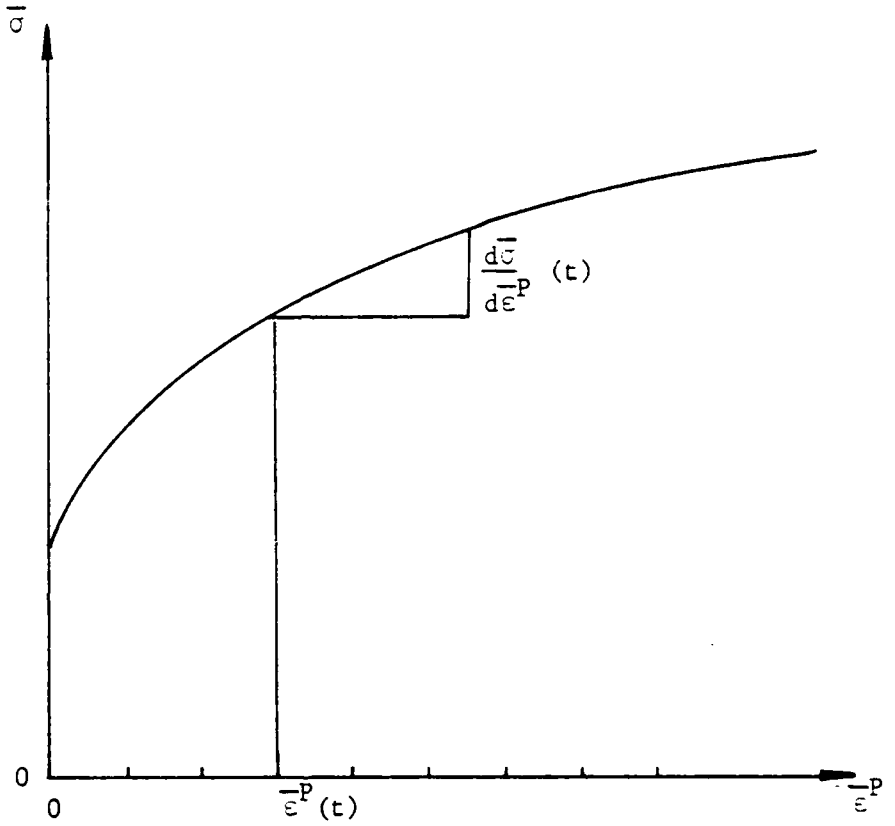

Fig. 1. Equivalent Uniaxial Stress Versus Equivalent Uniaxial Plastic Strain Diagram

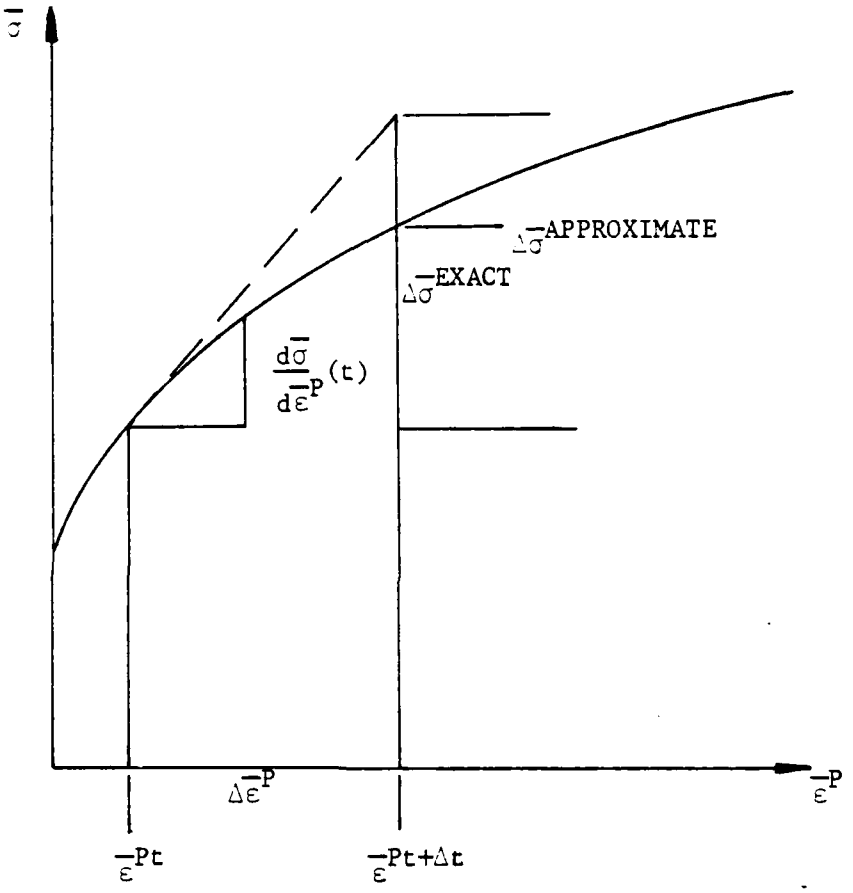

Fig. 2. Approximate Determination of $\frac{d\bar{\sigma}}{d\bar{\varepsilon}^P}$

In many computer codes the uniaxial stress-strain diagram is input in piecewise linear fashion as shown in Fig. 3. While it is not clear that this piecewise linearization is motivated by anything beyond simplification of input data, it has the added benefit that it helps alleviate the numerical integration problem noted above and described in Fig. 4. In fact, so long as the plastic strain increment $\Delta\bar{\varepsilon}^P$ does not subtend a slope discontinuity during a load step equations (11) indicate that approximation (12) will reproduce the piecewise linear curve exactly. Therefore, the accuracy of equations (13) is limited only by the accuracy with which one can reproduce the exact curve of stress versus plastic strain with a piecewise linear curve. Mathematically, the slope continuity condition is satisfied if one can find values of the equivalent plastic strain at slope discontinuities $\bar{\varepsilon}^P_i$, as shown in Fig. 3, such that for the current load increment

$$\bar{\varepsilon}^P_i \leq \bar{\varepsilon}^P \leq \bar{\varepsilon}^P_{i+1} \quad , \tag{14}$$

for all equivalent plastic strains in the range

$$\bar{\varepsilon}^P(t) \leq \bar{\varepsilon}^P \leq \bar{\varepsilon}^P(t+\Delta t) \quad . \tag{15}$$

However, condition (14) cannot be <u>a priori</u> guaranteed in practice because in a non-homogeneous boundary value problem the equivalent uniaxial plastic strain varies spatially. Whereas one integration point may undergo a very small or even zero (elastic) plastic strain increment during a specified increment in surface tractions, another point under high stress concentration may undergo a plastic strain increment which subtends one or more discontinuities in the piecewise linear equivalent uniaxial stress versus equivalent uniaxial plastic strain diagram. Thus, as can be seen from definitions (2) and (3) the equivalent uniaxial

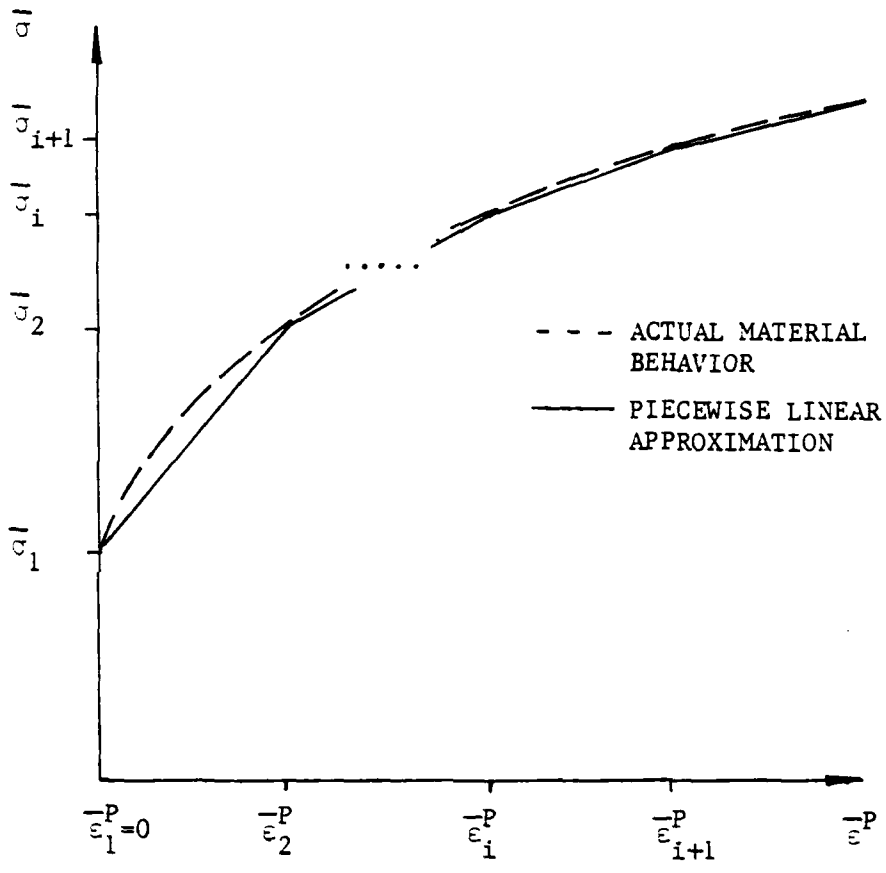

Fig. 3. Piecewise Linearization of the Equivalent Uniaxial Stress Versus Equivalent Uniaxial Plastic Strain Diagram

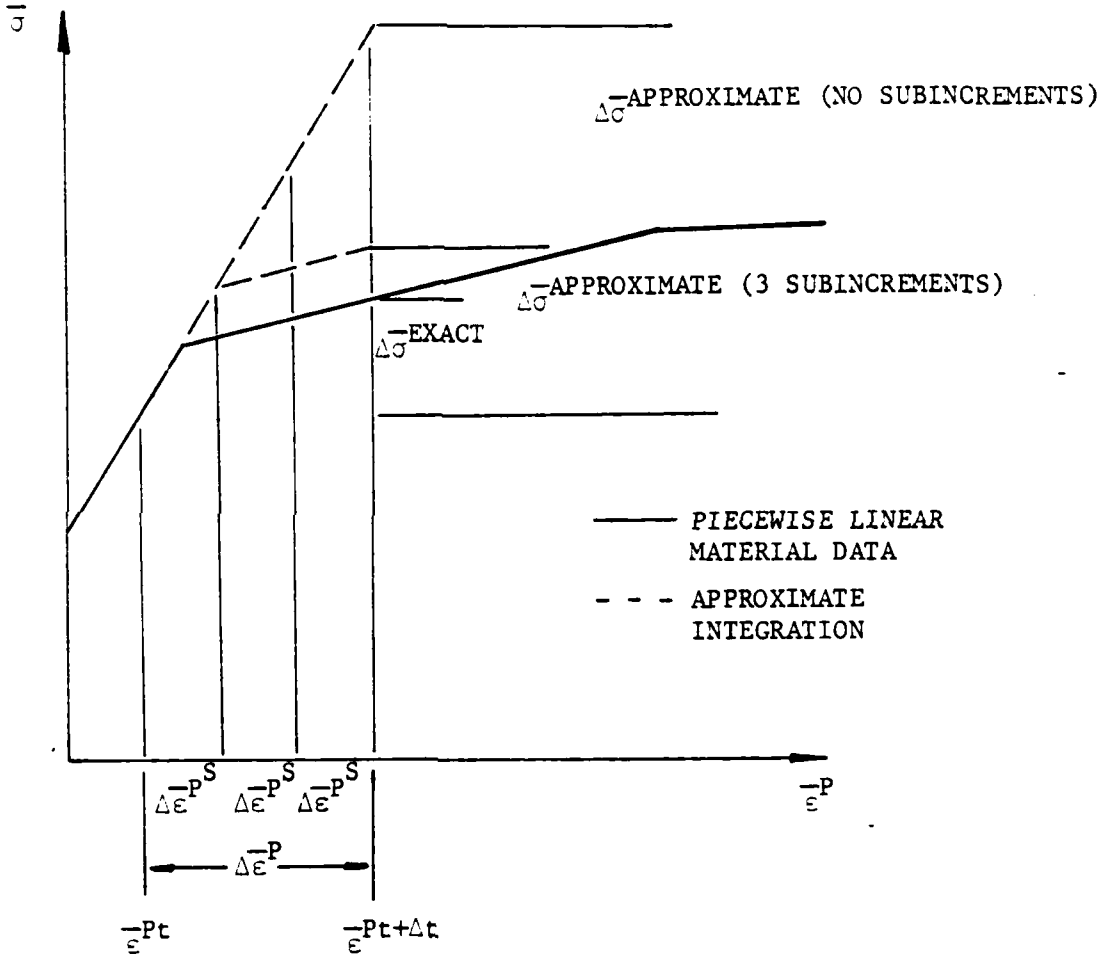

Fig. 4. Estimated Equivalent Uniaxial Stress Increment Using Subincrementation

plastic strain increment can be determined only after the stress increment tensor has been found.

REVIEW OF THE SUBINCREMENTATION METHOD

In order to improve the accuracy of approximation (13) subincrementation has been proposed [1,2]. In this method Stricklin, et al. define the equivalent uniaxial strain increment

$$d\bar{\varepsilon} = \sqrt{\frac{2}{3} d\varepsilon_{ij} d\varepsilon_{ij}} \quad . \tag{16}$$

This quantity is evaluated over a specified load step and is then compared to an input parameter called the allowable total strain increment ($d\bar{\varepsilon}_{AL}$) as follows

$$M = \frac{d\bar{\varepsilon}}{d\bar{\varepsilon}_{AL}} \quad , \tag{17}$$

where M is rounded off to the nearest integer greater than zero. Equations (6) are then evaluated M times for the strain subincrement

$$\Delta\varepsilon^{S}_{ij} \equiv \frac{\Delta\varepsilon_{ij}}{M} \quad , \tag{18}$$

and on each subincrement the effective modulus tensor is updated to reflect the current equivalent uniaxial plastic strain. Based on numerical evidence, Stricklin suggests that $d\bar{\varepsilon}_{AL}$ should be no greater than 0.0005 in./in., although our experience indicates that values as small as .00005 in./in. are sometimes required to maintain accuracy of solution.

In order to illustrate the effect of subincrementation let us examine a single example. Suppose we consider a bar subjected to a gradually increasing homogeneous uniaxial stress state. Because conditions

(1) and (3) are satisfied trivially we need only consider approximate constitutive equations (13). Since the input material properties will be described via a piecewise linear equivalent uniaxial stress versus equivalent uniaxial plastic strain diagram as shown in Fig. 3, and because this boundary value problem is equivalent to the experiment which produced the material input data, an exact analysis using equations (13) should reproduce Fig. 3 precisely. In fact, using subincrementation will yield the results shown in Fig. 4 when a single slope discontinuity is encountered in a given load step. It can be seen from the figure that the total error is incurred during the plastic strain subincrement subtending the slope discontinuity. The effect then of subincrementation is simply to improve the approximate integration of equations (6).

A PROPOSED MODIFICATION

It is apparent from the above discussion that subincrementation will often require multiple evaluations of equations (13) for each integration point. Since these equations must be evaluated at each integration point in the body and often several times for each load step in order to obtain equilibrium convergence, considerable computational time can be spent in this process. Detailed herein is a numerical procedure for integrating equations (7) which is both more accurate and more computationally efficient than subincrementation. We call this method the zeta method.

The method proposed here is a simple extension of a procedure utilized by Krieg and Duffey [18] for the transition step from elastic to elastic-plastic material behavior. The primary extension is that each

subsequent slope discontinuity in the piecewise linear equivalent uni-stress versus equivalent uniaxial plastic strain diagram is treated exactly like a subsequent yield surface. Since equations (13) are exact under conditions (14) and (15), no subincrementation will be required to obtain precise results between slope discontinuities.

In order to see how the zeta method works, consider a material point which is in a post-yielded state at time t and with equivalent uniaxial plast strain $\bar{\varepsilon}^{P}(t)$, as shown in Fig. 5.

According to Krieg and Duffey [18], the value of the stress tensor at the material point necessary to bring the equivalent uniaxial stress state to the i+1th slope discontinuity is defined by

$$\sigma_{ij}^{i+1} \equiv \sigma_{ij}{}^{t} + \zeta\, \hat{\Delta\sigma} \tag{19}$$

where $\hat{\Delta\sigma}_{ij}$ is the increment predicted by equations (13) using the input total strain increment $\Delta\varepsilon_{ij}$ and ζ is a scalar factor to be determined.

In order to determine zeta definitions (19) are substituted into the yield criterion used in the model. For example, if von Mises' yield criterion is utilized, equations (19) will result in

$$\frac{3}{2}\left[\sigma_{ij}{}^{t} + \zeta\hat{\Delta\sigma}_{ij} - \frac{(\sigma_{KK}+\zeta\hat{\Delta\sigma}_{KK})}{3}\,\delta_{ij}\right]\left[\sigma_{ij}{}^{t} + \zeta\hat{\Delta\sigma}_{ij} - \frac{(\sigma_{KK}+\zeta\hat{\Delta\sigma}_{KK})}{3}\,\delta_{ij}\right] = (\bar{\sigma}_{i+1})^{2}. \tag{20}$$

Solving the above equation for zeta will result in

$$\zeta = \frac{-B + \sqrt{(B^2 - 4AC)}}{2A}\ , \tag{21}$$

where

$$A = \hat{\Delta\sigma}_{ij}\hat{\Delta\sigma}_{ij}\ , \tag{22}$$

$$B = 2\sigma_{ij}\hat{\Delta\sigma}_{ij}\ , \tag{23}$$

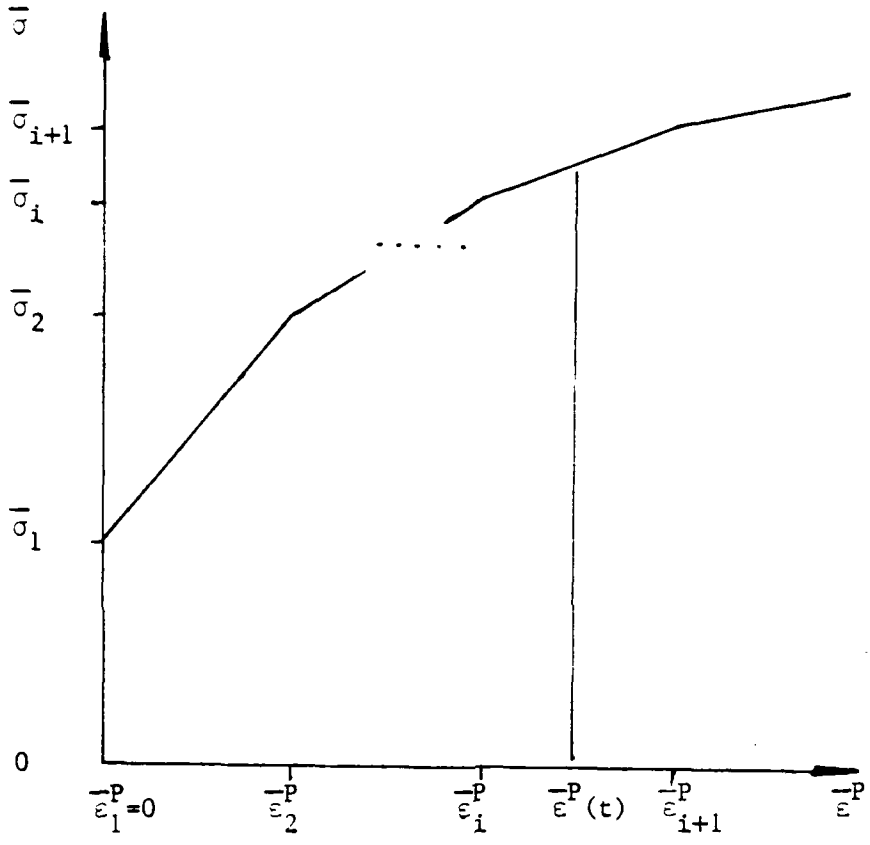

Fig. 5. Post-Yielded State for a Typical Material Point at Time t

and

$$C = \sigma_{ij}\sigma_{ij} - (\bar{\sigma}_{i+1})^2 \quad . \tag{24}$$

Utilizing equations (21) through (24) the value of zeta may be obtained. If zeta is greater than or equal to unity, the input total strain increment will not take the equivalent uniaxial stress beyond the next slope discontinuity and the results of equations (13) may be considered correct. In other words

$$\zeta \geq 1 \Rightarrow \Delta\sigma_{ij} = \hat{\Delta\sigma}_{ij} \quad . \tag{25}$$

If, on the other hand, zeta is less than unity, the predicted stress increment tensor is incorrect and equations (13) must be modified. This is accomplished by first constructing the input strain increment necessary to bring the equivalent uniaxial stress to the slope discontinuity:

$$\Delta\varepsilon_{ij}^{i+1} = \zeta\ \Delta\varepsilon_{ij} \quad , \tag{26}$$

where $\Delta\varepsilon_{ij}$ is the input strain increment. The values of $\Delta\varepsilon_{ij}^{i+1}$ are then substituted into equations (13) to produce

$$\Delta\sigma_{ij}^{i+1} = C_{ijkl}(\bar{\varepsilon}^P(t))\Delta\varepsilon_{ij}^{i+1} \quad , \tag{27}$$

the remaining portion of the stress increment tensor is calculated by first determining the remainder of the input strain increment

$$\Delta\varepsilon_{ij}^{R} \equiv (1 - \zeta)\Delta\varepsilon_{ij} \quad , \tag{28}$$

noting from definitions (26) and (28) that

$$\Delta\varepsilon_{ij} = \Delta\varepsilon_{ij}^{i+1} + \Delta\varepsilon_{ij}^{R} \quad . \tag{29}$$

The remainder of the strain increment tensor $\Delta\varepsilon_{ij}^{R}$ is then substituted into equations (13) to give the remainder of the stress increment tensor

$$\Delta\sigma^{R}_{ij} = C_{ijkl}(\bar{\varepsilon}^{P}_{i+1})\Delta\varepsilon^{R}_{ij} \quad . \tag{30}$$

Thus, the total stress increment tensor is given by

$$\Delta\sigma_{ij} = \Delta\sigma^{i+1}_{ij} + \Delta\sigma^{R}_{ij} \quad . \tag{31}$$

It is easily verified that the above procedure will result in an equivalent uniaxial stress and equivalent uniaxial plastic strain [utilizing definitions (2) and (3)] which lie on the equivalent uniaxial stress versus equivalent uniaxial plastic strain diagram. It should also be pointed out that although the actual yield surface is updated throughout plastic loading, the equivalent uniaxial stresses corresponding to slope discontinuities should at no time be altered.

Although the above procedure has been discussed here only in the context of isotropic hardening, it is also applicable to more complex yield criteria and work hardening rules [19,20].

COMPUTER CODE FLOWCHART

The following chart outlines in abbreviated form the application of the δ method for a given increment in the total strain tensor $\Delta\varepsilon_{ij}$ and equivalent uniaxial plastic strain at the start of the step $\bar{\varepsilon}^{P}(t)$.

a) Set $\Delta\sigma_{ij} = 0$.

b) Evaluate $C_{ijkl}(\bar{\varepsilon}^{P}(t))$.

c) Obtain $\Delta\hat{\sigma}_{ij}$ using equations (13).

d) Determine $\bar{\sigma}_{i+1}$ from Fig. 5.

e) Calculate A, B, and C using equations (22) through (24).

f) Determine zeta using equation (21).

g) If $\zeta \geq 1$ go to step q).

h) If $\zeta < 1$ evaluate $\Delta\varepsilon_{ij}^{i+1}$ using equations (26).

i) Determine $\Delta\sigma_{ij}^{i+1}$ using equations (27).

j) Set $\Delta\sigma_{ij} = \Delta\sigma_{ij} + \Delta\sigma_{ij}^{i+1}$.

k) Calculate $\Delta\varepsilon_{ij}^{R}$ using equations (28).

l) Set $\Delta\varepsilon_{ij} = \Delta\varepsilon_{ij}^{R}$.

m) Calculate $\Delta\varepsilon_{ij}^{P}$ using equations (3).

n) Determine $\Delta\bar{\varepsilon}^{P}$ using equation (2).

o) Set $\bar{\varepsilon}^{P}(t) = \bar{\varepsilon}^{P}(t) + \Delta\bar{\varepsilon}^{P}$.

p) Go to step b).

l) Set $\Delta\sigma_{ij} = \Delta\sigma_{ij} + \Delta\hat{\sigma}_{ij}$.

DISCUSSION OF RESULTS

In this section the results generated using the zeta method as well as the subincrementation method for solving the constitutive equations of classical plasticity are presented. Both solution techniques have been incorporated into a finite element computer program which uses constant strain triangular elements. The formulations have been cast into a 2-dimensional plane stress format.

In order to compare the efficiency of the two different methods their respective solution times will be compared. This was accomplished by using the built in timer (clock) subroutine used in the Fortran-H Extended language available on the AMDAHL 470 V6 located on the Texas A&M University campus. Two times will be given in the analysis: 1) time spent using the constitutive package, and 2) total time spent in solving the specified boundary value problem.

Two boundary value problems have been selected for comparing the two constitutive packages: a highly yielded uniaxial bar subjected

to uniaxial tension only and a thick walled pressure vessel subjected to internal pressure sufficient to yield a broad band of the vessel. Both specimens are assumed to be made of 5086-H34 aluminum with piecewise linearized room temperature properties shown in Figure 6. The finite element mesh used for the uniaxial bar as well as the load input diagram are shown in Figure 7. Only two elements are necessary to represent the bar because the boundary value problem is homogeneous. However, if the problem was inhomogeneous then mesh refinement would be necessary to increase the accuracy of the solution. It should nevertheless be pointed out here that the number of elements used in the mesh is directly proportional to the computational time required in the constitutive package. Another factor influencing the computation time is the non-linearity of the given stress strain curve. Increasing the number of piecewise linearities in the idealized uniaxial stress strain curve will increase the computational time required by the zeta method. Although this increase in piecewise linearizations will not greatly affect the computational time required by the subincrementation, it will have an adverse affect on the accuracy of this method.

The results of the uniaxial bar test are shown in Fig. 8 and the comparative solution times are given in Tables 1 and 2. Fig. 8 shows the output axial displacement versus time for the zeta method as well as the subincrementation with various allowable errors in equivalent uniaxial strain shown in parentheses. Table 1 shows a comparison of solution times for each load step, while Table 2 gives a more detailed comparison of solution times for the final time step. Several different cases were run using the subincrementation code in order to

FIGURE 6:

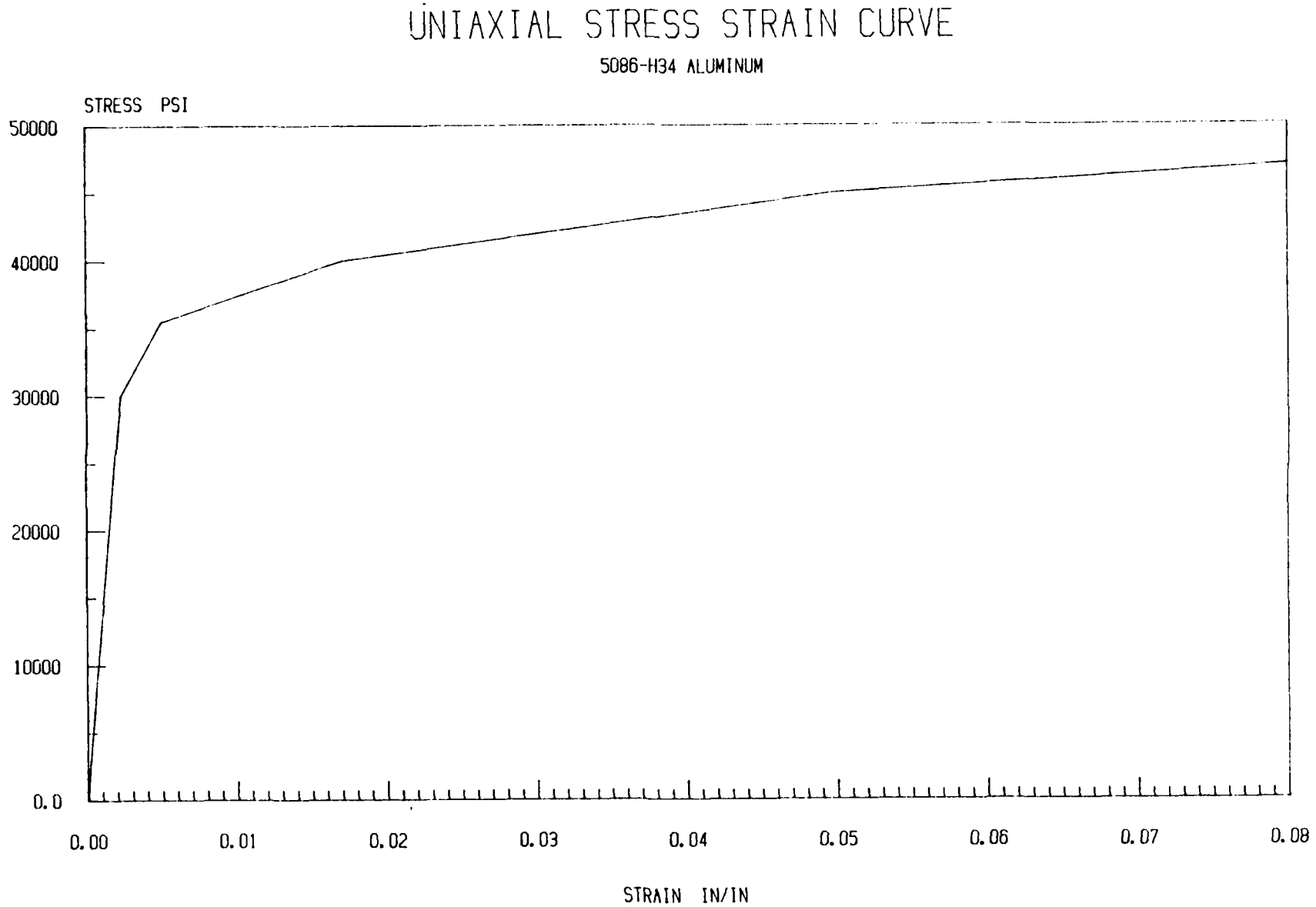

Figure 6 ,

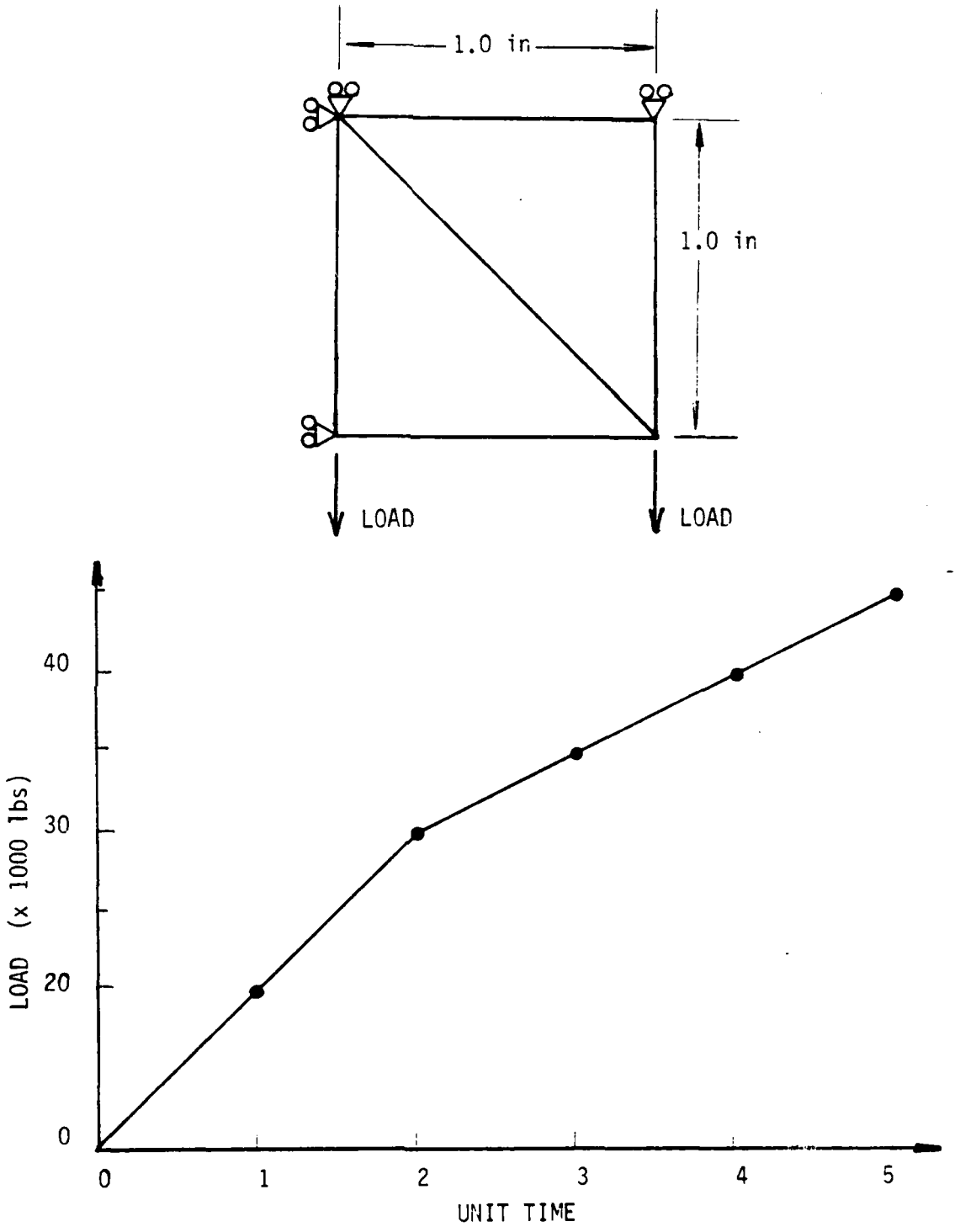

Figure 7. Uniaxial Bar Finite Element Mesh
And Input Load Diagram

FIGURE 8:

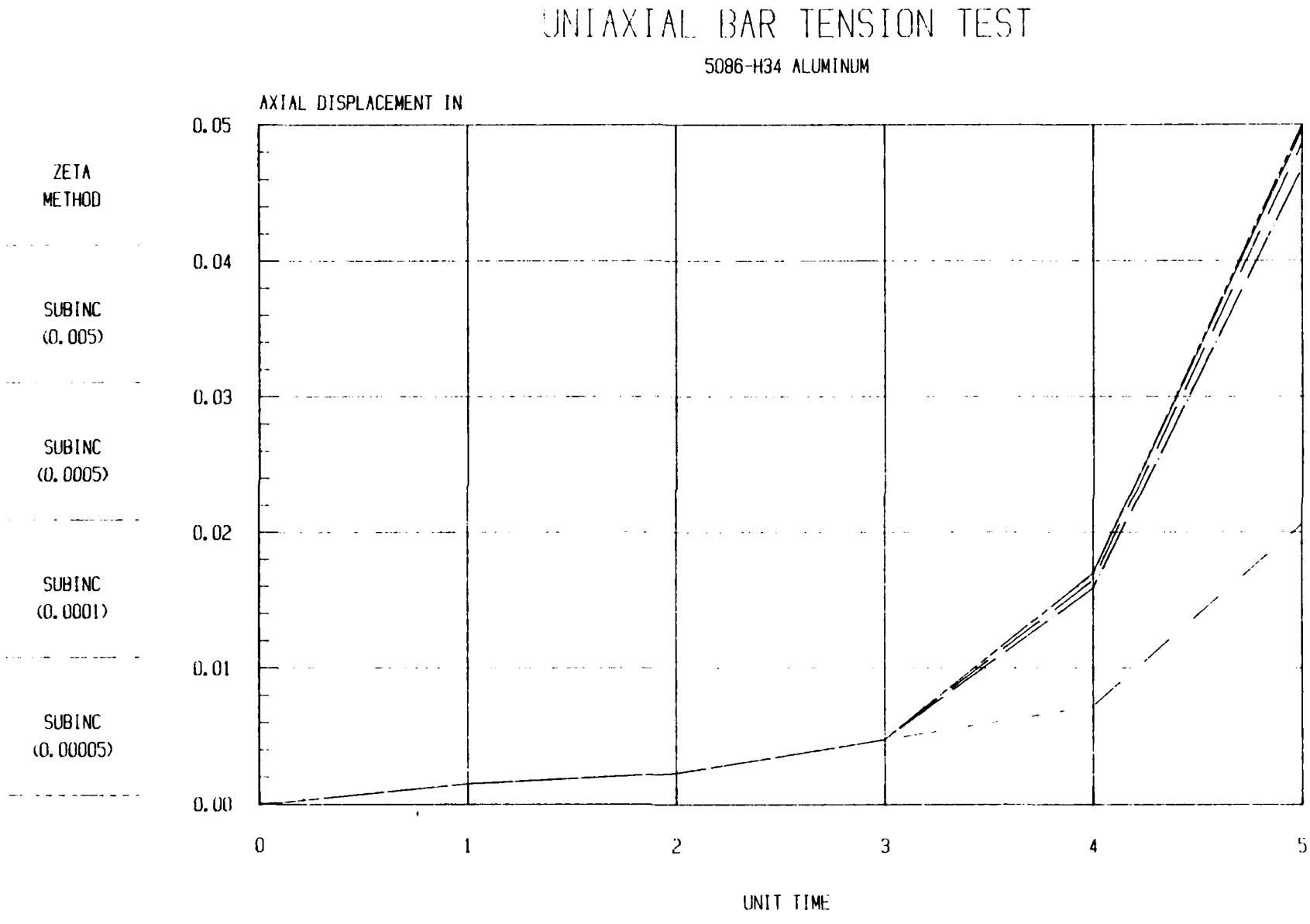
UNIAXIAL BAR TENSION TEST
5086-H34 ALUMINUM
AXIAL DISPLACEMENT IN
0.05
0.04
0.03
0.02
0.01
0.00
0
1
2
3
4
5
UNIT TIME
ZETA
METHOD
SUBINC
(0.005)
SUBINC
(0.0005)
SUBINC
(0.0001)
SUBINC
(0.00005)

TABLE 1: AXIAL DISPLACEMENT AND SOLUTION TIMES FOR THE UNIAXIAL BAR TEST

TIME	UNIAXIAL DISPLACEMENT					
	ZETA METHOD	SUBINC (0.005)	SUBINC (0.0005)	SUBINC (0.0001)	SUBINC (0.00005)	EXACT
1	0.0015384	0.0015384	0.0015384	0.0015384	0.0015384	0.0015384
2	0.0023077	0.0023077	0.0023077	0.0023077	0.0023077	0.0023
3	0.0047622	0.0047622	0.0047622	0.0047622	0.0047622	0.004754
4	0.0169661	0.0072167	0.0158503	0.0164200	0.0169230	0.017
5	0.0495370	0.02055	0.0466766	0.04850	0.498620	0.05
CONSTITUTIVE PACKAGE TIME (SEC)	0.0778959	0.006916	0.0582919	0.23093	0.4129838	
SUBINC/0.0778959		.088	.748	2.964	5.302	
TOTAL TIME (SEC)	0.15405	0.045	0.132184	0.35076	0.488462	
SUBINC/0.15405		.292	.858	2.277	3.171	

TABLE 2:

COMPARISON OF SOLUTION TIMES FOR

THE LAST LOAD STEP ON THE

UNIAXIAL BAR

	SOLUTION TIMES (sec)				
TIME	ZETA METHOD	SUBINC (0.005)	SUBINC (0.0005)	SUBINC (0.0001)	SUBINC (0.00005)
CONSTITUTIVE	0.063492	0.0027	0.0555	0.18764	0.37684
SUBINC/.063492		.043	.716	2.955	5.935
TOTAL TIME (SEC)	0.0968	0.00798	0.07761	0.22315	0.40994
SUBINC/.0968		.0824	.802	2.305	4.235

illustrate the difference in solutions and comparative times for different values of the allowable uniaxial stress increment $d\bar{\varepsilon}_{AL}$ used in determining the number of subincrements. In general, increasing the required accuracy of the subincrementation method also increases the computational time.

The results of this test show that in order to obtain solution accuracy by subincrementation which is comparable to the zeta method, the allowable strain increment must be of the order of 0.00005 in/in. In fact, the larger the allowable strain increment the less solution time required, and in fact for $d\bar{\varepsilon}_{AL}$ = 0.005 and 0.0005 the solution time was less for the subincrementation method. However, the resulting accuracy was very poor. Table 1 indicates that subincrementation ($\bar{\varepsilon}_{AL}$ = 0.00005 in./in.) requires 3.171 times as much computer time as the zeta method for the uniaxial bar problem. Although this is a rather large difference in relative times, since only a two element problem has been run, the difference in actual cost is small. However, on an extremely large scale problem obvious savings would result.

The finite element mesh used for the thickwall pressure vessel is shown in Fig. 9 and the load input diagram is shown in Fig. 10. The results of this test are shown in Fig. 11 as well as Tables 3 and 4. These results are for the final pressure of P = 30,000 PSI. It should be noted that if one applies increasing pressure to the specimen then more of the elements will yield in the outer regions of the thickwalled pressure vessel, resulting in a higher solution time because more time is spent in the constitutive package and more time in iterating on the correct nonlinear solution.

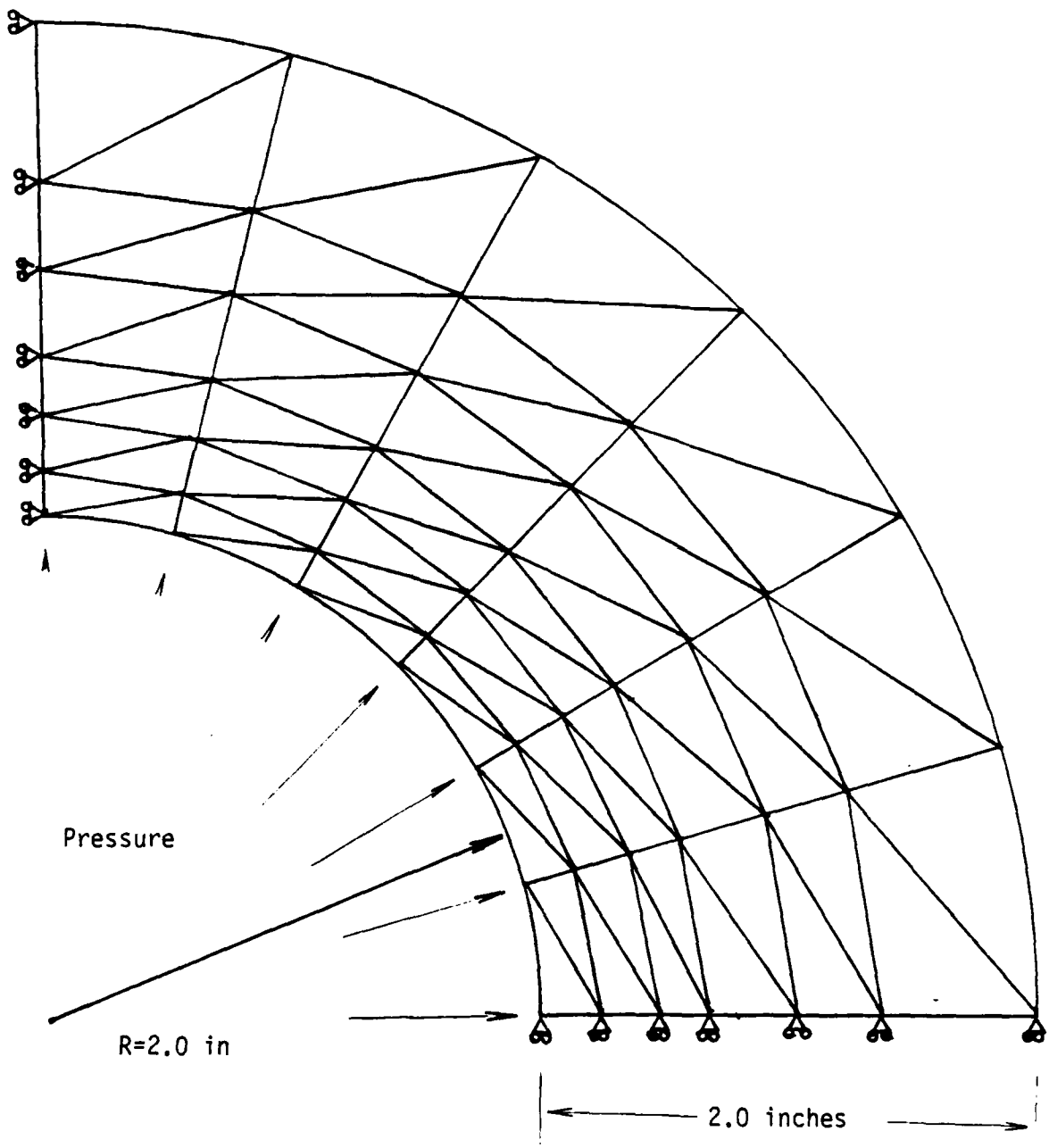

Fig. 9. Finite Element Mesh For
Thick Walled Pressure Vessel

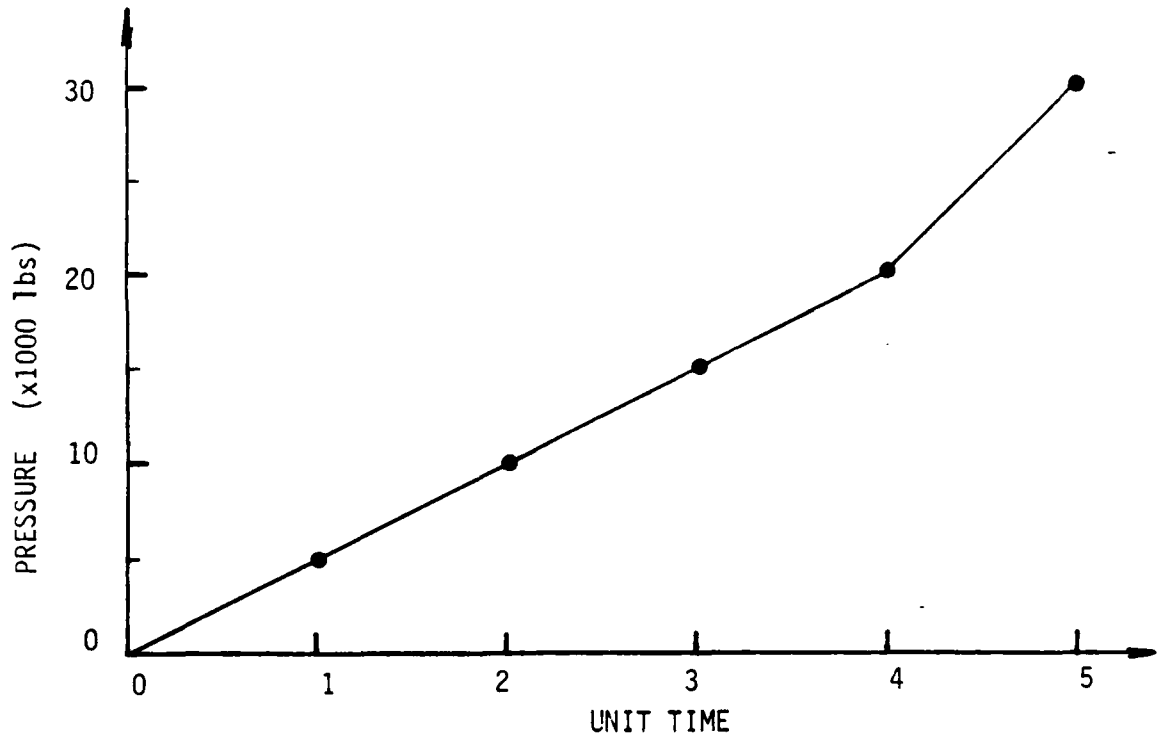

Fig. 10. Thick Walled Pressure Vessel
Input Diagram

Figure 11.

THICK WALLED PRESSURE VESSEL

5086-H34 ALUMINUM P=30000 PSI

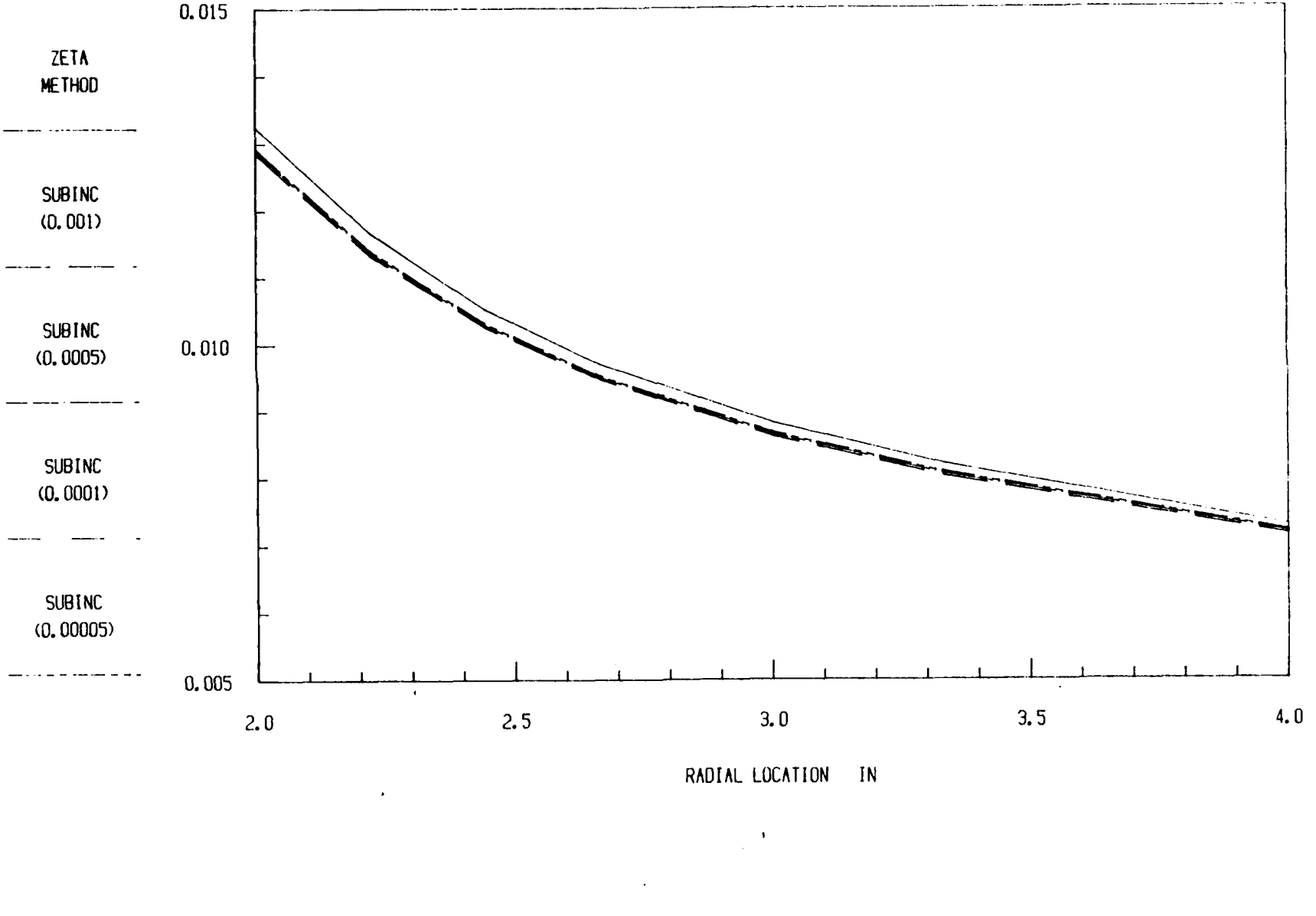

TABLE 3: RADIAL DISPLACEMENTS AND SOLUTION TIMES FOR THICK WALLED PRESSURE VESSEL

RADIAL LOCATION	RADIAL DISPLACEMENT (IN)				
	ZETA METHOD	SUBINC (0.001)	SUBINC (0.0005)	SUBINC (0.0001)	SUBINC (0.00005)
2.0	0.01324344	0.01285087	0.01289475	0.01292329	0.0129211
2.2222	0.01167517	0.01133769	0.01137959	0.01141027	0.01140665
2.4444	0.0105329	0.01026293	0.01029393	0.01032073	0.01031638
2.6666	0.00971329	0.00947785	0.00960516	0.00953320	0.00952741
3.0	0.00883162	0.00862648	0.00866162	0.00868949	0.00868414
3.3333	0.00821108	0.00802864	0.00806262	0.00809172	0.00808688
4.0	0.00728626	0.00714737	0.00717933	0.00720508	0.00720022
CONSTITUTIVE PACKAGE TIME (SEC)	0.691703	0.6132077	0.6854118	1.056744	1.503111
SUBINC/.691703		.886	.991	1.527	2.173
TOTAL TIME (SEC)	3.1546827	3.0397627	3.1661748	3.61964	4.0580
SUBINC/3.1546827		.964	1.003	1.147	1.286

TABLE 4:

COMPARISON OF SOLUTION TIMES FOR

THE LAST LOAD STEP ON THE

THICK WALLED PRESSURE VESSEL

TIMES	SOLUTION TIMES (sec) ZETA METHOD	SUBINC (0.001)	SUBINC (0.0005)	SUBINC (0.0001)	SUBINC (0.00005)
CONSTITUTIVE PACKAGE TIME (SEC)	0.476943	0.398788	0.468156	0.838656	1.278211
SUBINC/.476943		.830	.982	1.758	2.680
TOTAL TIME (SEC)	1.662752	1.565564	1.665976	2.143309	2.579693
SUBINC/1.662752		.941	1.002	1.289	1.551

The results of the test are basically the same as those for the uniaxial bar. From Table 3 it can be seen that for comparable solution accuracy the subincrementation method takes 1.527 to 2.173 times more constitutive time (depending on $\bar{\varepsilon}^{P}_{AL}$) than the zeta method and 1.147 to 1.286 times greater total time. Closer examination shows that even for the smallest $\bar{\varepsilon}^{P}_{AL} = 0.00005$ the solutions still differ from the zeta method and that there is no noticeable difference between solutions for $d\bar{\varepsilon}^{P}_{AL} = 0.0001$ and $d\bar{\varepsilon}^{P}_{AL} = 0.00005$. In fact, the results tend to be less accurate for $d\bar{\varepsilon}^{P}_{AL} = 0.00005$. This can be attributed to numerical roundoff error because the increments in the strain are so small that further improved accuracy is not possible. By constrast, there is no numerical roundoff error apparent in the zeta method.

CONCLUSION

The objective of this research has been to produce an alternative to subincrementation which results in a substantial improvement in computational efficiency. This new method has been shown by example to give not only improved efficiency, but also slightly greater accuracy of results. The following general conclusions can be made:

1) in order to produce results by the subincrementation method which are comparable in accuracy to the zeta method, significantly greater computation time is required by the former method;
2) increasing required accuracy in the allowable equivalent uniaxial strain increment ($\Delta\bar{\varepsilon}_{AL}$) can lead to roundoff error when subincrementation is utilized;

3) subincrementation necessarily produces errors in predicted stresses whenever a slope discontinuity is subtended in the uniaxial stress-strain curve,

4) the zeta method follows the uniaxial stress-strain curve exactly;

5) both subincrementation and the zeta method approximate the load path to be radial during each load increment,

6) piecewise linearization, although merely a numerical convenience in subincrementation, is necessary in order to utilize the zeta method;

7) the zeta method can be used with cyclic hardening models of plasticity, and

8) the zeta method may not be appropriate for use in rate dependent viscoplastic media.

ACKNOWLEDGEMENT

This research was supported by the Air Force Office of Scientific Research under contract no. F49620-83-C-0067.

REFERENCES

1. Yamada, Y., Yoshimura, N., and Sakurai, T., "Plastic Stress-Strain Matrix and Its Application for the Solution of Elastic-Plastic Problems by the Finite Element Method," Intl. J. Materials Science, Vol. 10, No. 5, pp. 343-354, 1968.

2. Stricklin, J.A., Haisler, W.E., and Von Riesemann, W.A., "Computation and Solution Procedures for Nonlinear Analysis by Combined Finite Element-Finite Difference Methods," Computers & Structures, Vol. 2, Nos. 5/6, pp. 955-974, 1972.

3. Bushnell, D., "Large Deflection Elastic-Plastic Creep Analysis of Axisymmetric Shells," Numerical Solution of Nonlinear Structural Problems, R.F. Hartung, Ed., AMD, Vol. 6, ASME, New York, pp. 103-138, 1973.

4. Coleman, B.D., and Noll, W., "The Thermodynamics of Elastic Materials with Heat Conduction and Viscosity," Archive for Rational Mechanics and Analysis, Vol. 13, p. 167, 1963.

5. Lubliner, J., "On Fading Memory in Materials of Evolutionary Type," Acta Mechanica, Vol. 8, pp. 75-81, 1969.

6. Fung, Y.C., Foundations of Solid Mechanics, Prentice-Hall, Englewood Cliffs, N.J., 1965.

7. Noll, W. and Truesdell, C.A., "The Non-linear Field Theories of Mechanics," Vol. 3, part 3, Encyclopedia of Physics, Springer, 1964.

8. Prandtl, L., Proc. Intern. Cong. Applied Mechanics, Delft, 1924.

9. Reuss, A., Z. Angew. Math. Mechanik., Vol. 10, p. 266, 1930.

10. Green, A.E. and Naghdi, P.M., "A General Theory of an Elastic-Plastic Continuum," Arch. Rational Mech. Anal., Vol. 18, pp. 251-281, 1965.

11. Schapery, R.A., "On a Thermodynamic Constitutive Theory and its Application to Various Nonlinear Materials," Proceedings IUTAM Symposium, Springer-Verlag, pp. 259-285, 1968.

12. Kratochvil, J. and Dillon, O.W., Jr., "Thermodynamics of Elastic-Plastic Materials as a Theory with Internal State Variables," Journal of Applied Physics, Vol. 40, No. 8, pp. 3207-3218, 1969.

13. Cook, R.D., Concepts and Applications of Finite Element Analysis, 2nd Edition, John Wiley & Sons, New York, 1981.

14. Owen, D.R.J. and Hinton, E., Finite Elements in Plasticity: Theory and Practice, Pineridge, Swansea, U.K., 1980.

AD-A162 140 A MODEL FOR PREDICTING THERMOMECHANICAL RESPONSE OF LARGE SPACE STRUCTURE (U) TEXAS A AND M UNIV COLLEGE STATION MECHANICS AND MATERIALS RE D H ALLEN ET AL 2/3

UNCLASSIFIED JUN 84 MM-4875-84-16 AFOSR-TR-85-1080 F/G 11/4 NL

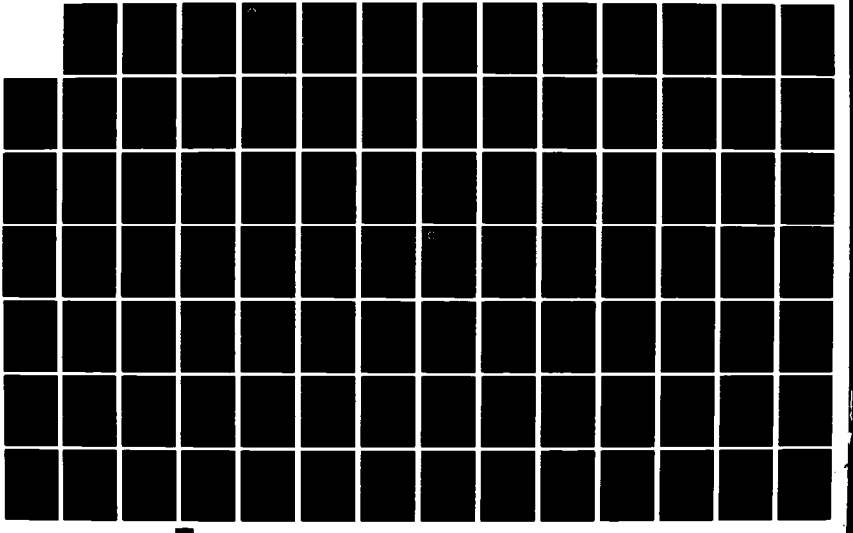

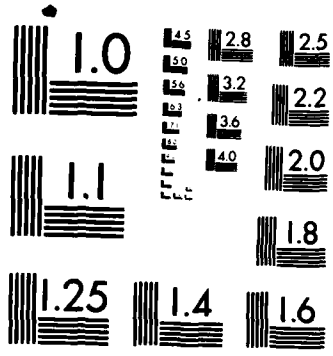

15. Hill, R., The Mathematical Theory of Plasticity, Oxford, London, 1956.

16. Hunsaker, B., Jr., "An Evaluation of Four Hardening Rules of the Incremental Theory of Plasticity," thesis, Texas A&M University, 1973.

17. Haisler, W.E., "AGGIE I, A Finite Element Program for Nonlinear Structural Analysis," Office of Naval Research, No. 3275-77-1, 1977.

18. Krieg, R.D. and Duffey, T.A., "Univalve II: A Code to Calculate the Large Deflection Dynamic Response of Beams, Rings, and Plates, and Cylinders," Sandia Laboratories, No. SC-RR-68-303, Albuquerque, New Mexico, October, 1968.

19. Hunsaker, B., Jr., Vaughan, D.K. and Stricklin, J.A., "A Comparison of the Capability of Four Hardening Rules to Predict a Materials Plastic Behavior," Journal of Pressure Vessel Technology, Vol. , pp. 66-74, 1976.

20. Haisler, W.E., "Numerical and Experimental Comparison of Plastic Work-Hardening Rules," Transactions 4th Intl. Conf. on Structural Mechanics in Reactor Technology, Vol. L, No. 4/7, 1977.

Appendix 6.3

Mechanics and Materials Center
TEXAS A&M UNIVERSITY
College Station, Texas

LARGE SPACE STRUCTURES TECHNOLOGY: A LITERATURE SURVEY

M. A. ZOCHER
S. KALYANASUNDARAM
E. W. NOTTORF
D. H. ALLEN
AND
W. E. HAISLER

MM 4875-84-13

JUNE 1984

SECURITY CLASSIFICATION OF THIS PAGE

REPORT DOCUMENTATION PAGE

1a REPORT SECURITY CLASSIFICATION Unclassified	1b. RESTRICTIVE MARKINGS
2a. SECURITY CLASSIFICATION AUTHORITY	3. DISTRIBUTION/AVAILABILITY OF REPORT Unlimited
2b. DECLASSIFICATION/DOWNGRADING SCHEDULE	
4. PERFORMING ORGANIZATION REPORT NUMBER(S) MM 4875-83-10	5. MONITORING ORGANIZATION REPORT NUMBER(S)
6a. NAME OF PERFORMING ORGANIZATION Aerospace Engineering Dept. / 6b. OFFICE SYMBOL (If applicable)	7a. NAME OF MONITORING ORGANIZATION Air Force Office of Scientific Research
6c. ADDRESS (City, State and ZIP Code) Texas A&M University College Station, Texas 77843	7b. ADDRESS (City, State and ZIP Code) Bolling AFB Washington, D. C. 20332
8a. NAME OF FUNDING/SPONSORING ORGANIZATION / 8b. OFFICE SYMBOL (If applicable)	9. PROCUREMENT INSTRUMENT IDENTIFICATION NUMBER F 49620-83-C-0067
8c. ADDRESS (City, State and ZIP Code)	10. SOURCE OF FUNDING NOS. PROGRAM ELEMENT NO. / PROJECT NO. / TASK NO. / WORK UNIT NO.
11. TITLE (Include Security Classification) Large Space Structure Technology: A Literary Survey	
12. PERSONAL AUTHOR(S) M. A. Zocher, S. Kalyanasundaram, E. W. Nottorf, D. H. Allen, W. E. Haisler	
13a. TYPE OF REPORT Interim / 13b. TIME COVERED FROM Mar 83 TO Apr 84	14. DATE OF REPORT (Yr., Mo., Day) June 84 / 15. PAGE COUNT 41
16. SUPPLEMENTARY NOTATION	
17. COSATI CODES FIELD / GROUP / SUB. GR.	18. SUBJECT TERMS (Continue on reverse if necessary and identify by block number)

19. ABSTRACT (Continue on reverse if necessary and identify by block number)

In recent years research on the subject of Large Space Structures (LSS) has dramatically increased. This research is of an extremely broad nature, extending from materials characterization to dynamic response as well as active control. This paper is intended to be a review of recent and important advances in this field of research. The subject matter is divided into six major headings: 1) expected applications of LSS; 2) the environment; 3) materials; 4) solution techniques for LSS; 5)damping technology; and 6) preliminary design/analysis/experimental investigation.

20 DISTRIBUTION/AVAILABILITY OF ABSTRACT UNCLASSIFIED/UNLIMITED [X] SAME AS RPT [ ] DTIC USERS [ ]	21 ABSTRACT SECURITY CLASSIFICATION
22a NAME OF RESPONSIBLE INDIVIDUAL Dr. Tony Amos	22b TELEPHONE NUMBER (Include Area Code) (202)767-4937 / 22c OFFICE SYMBOL

DD FORM 1473, 83 APR EDITION OF 1 JAN 73 IS OBSOLETE.

SECURITY CLASSIFICATION OF THIS PAGE

LARGE SPACE STRUCTURES TECHNOLOGY:

A LITERATURE SURVEY

by

M. A. Zocher

S. Kalyanasundaram

E. W. Nottorf

D. H. Allen

W. E. Haisler

Aerospace Engineering Department
Texas A&M University
College Station, Texas 77843

June, 1984

ABSTRACT

In recent years research on the subject of large space structures (LSS) has dramatically increased. This research is of an extremely broad nature, extending from materials characterization to dynamic response as well as active control. This paper is intended to be a review of recent and important advances in this field of research. The subject matter is divided into six major headings: 1) expected applications of LSS; 2) the environment; 3) materials; 4) solution techniques for LSS; 5) damping technology; and 6) preliminary design/analysis/experimental investigation.

OUTLINE

I. Expected Applications of LSS

II. The Environment

III. Materials

- A. Composites
  1. Temperature
  2. Moisture
  3. Radiation
  4. Microcracking
- B. Material Selection
- C. Metals
  1. Viscoplasticity
  2. Temperature
- D. Damage Models
  1. Fracture
  2. Metals
  3. Self-consistent scheme
  4. Damage Surfaces
  5. Equal-rank Assumption
  6. Internal State Variables
  7. Fracture Mechanics/Viscoelasticity

IV. Solution Techniques For LSS

- A. Surveys
- B. Finite Element Method
- C. Continuum Lattice Modeling
- D. Discrete Field Method
- E. Periodic Structure Approach

V. Damping Technology

- A. Constrained-Layer Damping
- B. Damping Materials and Systems
- C. Experimental Investigations
- D. Damping Design
- E. Active Control
- F. Miscellaneous

VI. Preliminary Design/Analysis/Experimental Investigation

A. Guidelines/Standards

B. Automated Fabrication

C. Deployable

D. Erectable

1. Erectable From Deployable Modules
2. Tetrahedral Truss, Octahedral Truss
3. Nonperiodic Truss
4. Truss Elements
5. Solar Power Satellite

E. Accuracy Potential

F. Miscellaneous

LIST OF ABBREVIATIONS

CAD	Computer Aided Design
CTE	Coefficient of Thermal Expansion
FY	Fiscal Year
G/E	Graphite/Epoxy
GEO	Geosynchronous Earth Orbit
JSC	Johnson Space Center
LaRC	Langley Research Center
LEO	Low Earth Orbit
LMSCO	Lockheed Missiles and Space Company
LSS	Large Space Structure(s)
LSST	Large Space Systems Technology
MPTS	Microwave Power Transmission System
NASA	National Aeronautics and Space Administration
PDE	Partial Differential Equation
SCAFE	Space Construction Automated Fabrication Experiment
SCATHA	Spacecraft Charging At High Altitudes
SPS	Solar Power Satellite
STS	Space Transportation System

I. Expected Applications of LSS

With the STS operational, the opportunity exists to exploit space through a myriad of enterprises that will be economically beneficial to mankind. Studies conducted to date point out many projects which will require the construction of very large structures in space. Possible applications of LSS include solar energy collection and transmission, communications, navigation, resources and environmental survey, border and coastal-water survery, area illumination, manufacturing, radio astronomy, and various scientific opportunities that a space station will provide.

Hedgepeth [1] conducted a survey of future requirements for large space structures in 1976. In it he states that the applications for LSS can be grouped into three categories: (1) large surfaces for power, (2) large antenna to receive and transmit energy over the rf loadwidth, and (3) space platforms to provide area for general utlizations. An example of an application-type paper Woodcock [2] would fall into Hedgepeth's first category. Folder and Dienemann [3], and Wannlund [4] project the need for large antennas. Holloway and Garrett [5], and Stone [6] examine the utilization of space platforms. Hagler [7] addresses the feasibility of two possible applications: (1) a 200m radio astronomy telescope, and (2) a 5000 MW sps.

Cord, Kruszewski, and Gustaferro [8], and Daros, Freitog, and Kline [9] project probable chronologies of development of LSS.

Hedgepeth, Mikulas, and Macneal [10] concern the economic feasibility of building large structures in space.

Since 1978, NASA-LaRC has sponsored an annual conference on LSST. Papers by James [11] and Cord [12] are introductions to the two volumes of the 1980 conference proceedings.

II. The Environment

To be feasible, LSS will have a function safely, reliably, and efficiently through several years of service. They must therefore be designed with particular emphasis given the environment in which they will be expected to function. Preliminary studies indicated that most, if not all, applications of LSS will place them in GEO. They must therefore be designed for the geosynchronous radiation environment and severe thermal cycling.

Ambient radiation is of particular concern to the designer because it causes: (1) a serious hazard for humans, (2) degrading and damaging effects on materials, (3) saturation of instruments, and (4) interference with scientific measurements and observations. Stassenopoulous [13] provides a study of the geostationary radiation environment.

Because spacecraft at GEO can charge to levels significant enough to impact the degrade system performance, there is a need for space vehicle design engineers to have a "worst case" charging environment. Gussenhoven and Mullen [14] discuss an environment that produced one of the largest satellite frame potentials on the SCATHA satellite in its first year of operation. Presented is an extremely severe geostationary environment having an exceptionally dense plasma population in the high energy range (20 keV). This is the only paper included in this survey regarding spacecraft charging, but much has been written and this paper lists many references.

The success of nearly every mission envisioned for LSS is critically dependent upon the maintenance of a stable, close-tolerance geomtry. Thus the prediction and control of structural deformations under the influence of the orbital environment become major design requirements and the candidates structure's characteristic responses become important considerations in concept selection. Brogren, Barclay, and Straayer [15] provide the de-

signer with a tool for making rapid estimates of the response of these structures to the thermal environment encountered in Earth orbit. Thermal analysis of relatively sparse structures in the space environment has customarily omitted consideration of shadowing by up-sun structural members. This convention has been frequently questioned in the case of lattice-type structures supporting very large, near planar, Earth-facing surfaces. For these, significant shadowing can occur whenever the solar vector is nearly tangent to the orbital path. Oneil, [16] deals with modelling this problem area.

Bosma and Levadou [17] examine passive thermal control coatings for Spacelab. This may indirectly be of interest to those studying thermal control for LSS.

III. Materials

The materials used for the construction of LSS will be exposed to an environment that will be seriously conducive to material degradation. The geosynchronous environment has an exceptionally dense plasma population in the high energy range, and there is little natural protection from the solar electromagnetic spectrum. The structure will be exposed to severe thermal cycling (one study indicates a range of from 88K to 377K, another from 77K to 394K).

Rosen and Hashin [18] have studied the relationship between the constituent and composite thermoelastic properties.

Schapery [19] has determined bounds on coefficients of thermal expansion for materials based on principles of thermoelasticity. This work is applicable for both istropic and anisotropic composite materials.

Halpin [20] has estimated expansion and stiffness for oriented short fiber composites with the use of Halpin-Tsai equations.

The effects of thermal expansion in metal-matrix composites have also been investigated by Wang and Sutula [21].

G/E composites have low density, high stiffness, and low CTE, making them prime candidates for the use in LSS. Cammahort, Rennhack, and Coons [22] have studied the effects of a thermal cycling enviroment on the dimensional stability and microstructural integrity of G/E composites. They subjected their specimen to 25 thermal cycles between the temperature of liquid nitrogen (77K) and that of boiling water (373K).

Bowles, Post, Herakovich, and Tenney [23] and Bowles and Tenney [24], describe an experimental program conducted to determine the feasibility of applying moiré interferometry to the measurement of thermally induced strains in composites. They have developed techniques for high sensitivity moiré interferometry by reflection, using a real reference grating of 1200 lines/mm. They have determined the CTE for four G/E laminates in the temperature range of 297K to 422K: (1) [0]; (2) [90]; (3) [0/±45/90]; and (4) [0/90±45].

The dimensional stability of materials used in LSS must be established at both low and high temperatures. The moiré interferometry system of references 23 and 24 is limited to making CTE measurements above room temperature. Short, Hyer, Bowles, and Tompkins [25] have developed an interferometer technique to measure small thermal strains associated with G/E composites over the temperature range of 116K to 366K.

When working with composite materials, the designer must be concerned with the effects of moisture absorption/desorption. Shen and Springer [26] have developed expressions for the moisture content of composite materials as a function of time. The results apply when both moisture content and the temperature of the environment are constant. Bergman and Dill [27] have

conducted experiments to determine the effect of absorbed moisture on the strength and stiffness properties of G/E composites. Zigrang and Bergman [28] have studied the response of G/E sandwich panels to moisture and temperature transients. The application prompting this study was the use of G/E honeycomb sandwich construction for the Shuttle payload bay doors.

Durability of composites in the GEO environment is considered to be the principle uncertainty associated with the long term [25-30 years) use of composites in thin-gage minimum weight LSS. Tenney, Slemp, Long, and Sykes [29] describe two programs conducted at LaRC in FY-79 to assess the radiation stability of current composites. The goal of one program is to determine the radiation damage mechanisms of resin matrix composites and formulate new polymer matrices that are inherently more stable in the space environment. The thrust of the second program is to develop the materials technology required for confident design of LSS such as antennas and platforms. Another long term concern for materials exposed to conditions found in space is stress corrosion cracking. Stress corrosion cracking is the result of both a sustained tensile stress and a corrosive environment such that a material fails prematurely. Marshall Space Flight Center [30] has investigated this problem and offers criteria for material design.

Because most polymeric materials are known to undergo changes in physical and/or mechanical properties when exposed to electron and proton radiation, a program designed to evaluate the effects of this radiation on selected candidate composite materials has been conducted at LaRC. Slemp and Santos [31] present some of the initial significant results from this research program. Fornes, Memory, Gilbert, and Long [32] present data gathered during experimentation conducted to evaluate the effects of radiation on the mechanical properties of epoxy based structural materials and to measure the fundamental radiation-

generated events which cause the changes. G/E composite specimens and epoxy resins were exposed to electron and gamma radiation, followed by mechanical property and fundamental measurements. Radiation induced changes in a structural material are initiated by energetic charged particle impact which transfers kinetic energy of the particle via its coulomb field into electronic excitation energy of the material. Kamorator, Wilson, Chang, and Xu [33] have investigated the energy absorption and events immediately following impact in an effort to arrive at an understanding of the radiation degradation of polymers.

For organic matrix composites, microcracking is one of the primary factors controlling the dimensional stability of the material. Permanent changes in the thermoelastic properties and/or permanent residual strains can result from this type of damage. Bowles [34] has studied the effect of microcracking on the CTE of G/E composites.

Hoggatt and Kushner [35] discuss a thermoplastic resin (polysulfane) and compare the structural and environmental properties and the fabrication and repairability of the thermoplastic composite with a typical epoxy composite. It is their conclusion that low labor costs exhibited by the thermoplastic composites make them a priority consideration for use in space structures. Fager [36] gives a good argument supporting the contention that G/E is the material to use in LSS.

A class of materials which have only recently become practical to use in structures are metal-matrix composites. Some advantages of these materials are better response at high temperatures and the possibility of using a matrix with high ductility to increase fracture toughness. Vinson, and Chow [37], and Renton [38], as well as Herakowich, Davis, and Dexter [39] discuss various applications of metal-matrix composites along with some material properties.

Divecha, Fishman, and Karmarkar [40] present production techniques, material properties, and practical application of Silicon Carbide/Aluminum Composites. It is necessary to develop a constitutive damage model of material behavior if a structure is to be designed to function under degraded material conditions. Much work has been done involving fracture mechanics in composite materials in general [41-48]. Yeow, et al. [49-51] have investigated the fracture behavior of Graphite/Epoxy composites. Hahn [52-55] has investigated the fracture rsponse of both polymeric and metal-matrix composites.

Some of the earliest work on modeling materials was for metals. Bodner et al. [56-59], and Krieg, Swearengen, and Rohde [60] have constructed microphenomenologically-based models for the response of metals.

Several damage models are currently available for use in composite materials. Maryolin [61] has done work on a constitutive model based on a prescribed distribution of penny shaped cracks. A damage field is constructed by the use of the crack distribution and crack radius. With this model, the effective moduli of the material can be calculated. Laws, Dvorak, and Hejazi [62] have modelled a unidirectional continuous fiber composite containing longitudinal slit cracks. By assuming different magnitudes of cracks, both a two-phase and three-phase model results. Horii and Nemat-Nasser [63] have developed a model involving randomly distributed cracks and frictional sliding. Both Margolin, Dvorak, and Nemat-Nasser use the self-consistent scheme (i.e., Eshelby's solution) in their models for the determination of the stiffness reduction.

A plane-stress continuum model for creep analysis of a unidirectional metal-matrix composite was developed by Min and Crossman [64]. This model used separate transverse and shear damage parameters to account for damage

caused by inhomogeneous local distribution of stress in the material.

Hashin and others [65-66] have modelled damage by the use of damage surfaces. These surfaces are based on S-N curves where N is the number of cycles to give fracture at a given stress S.

Chou and Croman [67] formulated a model using the equal rank assumption first introduced by Hahn and Kim [68]. This model assumes that fatigue life distribution has the same rank as in the static case. The assumption was based on an overall decrease in residual strength, rather than specific cracks.

Fonseka, and Krajcinovic [69,70] have developed a thermodynamically-based damage model for use on brittle materials with continuous damage. This model uses internal state variables. Another model using internal state variables was developed by Talreja [71-72]. Talreja's model is a continuum mechanics damage model which has damage from any loading condition expressed in terms of vector damage parameters. Allen [73] has proposed a damage model for composite materials based on a continuum/thermodynamics approach. In his model both local damage as well as global constitutive equations are averaged over the volume of the laminate. The internal state variables of damage that result are vector valued history dependent functions.

Schapery [74-76] has constructed a model for damage in a composite based on fracture mechanics and nonlinear viscoelasticity. This model has been primarily formulated for isotropic particulate composite materials, but can be extended to model continuous fiber composites.

Research has been performed at General Dynamics (Forth Work) [77] with damage modeling. Work has been done on a damage program outline and a preliminary damage model exists at this time.

IV. Solution Techniques for LSS

The solution techniques for LSS can be classified into several categories: Noor [78] classifies them into four categories: (1) Finite element modelling, (2) continuum lattice modelling, (3) discrete field method, and (4) periodic structure approach. This classification is based upon repetitive lattice trusses, which are expected to be the primary candidates for most of the large space structures. In an earlier status report on latticed structures [79] the analysis methods are divided into six categories: (1) discrete field analysis, (2) space frame analysis, (3) equivalent continuum analysis, (4) nonlinear analysis, (5) experimental analysis, and (6) dynamic analysis.

The paper by Roussos, Hyer and Thornton [80] develops a procedure by which many different damping functions (linear or nonlinear) may be incorporated in a structure. In the finite element formulation, a solution technique is developed by modifying the Newmark method for solving the set of nonlinear equations. Mehaney, Thornton and Dechaumphai [81,82] have developed integrated Thermal-Structural finite element analysis. In this integrated approach, thermal and structural finite elements are formulated with a common geometric discretization and the thermal and structural finite elements are fully compatible.

Adelman and Shore [83] describe the thermal analysis considerations for large space structures. The paper by A. K. Noor [84] summarizes recent developments in the application of reduction methods to nonlinear structural mechanics problems. Some of the aspects of reduction methods discussed include selection of basis vectors in nonlinear static and dynamic problems and the use of reduction methods in conjunction with mixed finite element models. A similar paper by Noor and Peters [85] describes a reduced basis technique and computational algorithm for predicting nonlinear static response of structures.

Soni and Bogner [86] present a computer program MAGNA-D for predicting the response of damped structures to steady state inputs. The analysis includes the damping effects of viscoelastic materials characterized by complex moduli and of coulomb friction at sliding interfaces.

One of the earlier papers on continuum modelling is by Heki and Saka [87]. This paper presents the stress analysis of lattice plates as anisotrpic continuum plates. In this approach effective rigidity of lattice plates have been derived for bending, stretching, shearing and coupling rigidity between them. Flower and Schmidt [88] present an analysis of space truss as equivalent plate. In this analysis it is assumed that all truss members behave linearly classically and are pin-pointed. Noor [89] presents a thermal analysis of double layered grids. These double layers are useful because of their low cost light weight and high stiffness. Also due to their ease of packaging, transporting and assembling in space, double layered lattice trusses are considered as prime candidates for large space structure application.

Nayfeh and Hefzy [90] present a continuum modeling technique of mechanical and thermal behavior of discrete large structures. This procedure can be applied to a wide variety of discrete structures. In another paper by the same authors [91] two models, cubic and octetruss are compared and their analysis indicates that from the stiffness-to-density ratio the cubic model is a better candidate for the large structures.

Noor, Anderson and Greene [92] have developed continuum models for large repetitive beam- and platelike structures with arbitrary configurations subjected to static, thermal and dynamic loadings. This model accounts for local effects in the repeating elements (which were neglected in most of the earlier models) of the actual structure. Noor and Anderson [93] present a simple procedure for predicting the thermoelastic and free vibration responses of large repetitive

beam-like trusses. In this procedure the original lattice structure is replaced by an equivalent continuum beam model. The equivalent beam model accounts for warping and shear deformation in the plane of the cross-section and is characterized by its thermoelastic strain and kinetic energies from which the equations of motion and constitutive relations can be derived.

A simple procedure is presented by Noor and Weisstein [94] for predicting the buckling loads associated with general instability of beam-like lattice trusses. Bazant and Christensen [95] present a micropolar analogy to model large grid frameworks under initial axial forces. This continuous approximation is formulated even for the case of variable member properties and variable initial axial forces. Also the boundary disturbances which rapidly decay with distance from boundary is demonstrated. The paper by Sun and Yang [96] present a continuum approach toward dynamics if gridworks. In this approach equations of motion, boundary conditions and constitutive equations are developed which can be used to analyze dynamic and static responses of gridwork consisting of orthogonally interesting beams rigidly connected at the joints. The transverse vibration and wave propagation are investigated by continuum theory. Comparison with finite-element solutions show that results obtained are accurate especially in the range of long wavelengths.

Noor and Nemeth [97] have developed micropolar models for the static, free vibration and buckling analysis of repetitive spatial beam-like lattices with rigid joints.

The discrete field method takes advantage of the regularity of the lattice and is based on construction of the equilibrium and compatibility equations at a typical joint and then using a Taylor Series expansion to replace these equations by difference equations. Renton [98-101] has analyzed fluxural-torsional behavior of grillages, triangular mesh grillages, space grids and

on the gridwork analogy for plates. Wah [102] outlines a procedure for analyzing laterally loaded gridworks.

The periodic structure approach is generally based on either: (a) the combined use of finite elements and transfer matrix methods, which is efficient only for rotationally symmetric or simple geometries, or (b) the exact representation of the stiff of an individual member from which the analysis of beam-like lattices with simple supported edges cam be performed. McDaniel and Chang [103] employ a finite element transfer matrix method to model dynamics of rotationally periodic large space structures. In this approach, the finite element transfer matrix method is employed to eliminate internal degrees of freedom from the basic unit of rotationally periodic large space structures. Eigenfunctions of the resulting periodic unit transfer matrix are used to obtain frequency responses of the complete structure without increasing the analysis variables. Interpolation procedures are developed which significantly reduce the required computations. The dimension of the transfer matrix, and the number of eigenvalues/eigenvectors extractions required in a given frequency range.

Anderson [104-106] has developed equations for general lattice structures having repetitive geometry for vibration and buckling analysis. This approach is based on represnting each member of the structure with the exact dynamic stiffness matrix and taking advantage of the repetitive geometry to obtain an eigenvalue problem involving the degrees-of-freedom at a single node in the lattice. According to Noor the limitations of the periodic structure approach can be removed by combining this approach with the continuum approach.

V. Damping Technology

Much research has gone into the area of constrained layer damping. Carne [107] examines constrained layer damping by using finite element analysis.

In this paper he gives a brief outline of the early development (1959 to 1973) of constrained layer damping technology. The first important paper on constrained layer damping was by Kerwin [108]. In it he develops theoretical expressions for the damping effectiveness of a constrained damping layer based on the shear energy - loss mechanism. This was followed by a more extensive paper by Ross, Ungar, and Kerwin. Using their theory, the loss coefficient and the increase in dynamic stiffness due to the constrained layer could be determined. Their theory is applicable for beams of infinite length or finite beams of infinite length or finite beams with simply supported boundary conditions. Ungar [109], using an energy method, was able to calculate the loss coefficient of more complicated beam structures. Yin, Kelly, and Barry [110] verified Ross, Ungar, and Kerwin. Their paper dealt with the constrained-layer damping mechanism for plates, beams, and tubular structures. DiTaranto [111] derived a 6th order PDE to describe the motion of sandwich beams, thus allowing boundary conditions other than simply supported for finite length beams. DiTaranto and Blasingame [112] applied the PDE to obtain generalized results for the composite loss factor and natural frequency of a sandwich beam. DiTaranto derived his 6th order PDE in terms of longitudinal displacements. Mead and Markus [113] rederived the equation based on lateral displacements, and then used it [114] to determine the characteirstic equation for the resonant frequency, loss factor and modal root. Yan and Dowell [115] derived a simpler 4th order PDE for the vibrating beam with constrained layer damping, and they published [116] some experimental results in verification of the theory. Mead [117] discusses some questions he has concerning the 4th order PDE. Carne's paper was written in 1975. In 1978 DiTaranto published "Summary of Constrained Damping Literature" [118]. This paper includes the literature survey of B.C. Nakra and has well over 100 papers referenced. More recent papers on constrained

damping include Rao [119] which uses an energy method, Johnson and Kienholz [120], and Bogner and Brockman [121] use the finite element method. Soovere [122] wrote of a program for the development of dampin applicable to stringers and frames on a wide-bodied transport. The use of constrained layer damping has been extended to rings and cylinders by DiTaranto [123] and Lu, Douglas, and Thomas [124].

Damping materials and systems are represented herein by three papers. Jones [125] wrote an introduction to damping materials and system. In it he lists 32 references. O'Kiefe [126] discussed application techniques and utilities for several types of damping systems. He described the microscopic mechanics of damping as well as some methods for improving performance over wider temperature and frequency ranges. Gibson [127] investigates the internal damping and dynamic stiffness of the G/E composite column of reference 160.

Experimental investigations of damping were conducted by Plunkett [128,129] and by Plunkett and Sax [130].

A few papers are included which are concerned with designing for vibration control. Rogers [131] wrote an outline guide for the design of vibration damping. Paul [132] illustrates damping thermal design methodology by discussion of two recent damping design projects. These concern the TF30P100 inlet guide vane and the B-1 aft equipment bay.

The following papers are directed toward active control: Horner [133], Herzberg, Johansen, and Stroud [134], Skelton [135,136], and Montgomery [137].

Snowden [138] is an often referenced text on the subject of vibration and damping.

Foss [139] derived orthogonality relationships between the eigenvectors of damped linear dynamic systems with lumped parameters, and was able to establish coordinates which uncouple the equations of motion.

VI. Preliminary Design/Analysis/Experimental Investigation

Any LSS will be built using the STS and must therefore be designed for compatibility with this system. Roebuck [140] describes shuttle considerations for the design of LSS. Culbertson and Bold [141] references many Shuttle user-oriented documents. Christensen [142] requests input necessary to develop LSS design guidelines and standards.

There are basically three methods of placing large structures in space: (1) automated fabrication, wherein a manufacturing system is placed in orbit which when supplied with raw materials will build truss like structures; (2) deployable structures built on Earth and collapsed into a compace transportation configuration to be unfurled in space; and (3) erectable structures built from pieces carried into orbit. Regardless of the method of construction, these will be first deployed in LEO and then transferred to GEO.

Powell [143], and Powell and Browning [144] describe a baseline LSS concept developed for the NASA-JSC, SCAFE. A beam builder and raw materials are placed in a 566 km circular orbit by the STS. The beam builder, working from the Shuttle, automatically fabricates four triangular beams, each 200m in length. The beam builder then moves along the length of these to build and attach shorter cross beams. The structure is to be built, and preliminary tests run, in a 7 day mission. Slysh and Kugath [145] describe a LSS automated assembly technique (LSAT) developed to provide a starting point for a feasibility examination of fully mechanized space structures assembly and maintenance. The LSAT concept is applicable to structures ranging in size from hundreds to tens of thousands of meters. Muench [146] describes an aluminum beam builder which has been built and ground tested by Grumman Aerospace. It could be used to produce the components necessary for assembling LSS. Goodwin [147] discusses the concept of a space platform to be used as a manufacturing base for the beam builder of

reference 100. The platform could house solar arrays, radiators, space construction equipment, laboratories, housing modules, etc.

The second means of placing LSS in orbit is the deployable method. These structures are assembled on Earth, packaged in a compact collapsed configuration to be unfurled in space. This type structure can never reach the dimensions necessary for many of the proposed applications of LSS, but can be utilized for larger aperture antennas. Fager and Garriott [148] describe a concept capable of deploying a reflector up to 91.5 M in diameter. Spring loaded trusses retract for transportation and are released in space. A 30.5 M diameter antenna can be packaged into a 3.05 M payload envelope. Deployment is automated. Chadwick and Woods [149] discuss the work being done at LMSCO to expand the maximum size of deployable antennas. Their work is based on the proved WRAP-RIB design. With new materials and design improvements, the WRAP-RIB structure can now be extended to support antennas of over 200 M in diameter. These designs can be packaged for ascent on the STS and are self deploying in space.

A hybrid method connecting the erectable concept with the deployable concept proposes the construction of LSS by the mating of deployable modules. Agan [150] contributes to the overall technical data base for various programs using deployable structures. His paper is generic in nature, intended to provide general information and data to emerging space programs employing erectable/deployable structural concepts. His basic structural building block is a double cell double folding cubic model (3M x 3M in cross-section and 6M long). Heartquist [151] relates the results of twin contracts awarded to General Dynamics-Convair and Martin Marietta to develop preliminary design of a 183M truss-like spacecraft. Armstrong, Skoumal, and Straayer [152] have conducted a building block structures study for LSS. Based on proposed uses of LSS, they decided that a modular planar truss structure and a long slender

boom concept would serve as building block approaches. The structural configurations chosen for the study were the tetrahedral planar turss and lattice column. Articulating joints and collapsing details are defined to allow packaging densities to approach values that effectively utilize the payload mass capability of the Shuttle. A deployable planar truss building block module is described in parametric form to allow a broad application base for this type of structure. Barclay, Brogren, and Skoumal [153] also deal with the subject of reference 152. A scenario is developed in [153] which would enable the placing of a 300M by 300M platform in LEO using the STS. The platform is assembled using 7 deployable tetrahedral modules [120M by 104M in size) mounted to an erectable truss structure consisting of 102 columns. The structural response was determined for: (1) a simple open truss subjected to the natural thermal radiation, and (2) a more complex truss subjected to on-board heating as well as the natural thermal radiation.

Erectable concepts deal with the building of LSS from beam or column elements transported to LEO by the STS. Much work has been done in this area at LaRC by Heard, Bush, Walz, Card, Mikulas, et al. This work has dealt primarily with the tetrahedral truss configuration. Mikulas, Bush, and Card [154] have written a good paper on the tetrahedral truss. In the paper, the truss is defined, analyzed (using a continuum method), and tested experimentally. The tetrahedral truss is an excellent configuration for preliminary studies because of its psuedo-isotropic elastic properties and because it is constructed of all identical column members. Also, work done by Boeing identified the tetrahedral truss as having the lightest weight and highest first mode frequency when compared to other generic trusses of equal depth and planform area. Reference 154 considers both aluminum and G/E tubular columns. Work by Bush, Mikulas, and Heard [155] is very similar to reference 154. Heard, Bush,

Walz, and Rehder [156] have conducted optimization studies to examine minimum mass structural proportions of deployable and erectable tetrahedral truss platforms subjected to the integrated effects of various design requirements. Considerations integrated into the design process are: (1) lowest natural frequencies of the platform and individual platform components; (2) packaging constraints imposed by the Shuttle cargo bay capacity; (3) initial curvature of the struts; (4) column buckling of the struts due to gravity gradient, orbital transfer, strut length tolerance, or design loads; and (5) lower limits for strut diameter and wall thickness. Katz and Pankopf [157] describe a three step procedure for assembling LSS. They use the tetrahedral truss and the nestable tapered column of reference 159.

Heard, Bush, and Walz [158] have tried to determine the size of LSS that is best suited to a deployable concept versus an erectable concept. They used the tetrahedral truss for mathematical modelling purposes. Preliminary orbital transfer investigations indicate that deployable platforms of up to 200M span may be placed in GEO with a single Shuttle flight using a constant thrust chemical propulsion system which limits initial accelration to 0.01g or less.

Park and Winget [159] wrote the only paper, found by this author, which proposed the use of nonperiodic LSS. The design and analysis of LSS for dynamic loads requires the consideration of wave propagation, transient response, and steady-state vibration problems. The desirable intrinsic structural characteristics of these problems are good dispersive properties, rapid decay of the transients, and an optimum distribution of frequency spectrum. Periodic trusses such as the tetrahedral truss or the octetruss have two major drawbacks. First, periodic trusses can be considered to be well tuned, and therefore they do not have good wave dispersion characteristics. Second, if the dimensions of the platform are fixed then the frequency spectrum of the structure is also

fixed, thus leaving no room for frequency modification other than through redesign and/or effective vibration control devices. Park and Winget propose improving wave dispersion and controlling the frequency spectrum by the internal rearrangements of nonperiodic lattices.

Preliminary studies indicate that LSS will be large area low mass truss type structures constructed of long slender lightly loaded compression elements may most likely of G/E. Bush and Mikulas [160] have developed a nestable tapered column to be used as the structural element of the tetrahedral truss developed at LaRC. The nestable tapered column permits achievement of weight critical as opposed to volume critical payloads for the STS. Structures using the nestable tapered column will have to be assembled in orbit eliminating the use of deployable modules. It is, however, the opinion of the authors that for very large (km size) structures, the gain in mass placed in orbit per launch makes the nestable tapered column feasible. The nestable tapered column concept will require a "break or center joint" in the middle of each truss element and a cluster joint for each node. Heard, Bush, and Agranoff [161] have investigated the effect of the mid-column break on stability behavior. Since the columns will function in an extremely low strain range they have also investigated the validity of using, for analysis predictions, standard material properties for G/E determined from coupons tested udner much larger strain ranges. Some preliminary buckling test results for the G/E nestable tapered column appear in reference 109. The purpose of reference 161 is to present detailed data on the columns and center joint of the nestable tapered columns concept, and to present buckling data for additional columns as well as a tripod arrangement of these columns using a cluster joint. Gibson [127] has investigated the damping characteristics and the dynamic stiffness of the G/E composite materials used in the restable tapered column. He has also compared the relationships between dynamic properties

derived from tests of small specimens and those of full scale columns. It is his conclusion that small specimens are representative. Mikulas [162] is concerned primarily with design methods for long lightly loaded columns, and with a technique for comparing the masses of different column concepts. He looks at four column concepts: (1) a tubular column, (2) a three longeron truss column constructed from tubular members, (3) a three longeron truss column constructed from solid rod members, and (4) a tubular column with open gridwork "isogrid" walls. Optimization of LSS is generally considered in terms of minimum weight. Yoo [163] considers the optimization of a three longeron truss column constructed from tubular members (one of the columns that Mikulas looked at). The optimization procedures are based on designing for a column with initial imperfections. Yoo compares his results to those of Mikulas. Many LSS make use of the low mass and deployability of pretensioned structures to achieve efficient designs. These structures use tension elements (cables, rods, and membranes) to provide stiffness and stability of structural systems. To understand the fundamental structural characteristics of pretensioned structures, Belvin [164] has performed analyses and tests of some simple configurations. The buckling and vibration behavior of a pretensioned stayed column are discussed in detail. Crawford and Benton [165] have determined the axial compressive strengths for lattice columns that are initially wavy in both local and overall modes. The compressive strength is found to be less than either the classical local or overall buckling strengths. These strength reductions are anticipated to be significant for lightweight space columns or large slenderness ratio. The study was prompted by a need to predict the axial compressive strength of lattice columns which were being considered for the diagonal spars of an 800M square solar sailing spacecraft.

The largest application of LSS technology being considered is the SPS. Studies have been conducted regarding satellites that would produce a useful output of from 5 to 10 GW at Earth receiving stations. The major dimensions of such a satellite will be several kilometers. For instance, Nansen and DiRamio [166] describe the structure for a SPS with the following dimensions for the solar collector: 21.28 by 5.30 by 0.47 km. It employs 660M by 660M square bays 470M deep as repeating elements. Most of the studies conducted thus far involve a planar solar array with either one or two attached MPTS's. The large solar collector is a source of electrical power (photovoltaic cells are utilized) which is converted to microwave electromagnetic energy and relayed from the collection site in GEO to the ground receiving system. The feasibility of the relay link depends on the capability of keeping the beam center of each MPTS pointed at the ground receiving antenna (rectenna), and the phase error over the aperture small enough so that efficiency is high. "Achievable Flatness in a Large Microwave Power Antenna Study" [167] is the structure of the MPTS, and (b) their contribution to slope error of the antenna array. "Satellite Power System, Concept Development and Evaluation Program - Reference System Report" [168] describes a reference system concept developed as the result of twin system definition studies conducted by Boeing Aerospace Company and Rockwell International. The reference system suggests implemeting two 5 GW SPS systems per year for 30 years starting in the year 2000. The concept uses a planar solar array (about 55 km^2) built on a graphite fiber reinforced thermoplastic structure. A one km diameter phased array MPTS is mounted on one end of the satellite.

As the need arises for larger antennas operating at higher frequencies, structural stiffness becomes a key design consideration. Structural stiffness will significantly influence thermal distortion, point accuracy, and natural

frequency. Fager [169] indicates that four design criteria must be considered regarding stiffness: contour control, thermal distortion, ground test capability, and most critical, pointing accuracy. He discusses this general problem area with respect to the geodetic truss. Analytical results indicate that a careful selection of materials and truss design, combined with accurate manufacturing techniques, can result in very accurate surfaces for large space antennas. The purpose of the paper by Hedgepth [170] is to investigate the influence of the accuracy requirements on the design geometry of the structure for four general types of structural configurations: tetrahedral truss, geodesic dome, radial rib, and pretensioned truss. Requirements on the panel sizes for a mesh reflection surface are obtained. The influence of fabrication imperfections on the surface error is also evaluated. An initial evaluation is taken of the effect of thermal stress on the accuracy. Finally, an evaluation is made of the diameter-wavelength ratios potentially feasible as limited by fabrication imperfections and thermal strains. As mentiond already, one of the sources of error in rf antennas is the lack of dimensional precision of the surface. Hedgepeth [171] presents an approach for estimating the amount of error caused by random dimensional imperfections of the many structural elements which make up a truss-type antenna. A principle of equivalence between the analyses of statistical error and of the natural vibration frequencies of the structure is developed.

Bellagamba and Yang [172] have developed a technique for constrained parameter optimization and have applied it to the minimum-mass design of truss structures. The procedure employs and exterior penalty function to transform the constrained objective function into an unconstrained index of performance which is minimized by the Gauss method.

Soon, very large spacecraft will be assembled in LEO and then transferred to GEO. These lightweight and very flexible spacecraft will require specially

designed propulsive systems for the orbital transfer. Interactions between such structures and the propulsive thrust forces can have significant influence on the overall spacecraft configuration, structural design, and control functions to a greater degree than experienced with more conventional spacecraft. Kunz [173] examines some of these structural/propulsive interactions, deduces significant propulsion requirements, and illustrates some concepts with design characteristics.

Oren and Cox [174] provide an evaluation of heat rejection techniques applicable to multihundred-kW space platforms.

LSS preliminary and conceptual design requires extensive iterative analysis because of the effects of structural, thermal, and control intercoupling. LaRC is developing a CAD program that will permit integrating and interfacing of required LSS analyses. The primary objective of this program is the implementation of modeling techniques and analysis algorithms that permit interactive design and trade-off studies of LSS concepts. Farrell [175] presents an overview of the status of the program and the capabilities added by Martin Marietta.

ACKNOWLEDGEMENT

The authors gratefully acknowledge the support for this research, which was provided by the Air Force Office of Scientific Research under contract no. F49620-83-C-0067.

References

I. Expected Applications of LSS

1. Hedgepeth, J. M., "Survey of Future Requirements for Large Space Structures," NASA-CR-2621, 1976.

2. Woodcock, G. R., "Solar Satellites, Space Key to Our Power Future," Astronautics and Aeronautics, Vol. 15, July/Aug., pp. 30-43, 1977.

3. Foldes, P., Dienemann, M. W., "Large Multibeam Antennas for Space, [AIAA 79-0942], Journal of Spacecraft and Rockets, Vol. 17, No. 4, pp. 363-371, 1980.

4. Wannlund, W. R., "Large Antenna Structure Technologies Required for 1985-2000," NASA-CP-2035, 1978.

5. Holloway, P. F., Garrett, L. B., "Concepts for, and Utility of, Future Space Central Power Sations," [AIAA 81-0449], Journal of Spacecraft and Rockets, Vol. 19, No. 2, pp. 97-98, 1982.

6. Stone, G. R., "Structural Requirements and Technology Needs of Geostationary Platforms," NASA-CP-2168, 1980.

7. Hagler, T. A., "Building Large Structures in Space," Astronautics and Aeronautics, Vol. 14, May, pp. 56-61, 1976.

8. Card, M. F., Kruszewski, E. T., Guastaferro, A., "Technology Assessment and Outlook," Astronautics and Aeronautics, Vol. 16, Oct., pp. 48-54, 1978.

9. Daros, C. J., Freitag, R. G., Kline, R. L., "Toward Large Space Systems," Astronautics and Aeronautics, Vol. 15, May, pp. 22-30, 1977.

10. Hedgepeth, J. M., Mikulas, M. M. Jur., Macneal, R. H., "Practical Design of Low Cost Large Space Structures," Astronautics and Aeronautics, Vol. 16, Oct., pp. 30-34, 1978.

11. James. R. L. Jr., "Large Space Systems Technology Overview," NASA-CP-2168, 1980.

12. Cord, M. F., "Base Technology Overview," NASA-CP-2168, 1980.

II. The Environment

13. Stassinopoulos, E. G., "The Geostationary Radiation Environment," [AIAA 80-4026], Journal of Spacecraft and Rockets, Vol. 17, No. 2, pp. 145-152, 1980.

14. Gussenhoven, M. S., Mullen, E. G., "Geosynchronous Environment for Severe Spacecraft Charging," [AIAA 80-0271], Journal of Spacecraft and Rockets, Vol. 20, No. 1, pp. 26-34, 1983.

15. Brogren, E. W., Barclay, D. L., Stroayer, J. W., "Simplified Thermal Estimation Techniques for Large Space Structures," NASA-CR-145253, 1977.

16. O'Neill, R. F., "Recent Developments in Thermal Analysis of Large Space Structures," NASA-CP-2258, 1982.

17. Bosma, J., Levadou, F., "Ultraviolet Irradiation Effects on Candidate Spacelab Thermal Control Coatings," [AIAA 78-1621], Journal of Spacecraft and Rockets, Vol. 17, No. 6, pp. 558-564, 1980.

III. Materials

A. Composites

1. Temperature

18. Rosen, B. Walter, and Hashin, Zvi, "Effective Thermal Expansion Coefficients and Specific Heats of Composite Materials," International Journal Engineering Science, Vol. 8, pp. 157-173.

19. Schapery, R. A., "Thermal Expansion Coefficients of Composite Materials Based on Energy Principles," J. Composite Materials, Vol. 2, No. 3, p. 380.

20. Halpin, J. C., "Stiffness and Expansion Estimates for Oriented Short Fiber Composites," J. Composite Materials, Vol. 3, p. 732.

21. Wang, Frederick, E., and Sutula, Raynmond A., "On the Effects of Thermal Expansion in metal-matrix-composites," Proceedings of the 1978 International Conference on Composite Materials, p. 822.

22. Camahort, J. L., Rennhack, E. H., Coons, W. C., "Effects of Thermal Cycling Environment on Graphite/Epoxy Composites," ASTM STP 602, 37-49, 1976.

23. Bowles, D. E., Post, D., Herakovich, C. T., Tenney, D. R., "Moiré Interferometry for Thermal Expansion of Composites," Experimental Mechanics, Vol. 21, No. 12, pp. 441-447, 1981.

24. Bowles, D. E., Tenney, D. R., "Thermal Expansion of Composites: Methods and Results," NASA-CP-2168, 1980.

25. Short, J. S., Hyer, M. W., Bowles, D. E., Tompkins, S. S., "Thermal Expansion of Graphite Epoxy Between 116 K and 366 K," NASA-CP-2215, 1981.

2. Moisture

26. Shen, C-H, Springer, G. S., "Moisture Absorption and Desorption of Composite Materials," Journal of Composite Materials, Vol. 10, Jan., pp. 2-20, 1976.

27. Bergman, H. W., Dill C. W., Effect of Absorbed Moisture on Strength and Stiffness Properties of Graphite-Epoxy Composites," Proc. 8th National SAMPE Technical Conf., pp. 244-256, 1976.

28. Zigrang, D. J., Bergmann, H. W., "Response of Graphite/Epoxy Sandwich Panels to Moisture and Temperature Transients," [AIAA 80-4052], Journal of Spacecraft and Rockets, Vol. 17, No. 3, pp. 219-225, 1980.

3. Radiation

29. Tenney, D. R., Slemp, W. S., Long, E. R. Jr., Sykes, G. F., "Advanced Materials for Space," NASA-CP-2118, 1979.

30. NASA, "Design Criteria for Controlling Stress Corrosion Cracking," MSFC-SPEC-522A, November 18, 1977.

31. Slemp, W. S., Santos, B., "Radiation Exposure of Selected Composites and Thin Films," NASA-CP-2168, 1980.

32. Fornes, R. E., Memory, J. D., Gilbert, R. D., Long, E. R. Jr., "The Effects of Electron and Gamma Radiation on Epoxy Based Materials, NASA-CP-2215, 1981.

33. Kamaratos, E., Wilson, J. W., Chang, C. K., Xu, Y. J., "Basic Physical and Chemical Processes in Space Radiation Effects on Polymers," NASA-CP-2215, 1981.

4. Microcracking

34. Bowles, D. E., "The Effects of Microcracking on the Thermal Expansion of Graphite-Epoxy Composites," NASA-CP-2215, 1981.

B. Material Selection

35. Hoggatt, J. T., Kushner, M., "Applicability of Thermoplastic Composites for Space Structures," NASA-CP-2035, 1978.

36. Fager, J. A., "Application of Graphite Composites to Future Spacecraft Antennas," Satellite Communications: Advanced Technologies-Progress in Astronautics and Aeronautics, Vol. 55, pp. 21-33, 1977.

37. Vinson, J. R., and Chow, Tsu-Wei, "Metal-Matrix Composite Materials," Composite Materials and their use in Structures, John Wiley & Sons, N. Y., pp. 74-95.

38. Renton, W. James, "Introduction to Hybrid and Selected Metal-Matrix Composites," Hybrid and Select Metal-Matrix Composites: A State of the Art Preview, AIAA, 1977, pp. 1-11.

39. Herakovich, C. T., Davis, J. G., and Dexter, H. B., "Reinforcement of Metals with Advanced Filamentary Composites," Composite Materials: Testing and Design (Third Conference), ASTM STP 546, 1974, pp. 523-541.

40. Divecha, A. P., Fishman, S. G., and Karmarkar, S. D., "Silicon Carbide Reinforced Aluminum-A Formable Compsite," Journal of Metals, September 1981, pp. 12-17.

D. Damage Models

1. Fracture

41. Liebowitz, H., Subramonian, N., and Lee, J. D., "Mechanics of Fracture-Fundamentals and Some Recent Developments," Israel Journal of Technology, Vol. 17, 1979, pp. 273-294.

42. Erdogan, F., and Gupta, G. D., Layered Composites With an Interface Flaw," Int. J. Solids Structures, Vol. 7, 1971, pp. 1089-1107.

43. Kinra, V. K., and Vu, B. Q., "Brittle Fracture of Plates in Tension-Virgin Waves and Boundary Reflections," Journal of Applied Mechanics, Vol. 47, March 1980, pp. 45-50.

44. Badaliance, R., and Sih, G. C., "An Approximate Three-Dimensional Theory of Layered Plates Containing Through Thickness Cracks," Engineering Fracture Mechanics, Vol. 7, 1975, pp. 1-22.

45. Tada, H., Paris, P. C., and Irwin, G. R., The Stress Analysis of Cracks Handbook, Del Research Corporation, Hellertown, Pa., 1973.

46. Altus, E. and Rotem, A., "A 3-D Fracture Mechanics Approach to the Strength of Composite Materials," Engineering Fracture Mechanics, Vol. 14, pp. 637-644.

47. Chen, E. P., and Sih, G. C., "Stress Intensity Factor For a Three-Layered Plate With a Crack in the Center Layer," Engineering Fracture Mechanics, Vol. 14, pp. 195-214.

48. Sih, G. C., Hilton, P. D., Badaliance, R., Shenberger, P. S., and Villarreal, G., "Fracture Mechanics for Fibrous Composites," Analysis of the Test Methods for High Modulus Fibers and Composites, ASTM STP 521, 1973, pp. 98-132.

49. Yeow, Y. T., Morris, D. ., and Brinson, H. F., "The Fracture Behavior of Graphite Epoxy Laminates," Experimental Mechanics, Vol. 19, pp. 1-8, 1979.

50. Brinson, H. F., and Yeow, Y. T., "An Experimental Study of the Fracture Behavior of Laminated Graphite/Epoxy Composites," Composite Materials: Testing and Design, ASTM STP 617, pp. 18-38, 1977.

51. Yeow, Y. T., Morris, D. H., and Brinson, H. F., "A Correlative Study Between Analysis and Experiment on the Fracture Behavior of Graphite/Epoxy Composites," Journal Testing Evaluation, Vol. 7, pp. 117-125, 1979.

52. Morris, D. H. and Hahn, H. T., "Fracture Resistance Characterization of Graphite/Epoxy Composites," Composite Materials: Testing and Design, ASTM STP 617, pp. 5-17, 1977.

53. Awerbuch, J. and Hahn, H. T., "Hard Object Impact Damage of Metal Matrix Composites," J. Composite Materials, Vol. 10, pp. 231-257.

54. Awerbuch, J., and Hahn, H. T., "Crack-tip Damage and Fracture Toughness of Boron/Aluminum Composites," J. Composite Materials, Vol. 13, pp. 82-107.

55. Awerbuch, J., and Hahn, H. T., "Crack-tip Damage and Fracture Toughness of Borsic/Titanium Composite," Experimental Mechanics, October 1980, pp. 334-344.

2. Metals

56. Bodner, S. R., and Partom, Y., "Constitutive Equation for Elastic-Viscoplastic Strain-Hardening Materials," Journal of Applied Mechanics, Vol. 42, No. 2, pp. 385-389, 1975.

57. Bodner, S. R., "Representation of Time Dependent Mechanical Behavior of Rene 95 by Constitutive Equations," Air Force Materials Laboratory, AFML-TX-79-4116, 1979.

58. Bodner, S. R., Partom, I., and Partom, Y., "Uniaxial Cyclic Loading of Elastic-Viscoplastic Materials," Journal of Applied Mechanics, 1979.

59. Stouffer, D. C., and Bodner, S. R., "A Relationship Between Theory and Experiment for a State Variable Constitutive Equation," Air Force Materials Laboratory, AFWAL-TR-80-4194, 1981.

60. Krieg, R. D., Swearengen, J. C., and Rhode, R. W., "A Physically-Based Internal Variable Model for Rate-Dependent Plasticity," Proceedings ASME/CSME PVP Conference, pp. 15-27, 1978.

3. Self-Consistent Schemes

61. Margolin, L. G., "Effective Moduli of a Cracked Body," Int. Journ. of Fracture, Voo. 22, pp. 65-79.

62. Laws, N., Dvorak, G. J., and Hejazi, M., "Stiffness Changes in Unidirectional Composites Caused by Crack Systems," Mechanics of Materials 2, 1983, pp. 123-127.

63. Horii, H., and Nemat-Nasser, S., "Overall Moduli of Solids with Microcracks: Load-Induced Anisotropy," Jr. Mech. Phys. Solids, Vol. 31, No. 2, pp. 155-171.

64. Min, B. K., and Crossman, W., "Analysis of Creep for Metal Matrix Composites," J. Composite Materials, Vol. 16, pp. 188-203.

4. Damage Surfaces

65. Hashin, Z., and Rotem, A., "A Cumulative Damage Theory of Fatigue Failure," AFOSR 76-3015, TAU-SOE/395-77, February 1977.

66. Hashin, Z., and Laird, C., "Cumulative Damage Under Two Level Cycling: Some Theoretical TR-3, August 1979.

5. Equal Rank Assumption

67. Chou, P. C., and Croman, R., "Residual Strength in Fatigue Based on the Strength-Life Equal Rank Assumption," Journal Composite Materials, Vol. 12, April 1978, pp. 177-194.

68. Hahn, H. T., and Kim, R. Y., "Proof Testing of Composite Materials," Journal Composite Materials, Vol. 9, July 1975, pp. 297-311.

6. Internal State Variables

69. Krajcinovic, D., and Foneska, G. U., "The Continuous Damage Theory of Brittle Materials Part 1: General Theory," Journal of Applied Mechanics, Vol. 48, pp. 809-815.

70. Foneska, G. U., and Krajcinovic, D., "The Continuous Damage Theory of Brittle Materials Part 2: Uniaxial and Plane Response Modes," Journal of Applied Mechanics, Vol. 48, pp. 816-824.

71. Talreja, J. R., "Fatigue of Composite Materials: Damage Mechanisms and Fatigue-Life Diagrams," Proc. R. Soc. Lond., A378, pp. 461-475, 1981, Printed in Great Britain.

72. Talreja, R., "A Continuum Mechanics Characterization of Damage in Composite Materials," Visiting Scientist, ESM, Virginia Polytechnic Institute, 1982.

73. Allen, D. H., "A Damage Model for Continuous Fiber Composites," Mechanics and Materials Center, Texas A&M University, in preparation.

7. Fracture Mechanics/Viscoelasticity

74. Schapery, R. A., "A Method for Predicting Crack Growth in Nonhomogeneous Viscoelastic Media," Int. Journal of Fracture, Vol. 14, 1978, pp. 293-309.

75. Schapery, R. A., "On Viscoelastic Deformation and Failure Behavior of Composite Materials with Distributed Flows," Advances in Aerospace Structures and Materials, AD-01, 1981, pp. 5-20.

76. Schapery, R. A., "Models for Damage Growth and Fracture in Nonlinear Viscoelastic Particulate Composites," MM 3168-82-5, Mechanics and Materials Center, Texas A&M University, August 1982.

77. General Dynamics, "Cumulative Damage Model for Advanced Composite Materials," Progress Report No. 3, Contract No. F33615-81-C-5049, Air Force Materials Laboratory, September 1982.

IV. Solution Techniques for LSS

A. Surveys

78. Noor, A. K., "Assessment of Current State of the Art in Modeling Techniques and Analysis Methods for Large Space Structures," NASA-CP-2258, 1982.

79. "Lattice Structures: State-of-the-Art Report", Journal of the Structural Division, ASCE, Vol. 102, No. ST11, pp. 2197-2230, 1976.

B. Finite Element Method

80. Roussos, L. A., Hyer, M. W., Thornton, E. A., "Finite Element Model With Nonviscous Damping," "AIAA 81-0490], AIAA Journal, Vol. 20, No. 6, pp. 831-838, 1982.

81. Mehaney, J., Thornton, E. A., Dechaumphai, P., "Integrated Thermal-Structural Analysis of Large Space Structures," NASA-CP-2216, 1982.

82. Thornton, E. A., Mehaney, J., Dechaumphai, P., "Finite Element Thermal-Structural Modelling of Orbiting Truss Structures," NASA-CP-2215, 1981.

83. Adelman, H. M., Shore, C. P., "Thermal Analysis Considerations for Large Space Structures," NASA-CP-2258, 1982.

84. Noor, A. K., "Recent Advances in Reduction Methods for Nonlinear Problems," Computers and Structures, Vol. 13, pp. 31-44, 1981.

85. Noor, A. K., Peters, J. M., "Reduction Basis Technique for Nonlinear Analysis of Structures," [AIAA 79-0747], AIAA Journal, Vol. 18, No. 4, pp. 455-462, 1980.

86. Soni, M. L., Bogner, F. K., "Finite Element Vibration Analysis of Damped Structures," [AIAA 81-0489], AIAA Journal, Vol. 20, No. 5, pp. 700-707, 1982.

C. Continuum Lattice Modeling

87. Heki, K., Saka, T., "Stress Analysis of Lattice Plates as Anisotropic Continuum Plates," Proceedings of the 1971 IASS Pacific Symposium, Part II on Tension Structures and Space Frames, Tokyo and Kyoto, pp. 663-674, 1972.

88. Flower, W. R., Schmidt, L. C., "Analysis of Space Truss as Equivalent Plate," Journal of the Structural Division, ASCE, Vol. 97, No. 12, pp. 2777-2789, 1971.

89. Noor, A. K., "Thermal Stress Analysis of Double-Layered Grids," Journal of the Structural Division, ASCE, Vol. 104, No. 2, pp. 251-262, 1978.

90. Nayfeh, A. H., Hefzy, M. S., "Continuum Modeling of the Mechanical and Thermal Behavior of Discrete Large Structures," [AIAA 80-0679], AIAA Journal, Vol. 19, No. 6, pp. 766-773, 1981.

91. Nayfeh, A. H., Hefzy, M. S., "Continuum Modeling of Three-Dimensional Truss-Like Space Structures," AIAA Journal, Vol. 16, No. 8, pp. 779-787, 1978.

92. Noor, A. K., Anderson, M. S., Greene, W. H., "Continuum Models for Beam- and Platelike Lattice Structures," [AIAA 78-493], AIAA Journal, Vol. 16, No. 12, pp. 1219-1228, 1978.

93. Noor, A. K., Anderson, C. M., "Analysis of Beam-Like Lattice Trusses," Computer Methods in Applied Mechanics and Engineering, Vol. 20, No. 1, pp. 53-70, 1979.

94. Noor, A. K., Weisstein, L. S., "Stability of Beamlike Lattice Trusses," Computer Methods in Applied Mechanics and Engineering, Vol. 25, pp. 179-193, 1981.

95. Bazant, Z. P., Christensen, M., "Analogy Between Micropolar Continuum and Grid Frameworks Under Initial Stress," International Journal of Solids and Structures, Vol. 8, No. 3, pp. 327-346, 1972.

96. Sun, C. T., Yang, T. Y., "A Continuum Approach Toward Dynamics of Gridworks," Journal of Applied Mechanics, Transactions of ASME, Vol. 40, pp. 186-192, 1973.

97. Noor, A. K., Nemeth, M. P., "Analysis of Spatial Beam-Like Lattices With Rigid Joints," Computer Methods in Applied Mechanics and Engineering, Vol. 24, No. 1, pp. 35-59, 1980.

D. Discrete Field Method

98. Renton, J. D., "A Finite Difference Analysis of the Flexural-Torsional Behavior of Grillages," International Journal of Mechanical Sciences, Vol. 6, pp. 209-224, 1964.

99. Renton, J. D., "General Properties of Space Grids," International Journal of Mechanical Sciences, Vol. 12, pp. 801-810, 1970.

100. Renton, J. D., "On the Analysis of Triangular Mesh Grillages," International Journal of Solids and Structures, Vol. 2, pp. 307-318, 1966.

101. Renton, J. D., "On the Gridwork Analogy for Plates," Journal of the Mechanics and Physics of Solids, Vol. 13, pp. 413-420, 1965.

102. Wah, T., "Analysis of Laterally Louded Gridworks," Journal of the Engineering Mechanics Division, ASCE, Vol. 90, No. EM2, pp. 83-106, 1964.

E. Periodic Structure Approach

103. McDaniel, T. J., Chang, K. J., "Dynamics of Rotationally Periodic Large Space Structures," Journal of Sound and Vibration, Vol. 68, No. 3, pp. 351-368, 1980.

104. Anderson, M. S., "Buckling and Vibration of Periodic Lattice Structures," NASA-CP-2168, 1980.

105. Anderson, M. S., "Buckling of Periodic Lattice Structures," [AIAA 80-0681], AIAA Journal, Vol. 19, No. 6, pp. 782-788, 1980.

106. Anderson, M. S., "Vibration of Prestressed Periodic Lattice Structures," [AIAA 81-0620], AIAA Journal, Vol. 20, No. 4, pp. 551-555, 1982.

V. Damping Technology

A. Constrained-Layer Damping

107. Carne, T., "Constrained Layer Damping Examined by Finite Element Analysis," Proceedings of the 12th Annual Meeting, Society of Engineering Science, Austin, Texas, Oct. 20-22, pp. 567-576, 1975.

108. Kerwin, E. M. Jr., "Damping of Flexural Waves by a Constrained Viscoelastic Layer," Journal of the Acoustical Society of America, Vol. 31, No. 7, pp. 952-962, 1959.

109. Ungar, E. E., "Loss Factors of Viscoelastically Damped Beam Structures," Journal of the Acoustical Society of America, Vol. 34, No. 8, pp. 1082-1089, 1962.

110. Yin T. P. Kelly, T. J., Barry, J. E., "A Quantitative Evaluation of Constrained-Layer Damping," Journal of Enginering for Industry, Vol. 89, pp. 773-784, 1967.

111. DiTaranto, R. A., "Theory of Vibratory Bending for Elastic and Viscoelastic Layered Finite-Element Beams," Journal of Applied Mechanics, Vol. 32, pp. 881-886, 1965.

112. DiTaranto, R. A., Blasingame, W., "Composite Damping of Vibrating Sandwich Beams," Journal of Engineering for Industry, Vol. 89, pp. 633-638, 1967.

113. Mead, D. J., Markus, S., "The Forced Vibration of a Three-Layer, Damped Sandwich Beam With Arbitrary Boundary Conditions," Journal of Sound and Vibration, Vol. 10, No. 2, pp. 163-175, 1969.

114. Mead, D. J., Markus, S., "Loss Factors and Resonant Frequencies of Encastre Damped Sandwich Beams," Journal of Sound and Vibration, Vol. 12, No. 1, pp. 99-112, 1970.

115. Yan, M. J., Dowell, E. H., "Governing Equations for Vibrating Constrained-Layer Damping Sandwich Plates and Beams," Journal of Applied Mechanics, Vol. 39, pp. 1041-1047, 1972.

116. Yan, M. J.,, Dowell, E. H., "High Damping Measurements and a Preliminary Evaluation of an Equation for Constrained-Layer Damping," AIAA Journal, Vol. 11, No. 3, pp. 388-390, 1973.

117. Mead, D. J., "Governing Equations For Vibrating Constrained-Layer Damping Sandwich Plates and Beams," Journal of Applied Mechanics, Vol. 40, pp. 639-640, 1973.

118. DiTaranto, R. A., "Summary of Constrained Damping Literature," AFFDL-TM-78-78-FBA, 1978.

119. Rao, D. K., "Frequency and Loss Factors of Sandwich Beams Under Various Boundary Conditions," Journal of Mechanical Engineering Science, Vol. 20, No. 5, pp. 271-282, 1978.

120. Johnson, C. D., Kienholz, D. A., "Finite Element Prediction of Damping in Structures With Constrained Viscoelastic Layers," [AIAA 81-0486], AIAA Journal, Vol. 20, No. 9, pp. 1284-1290, 1982.

121. Bogner, F. K., Brockman, R. A., "Vibration Damping Analysis by Finite Elements," AFFDL-TM-78-78-FBA, 1978.

122. Soovere, J., "High Modulus Graphite Fiber Constrained Layer Damping Treatment for Heavy Aerospace Structures," AFFDL-TM-78-78-FBA, 1978.

123. DiTaranto, R. A., "Free and Forced Response of a Laminated Ring," Journal of the Acoustical Society of America, Vol. 53, No. 3, pp. 748-757, 1973.

124. Lu, Y. P., Douglas, B. E., Thomas, E. V., "Mechanical Impedance of Damped Three-Layered Sandwich Raings," AIAA Journal, Vol. 11, No. 3, pp. 300-304, 1973.

B. Damping Materials and Systems

125. Jones, D. J. G., "Introduction to Damping Materials and Systems for Vibration Control in Structures," AFFDL-TM-78-78-FBA, 1978.

126. O'Keefe, E. J., "Developments in Damping Technology," AFFDL-TM-78-78-FBA, 1978.

127. Gibson, R. F., "Vibration Damping Characteristics of Graphite/Epoxy Composites for Large Spce Structures," NASA-CP-2215, 1981.

C. Experimental Investigations

128. Plunkett, R., "Transient Response of Real Dissipative Structures," Shock and Vibration Bulletin, pp. 1-5, 1972.

129. Plunkett, R., "Measurement of Material and System Damping," AFFDL-TM-78-78-TBA, 1978.

130. Plunkett, R., Sax, M., "Nonlinear Material Damping for Nonsinusoidal Strain," Journal of Applied Mechanics, Vol. 45, Dec., pp. 883-888, 1978.

D. Damping Design

131. Rogers, L., "Necessary Steps for Successful Viscoelastic Damping Applications," AFFDL-TM-78-78-FBA, 1978.

132. Paul D. B., "Spatial and Temporal Temperature Distribution Considerations," AFFDL-TM-78-78-FBA, 1978.

E. Active Control

133. Hroner, G. C., "Optimum Damper Locations for a Free-Free Beam," NASA-Cp-2168, 1980.

134. Herzberg, R. J., Johansen, K. F., S-roud, R. C., "Dynamics and Control of Large Satellites," Astronautics and Aeronautics, Vol. 16, Oct., pp. 35-39, 1978.

135. Skelton, R. E., "Algorithm Development for the Control Design of Flexible Structures," NASA-CP-2258, 1982.

136. Skelton, R. E., "Large Space System Control Technology Model Order Reduction Study," NASA-CP-2118, 1979.

137. Montgomery, R. C., "Control Theoretics for Large Structural Systems," NASA-CP-2168, 1980.

F. Miscellaneous

138. Snowden, J. C., Vibration and Shock in Damped Mechanical Systems, John Wiley & Sons, N. Y., London, Sydney, 1968.

139. Foss, K. A., "Co-Ordinates Which Uncouple the Equations of Motion of Damped Linear Dynamic Systems," Journal of Applied Mechanics, Vol. 25, Sept., pp. 361-364, 1958.

VI. Preliminary Design/Analysis/Experimental Investigation

A. Guidelines/Standards

140. Roebuck, J. A. Jr., "A Document Describing Shuttle Considerations for the Design of Large Space Structures," NASA-Cp-2168, 1980.

141. Culbertson, P. E., Bold, T. P., "Opening a New Era," Astronautics and Aeronautics, Vol. 15, April, pp. 20-25, 1977.

142. Christensen, R. H., "Designing Structures for Large Space Systems," NASA-CP-2035, 1978.

B. Automated Fabrication

143. Powell, D. J., "Space Fabrication and Assembly of Graphite Composite Trusses," NASA-CP-2035, 1978.

144. Powell, D. J., Browning, L., "Automated Fabrication of Large Space Structures," Astronautics and Aeronautics, Vol. 16, Oct., pp. 24-29, 1978.

145. Slysh, P., Kugath, D. A., "Large Space Structure Automated Assembly Technique," [AIAA 79-9039], Journal of Spacecraft and Rockets, Vol. 17, No. 4, pp. 354-362, 1980.

146. Muench, W. K., "Automatic Fabrication of Large Space Structures-The Next Step," [AIAA 78-1651], Journal of Spacecraft and Rockets, Vol. 17, No. 3, pp. 286-288, 1980.

147. Goodwin, C. J., "Space Platforms for Building Large Space Structures," Astronautics and Aeronautics, Vol. 16, Oct., pp. 44-47, 1978.

C. Deployable

148. Fager, J. A. Garriott, R., "Large-Aperture Expandable Truss Microwave Antenna," IEEE Trans. on Antennas and Propagation, Vol. AP-17, No. 4, pp. 452-458, 1969.

149. Chadwick, G. C., Woods, A. A. Jr., "Large Space Deployable Antenna Systems," NASA-CP-2035, 1978.

D. Erectable

1. Erectable From Deployable Modules

150. Agan, W. E., "Erectable Concepts for Large Space System Technology," NASA-CP-2168, 1980.

151. Heartquist, P. E., "USAF Antenna On-Orbit Assembly," NASA-CP-2035, 1978.

152. Armstrong, W. H., Skoumal, D. E., Straayer, J. W., "Large Space Erectable Structures, Building Block Structures Study," NASA-CR-151449, 1977.

153. Barclay, D. L., Brogren, E. W., Skoumal, D. E., "Structural/Thermal Considerations for Design of Large Space Platform Structures," NASA-CP-2035, 1978.

2. Tetrahedral Truss, Octahedral Truss

154. Mikulas, M. M. Jr., Bush, H. G., Card, M. F., "Structural Stiffness, Strength and Dynamic Characteristics of Large Tetrahedral Space Truss Structures," NASA-TMX-74001, 1977.

155. Bush, H. G., Mikulas, M. M. Jr., Heard, W. L. Jr., "Some Design Considerations for Large Space Structures," [AIAA 77-395], AIAA Journal, Vol. 16, No. 4, pp. 352-359, 1978.

156. Heard, W. L., Bush, G. H., Walz, J. E., Rehder, J. J., "Structural Sizing Considerations for Large Space Platforms," [AIAA 80-0680], Journal of Spacecraft and Rockets, Vol. 19, No. 6, pp.211-217, 1982.

157. Katz, E., Pankopf, D. L., "Making a Start on Shuttle-Erectable Structures," Astronautics and Aeronautics, Vol. 16, Oct., pp. 40-43, 1978.

158. Heard, W. L. Jr., Bush, H. G., Walz, J. E., "Structural Sizing Considerations for large Space Structures," NASA-CP-2215, 1981.

4. Truss Elements

159. Park, K. C., Winget, J. M., "The Potential of Nonperiodic Truss Structures for Space Applications," Large Space Systems Technology-1981 Third Annual Technical Review, November, 1981.

160. Bush, H. G., Mikulas, M. M. Jr., "A Nestable Tapered Column Concept for Large Space Structures," NASA-TMX-73927, 1976.

161. Heard, W. L. Jr., Bush, H. G., Agraneff, N., "Buckling Tests of Structural Elements Applicable to Large Erectable Space Trusses, NASA-TM-78628, 1978.

162. Mikulas, M. M. Jr., "Structural Efficiency of Long Lightly Loaded Truss and Isogrid Columns for Space Applications," NASA-TM-78687, 1978.

163. Yoo, C.H., "Optimization of Triangular Laced Truss Columns With Tubular Compression Members for Space Application," AIAA Journal, Vol. 17, No. 8, pp. 921-924, 1979.

164. Belvin, W.K., "Vibration and Buckling Studies of Pretensioned Structures," NASA-CP-2215, 1981.

165. Crawford, R.F., Benton, M.D., "Strength of Initially Wave Lattice Columns," [AIAA 79-0753], AIAA Journal, Vol. 18, No. 5, pp. 581-584, 1980.

5. Solar Power Satellite

166. Hansen, R.H., DiRamio, H., "Structures for Solar Power Satellites," Astronautics and Aeronautics, Vol. 16, Oct., pp. 55-59, 1978.

167. "Achievable Flatness in a Large Microwave Power Antenna Study," General Dynamics-Convair, Rept. No. CASD-NAS-78-011, Aug., 1978.

168. "Satellite Power System, Concept Development and Evaluation Program-Reference Reference System Report," DOE and NASA, DOE/ER-0023, Oct., 1978.

E. Accuracy Potential

169. Fager, J.A., "Large Space Erectable Antenna Stiffness Requirements," Journal of Spacecraft and Rockets, Vol. 17, No. 2, pp. 86-92, 1980.

170. Hedgepeth, J.M., "Accuracy Potential for Large Space Antenna Reflectors With Passive Structure", [AIAA 82-4136], Journal of Spacecraft and Rockets, Vol. 19, No. 3, pp. 211-217, 1982.

171. Hedgepeth, J.M., "Influence of Fabrication Tolerances on the Surface Accuracy of Large Antenna Structures," [AIAA 82-4116], AIAA Journal, Vol 20, No. 5, pp. 680-686, 1982.

F. Miscellaneous

172. Bellagamba, L., Yang, T.Y., "Minimum-Mass Structures with Constraints on Fundamental Natural Frequency," [AIAA 81-4295], AIAA Journal, Vol. 19, No. 11, pp. 1452-1458, 1981.

173. Kunz, K.E., "Orbital Transfer Propulsion and Large Space Systems," [AIAA-80-4131], Journal of Spacecraft and Rockets, Vol. 17, N R 6, pp. 495-500.

174. Oren, J.A., Cox, R.L., "Thermal Management for Large Space Platforms," [AIAA 81-0451], Journal of Spacecraft and Rockets, Vol. 19, No. 3, pp. 278-283, 1982.

175. Farrell, C.E., "Large Advanced Space Systems (LASS) Computer-Aided Design Program Additions," NASA-CP-2215, 1981.

Appendix 6.4

Mechanics and Materials Center
TEXAS A&M UNIVERSITY
College Station, Texas

EFFECT OF DEGRADATION OF MATERIAL PROPERTIES ON THE DYNAMIC RESPONSE OF LARGE SPACE STRUCTURES

S. KALYANASUNDARAM
J. D. LUTZ
W. E. HAISLER
D. H. ALLEN

MM 4875-84-14

JUNE 1984

SECURITY CLASSIFICATION OF THIS PAGE

REPORT DOCUMENTATION PAGE

1a. REPORT SECURITY CLASSIFICATION: Unclassified	1b. RESTRICTIVE MARKINGS
2a. SECURITY CLASSIFICATION AUTHORITY	3. DISTRIBUTION/AVAILABILITY OF REPORT: Unlimited
2b. DECLASSIFICATION/DOWNGRADING SCHEDULE	
4. PERFORMING ORGANIZATION REPORT NUMBER(S): MM 4875-84-14	5. MONITORING ORGANIZATION REPORT NUMBER(S)
6a. NAME OF PERFORMING ORGANIZATION: Aerospace Engineering Department; 6b. OFFICE SYMBOL (If applicable)	7a. NAME OF MONITORING ORGANIZATION: Air Force Office of Scientific Research Bolling AFB Washington, D. C. 20332
6c. ADDRESS (City, State and ZIP Code): Texas A&M University College Station, Texas 77843	7b. ADDRESS (City, State and ZIP Code)
8a. NAME OF FUNDING/SPONSORING ORGANIZATION; 8b. OFFICE SYMBOL (If applicable)	9. PROCUREMENT INSTRUMENT IDENTIFICATION NUMBER: F 49620-83-C-0067
8c. ADDRESS (City, State and ZIP Code)	10. SOURCE OF FUNDING NOS.

PROGRAM ELEMENT NO.	PROJECT NO.	TASK NO.	WORK UNIT NO.

11. TITLE (Include Security Classification): Effect of Degradation of Material Properties on the dynamic Response of Large Space Structures

12. PERSONAL AUTHOR(S): S. Kalyanasundaram, J. D. Lutz, W. E. Haisler, and D. H. Allen

13a. TYPE OF REPORT	13b. TIME COVERED	14. DATE OF REPORT (Yr., Mo., Day)	15. PAGE COUNT
Interim	FROM Mar 83 TO Apr 84	June, 1984	27

16. SUPPLEMENTARY NOTATION

17. COSATI CODES			18. SUBJECT TERMS (Continue on reverse if necessary and identify by block number)
FIELD	GROUP	SUB. GR.	

19. ABSTRACT (Continue on reverse if necessary and identify by block number)

In this paper the effect of degradation of material properties on structural frequencies and mode shapes of Large Space Structures is investigated. The difficulty and cost of maintenance of LSS make it a necessity to design these structures to operate with a certain degree of damage. The techniques for achieving modal control will require a more accurate knowledge of modal characteristics.

The sensitivity studies conducted on selected space truss and plane frame problems indicate that the degradation of material properties may have a significant effect on the structural mode shapes and frequencies. For even small amounts of degradation (10%), frequencies and location of nodes may change significantly. It is clear that these effects must be taken into consideration when designing the control system for Large Space Structures.

20. DISTRIBUTION/AVAILABILITY OF ABSTRACT	21. ABSTRACT SECURITY CLASSIFICATION	
UNCLASSIFIED/UNLIMITED ☒ SAME AS RPT ☐ DTIC USERS ☐		
22a. NAME OF RESPONSIBLE INDIVIDUAL: Dr. Tony Amos	22b. TELEPHONE NUMBER (Include Area Code): (202) 767-4937	22c. OFFICE SYMBOL

DD FORM 1473, 83 APR EDITION OF 1 JAN 73 IS OBSOLETE

SECURITY CLASSIFICATION OF THIS PAGE

EFFECT OF DEGRADATION OF MATERIAL PROPERTIES ON THE DYNAMIC RESPONSE OF LARGE SPACE STRUCTURES

by

S. Kalyanasundaram, Graduate Assistant
Dept. of Aerospace Engineering
Texas A&M University
College Station, Texas 77843

J. D. Lutz, Graduate Assistant
Dept. of Aerospace Engineering
Texas A&M University
College Station, Texas 77843

W. E. Haisler, Professor
Dept of Aerospace Engineering
Texas A&M University
College Station, Texas 77843

D. H. Allen, Assistant Professor
Dept. of Aerospace Engineering
Texas A&M University
College Station, Texas 77843

June 1984

Effect of Degradation of Material Properties on the Dynamic Response of Large Space Structures

by

S. Kalyanasundaram, J. D. Lutz, W. E. Haisler, and D. H. Allen

ABSTRACT

In this paper the effect of degradation of material properties on structural frequencies and mode shapes of Large Space Structures is investigated. The difficulty and cost of maintenance of LSS make it a necessity to design these structures to operate with a certain damage. The techniques for achieving modal control will require a more accurate knowledge of modal characteristics.

The sensitivity studies conducted on selected space truss and plane frame problems indicate that the degradation of material properties may have a significant effect on the structural mode shapes and frequencies. For even small amounts of degradation(10%), frequencies and location of nodes may change significantly. It is clear that these effects must be taken into consideration when designing the control systems for large space structures.

INTRODUCTION

It is projected that advanced aerospace materials will be required in the future generation of space structures. To make the optimum use of these materials, the effect of environmental conditions and complicated loading histories need to be studied. One of the important consequences of the extreme loading conditions will be the degradation of the material properties of the structural components.

The observed reduction in stiffness is often a good indication of damage development in the life of these structural components. Degradation of material properties usually leads to the reduction of stiffness which affects the dynamic response. In this report, sensitivity studies will be presented which investigate the effect of stiffness on structural frequencies and mode shapes.

IMPORTANCE OF STRUCTURAL FREQUENCIES AND MODE SHAPES

The advent of the Space Shuttle has made possible the development of Large Space Structures (LSS). Control systems for stabilizing and maneuvering these very large space structures, especially those for precise pointing, will require extensions of our present technology.

Large size by itself does not arouse concern, but the structural flexibility resulting from minimizing the structural weight, while increasing physical dimension may present problems. At some point, deformations from structural flexibility result in sufficiently large amplitudes and very low frequencies (.01 to 10Hz) which create new complications for control designers.

As an example of the precision being sought [1], a typical radiometry application may utilize a 200-m antenna with a effective beam width of 0.01 deg. and have requirements limiting the vibratory beam shift to less than 0.005 deg. and dynamic surface distortions to less than 1mm. Maneuvering or maintaining altitude of such

a satellite leads to flexible body motion and this must be well predicted and controlled.

The importance of interaction between the control systems and vibratory response has influenced alot of research in LSS control system [2-4]. The current practice of guaranteeing a large seperation between modal frequencies and the bandwidth of control will not be adequate in future applications. The combination of large size and payload-weight restrictions will drive structural frequencies down and need for more accurate pointing will drive the control system bandwidth up. When the frequency separation becomes impossible, there exists a need for adaptive control systems. This leads to further research in design of structural control systems actuatorsensor placement and distributed sensing and actuator as opposed to co-located sensors and actuator .

The techniques for achieving modal control will require a more accurate knowledge of modal characterisctics. Optimum sensor and actuator placement will be greatly influenced by modal effects which must be known to a greater degree of precision.

The difficulty and cost of maintenance of LSS make it a necessity to design these structures to operate with a certain degree of damage. Current research on damage characterization of advanced aerospace materials [5-9] indicates a stiffness reduction as high as 25% that can occur during the life span of these materials. Thus, there is clearly a need to study the effect of stiffness reduction in structural frequencies and mode shapes.

MODEL DESCRIPTION

The effect of stiffness reduction (resulting from material damage) is investigated in this report for selected space truss and plane frame problems. The frequencies and mode shapes were found using finite element programs incorporating standard space truss and plane frame elements.

The damage is modeled in this study as a reduction in stiffness for all the structural elements. The amount of reduction in stiffness is assumed to be proportional to the stress in the structural element with a maximum reduction occuring in the highest stressed element.

The following equations govern the severity and distribution of damage:

$$E' = E_o\left[\frac{1-k\sigma}{Y}\right]$$

E' = Reduced modulus of the element

E_o = undegraded modulus of the element

k= Constant of degradation

σ= stress in the element

Y = Yield stress

The linear form of the material damage law is used herein for simplicity. In reality, the damage law will be more complex and history dependent. Damage laws are currently being developed [9-11] and will be considered in future research. The effect of residual stress is not considered here and a quasi-elastic behavior is assumed.

In addition to the above model, random reduction in stiffness was also considered to study the effect of degradation of some members that might experience severe loading histories.

Figure [1] illustrates the geometry of the example space truss. This structure has 10 bays and is fixed at one end. 124 space truss elements are used in the finite element model. In the initial undegraded configuration, the material properties are

124 ELEMENT SPACE TRUSS

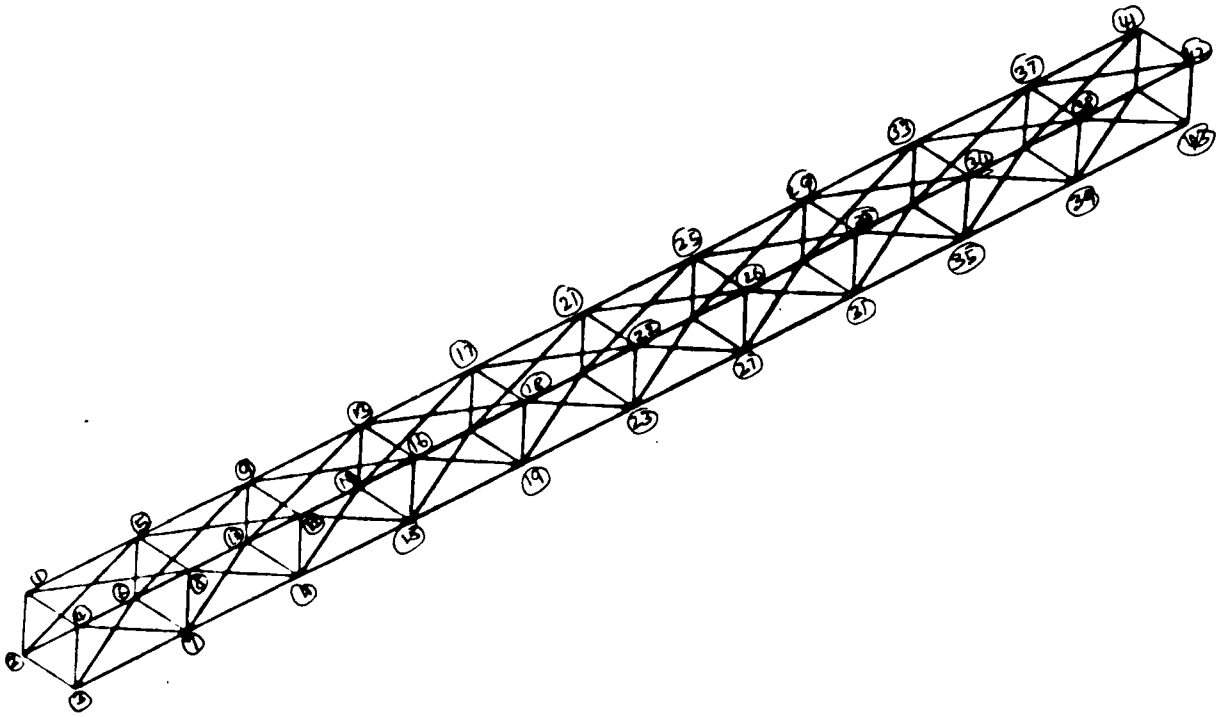

FIGURE NO. 1

21 ELEMENT PLANE FRAME

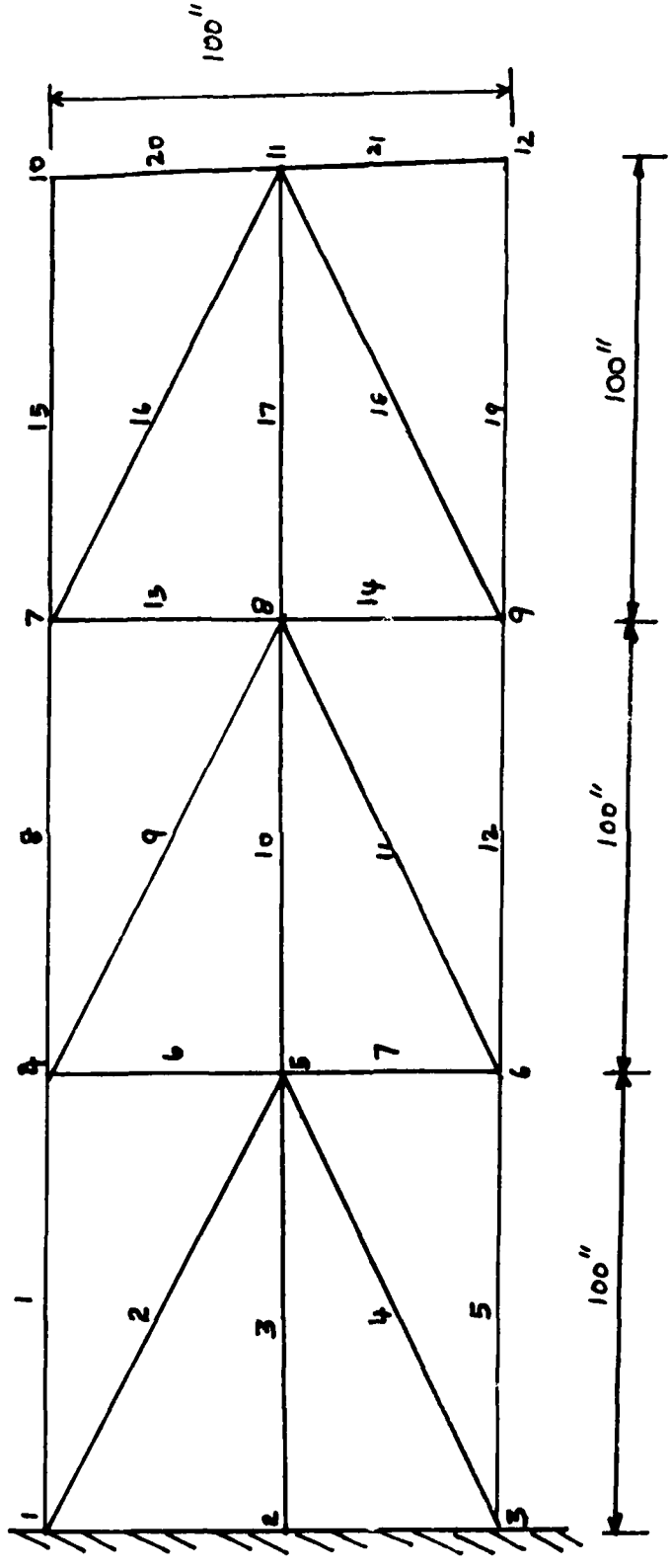

FIGURE NO. 2

12 ELEMENT PLANE TRUSS

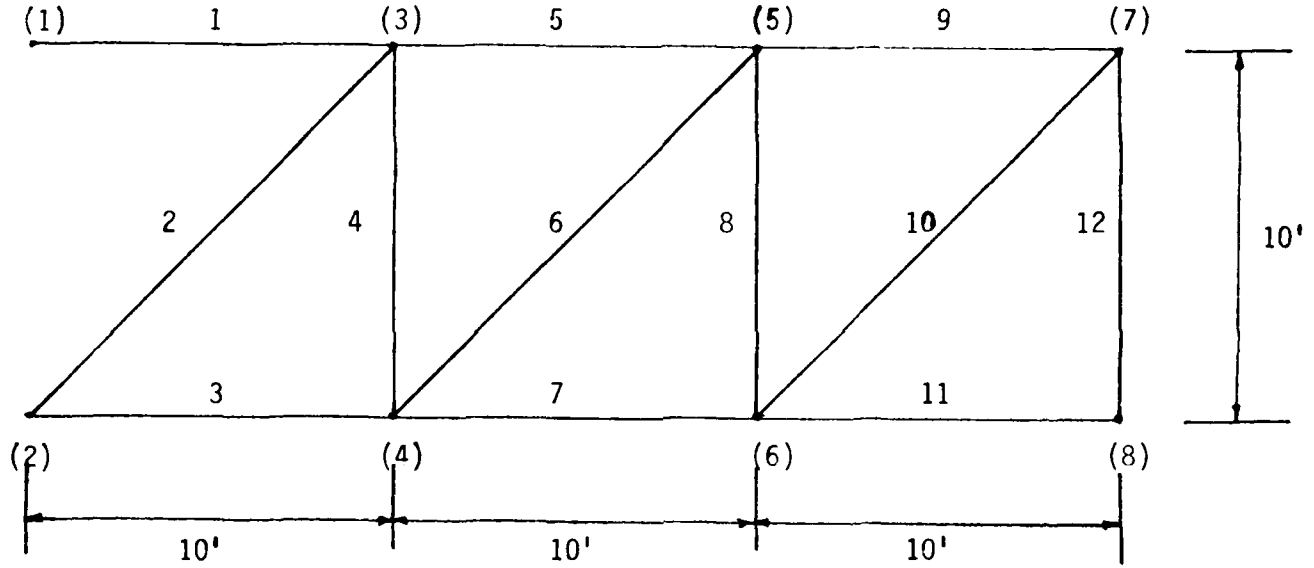

FIGURE NO. 3

same for all members with the following values:

Material type - Graphite Epoxy (Hexel)

Young's modulus $E = 21.5 \times 10^6$ psi

Cross sectional area $A = 1.0$ in^2

Density $\rho = 0.065$ lb/in^3

Figure [2] is the finite element model of the plane frame. 21 frame elements are used. The undegraded material properties (same for all members) are given below:

Material type - graphite epoxy (Hexel)

Young's modulus $E = 16 \times 10^6$ psi

Cross sectional area $A = 1.37$ in^2

Moment of Inertia $I_z = 0.033$ in^4

density $\rho = 0.06$ lb/in^3

Figure [3] is the plane truss model with the same material properties as the space truss model.. 12 Truss elements are used to model this case to study the effect of random reduction in stiffness.

DISCUSSION OF RESULTS

In figure [14], the first two natural frequencies are plotted for different magnitude of damage for the space truss. The properties were degraded by using stress obtained from displacements corresponding to the first mode shapes. Consequently the damage or stiffness degradation varies spatially from element to element and, in general, is greatest at the fixed end ($x = 0$)

The effects of damage on frequencies of the truss are clear. Increase of damage results in a decrease of frequencies due to the reduction in the stiffness. A maximum

damage of 25% results in a frequency reduction of nearly 10% for the first two natural frequencies.

The vertical deflection of the free end of the truss corresponding to the first mode is plotted in Figure (5) for the case of undegraded and 25% degraded cases. Damage has little effect on this mode shape with the difference in deflection at any node being less than 2%. The second mode shape gives interesting results. Figure (6) shows deflections for different damage. The plot indicates a change in modal deflection of 9% for 5% damage to nearly 73% change for 25% damage. The location of the mode (zero displacement) changes drastically. Such a movement of the systems mode would require very "robust" control. The third mode shape produces similar results with large changes in the modal displacement and is plotted in Figure 7. Thus the damage has a significant effect on natural frequencies and mode shapes.

For the study of random damage effects on the 12 element plane truss (Figure 3), the following three cases are used: 50% stiffness reduction to element 9 (2) 50% stiffness reduction to elements 8, 9, and 10, and (3) 50% stiffness reduction to elements 4, 5, 6, 8, 9, 10 and 12. Figure (8) gives the plot of the first two frequencies for different cases. The frequencies decrease as tthe properties of more elements are degraded. This is due to the reduction in stiffness. Figures 9 and 10 compare the first two mode shapes for the different cases. There are some variations in the mode shapes for the different cases.

The effect of damage on the plane frame problem is investigated by varying the maximum reduction of stiffness from 5% to 25%. It is found that the vertical members and the members near the fixed end are more affected when the properties were degraded in a similar fashion to space truss problem (i.e., using stress calculated from displacement corresponding to the first mode). Figure 11 illustrates the effect of damage in the first three frequencies. The frequencies decrease with the increase of damage from 5% to 25%. Figures 12, 13 and 14 give plots of vertical displacements corresponding to the first threee mode shapes along the elements 1, 18 and 15. There

is a small variation corresponding to the first and third mode shapes. For the second there is significant variation in the mode shape for damaged and undamaged cases.

For the study of random damage effects on the plane frame, the following three cases are used: (1) 25% stiffness reduction to element 15, (2) 25% stiffness reduction to elements 8, 15 and (3) 25% stiffness reduction to elements 8, 15 and 1. These elements are located at the top of the frame and might be damaged in this fashion due to localized impactm heating, etc. The frequencies decrease as stiffness of more number of elements are reduced and the first three mode shapes are plotted in figures 15,16 and 17

To investigate the effect of damage on the transient response, the space truss model (figure 1.) is subjected to an impact load of 10,000 lbs at nodes 29 and 30 in the transverse direction. The duration of the load is one second. Figure 18 gives the plot of vertical displacement vs. time for the node 41 at the free end. There is a change in both the frequency and the amplitude of response.

The next loading is a cycle temperature loading with a period of one day. The temperature distribution is uniform over the structure. Figure 19 depicts the vertical response of node 41 vs. time for a maximum temperature difference of 250^{o} at the mid point of each element. The amplitude increases with the loss of stiffness. The amplitude increases by 17% for the most severly damaged case (a maximum of 25% stiffness reduction).

CONCLUSION

This study confirms the need for a more accurate knowledge of modal characteristics for large space structures. Degradation of material properties may have a significant effect on the structural mode shapes and frequencies. For even small amounts of degradation (10%), frequencies and location of nodes may change significantly. It is clear that these effects must be taken into consideration when designing the control systems for large space structures.

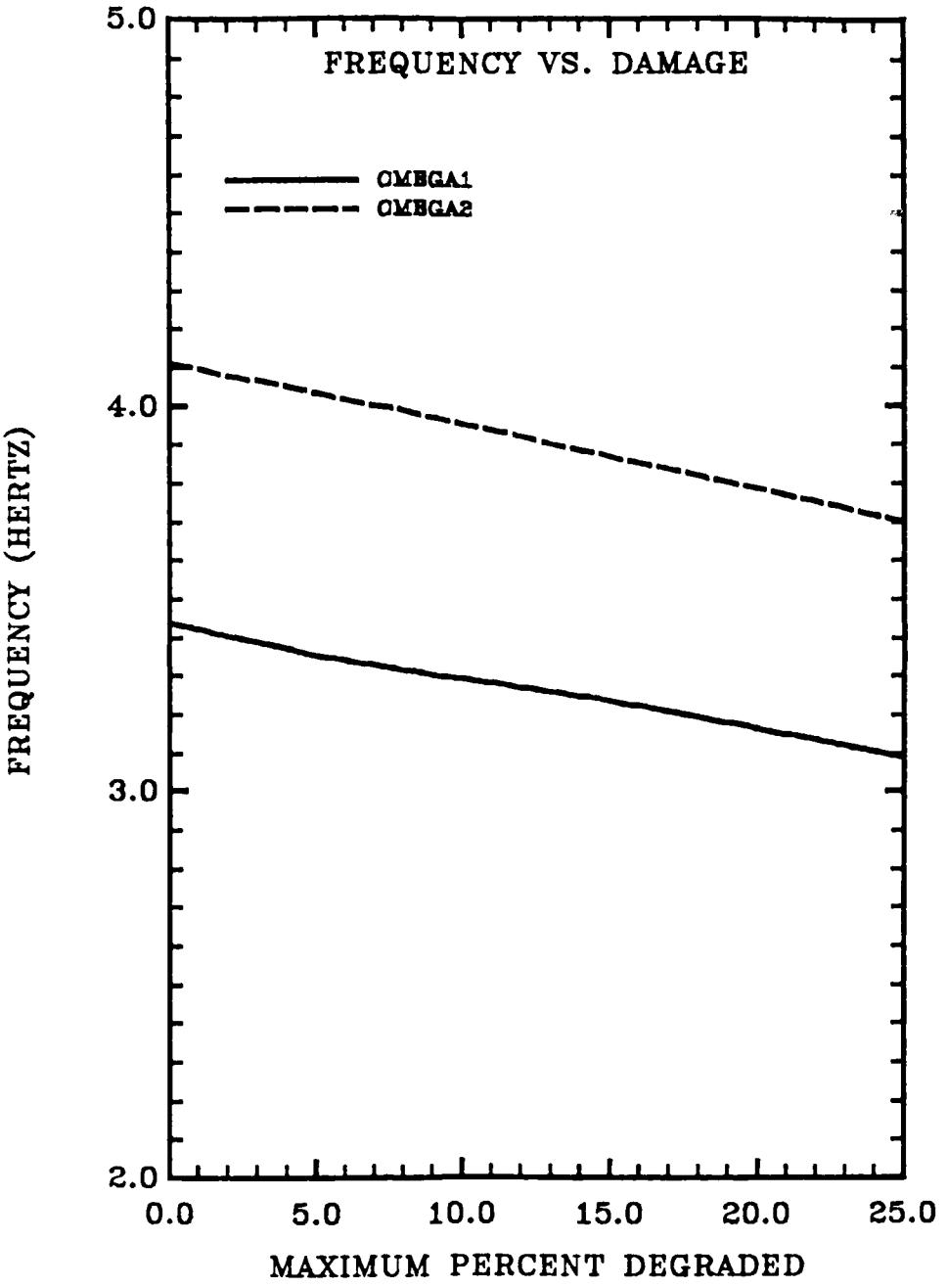
FREQUENCY VS. DAMAGE
OMEGA1
OMEGA2
FREQUENCY (HERTZ)
5.0
4.0
3.0
2.0
0.0
5.0
10.0
15.0
20.0
25.0
MAXIMUM PERCENT DEGRADED

FIGURE NO. 4

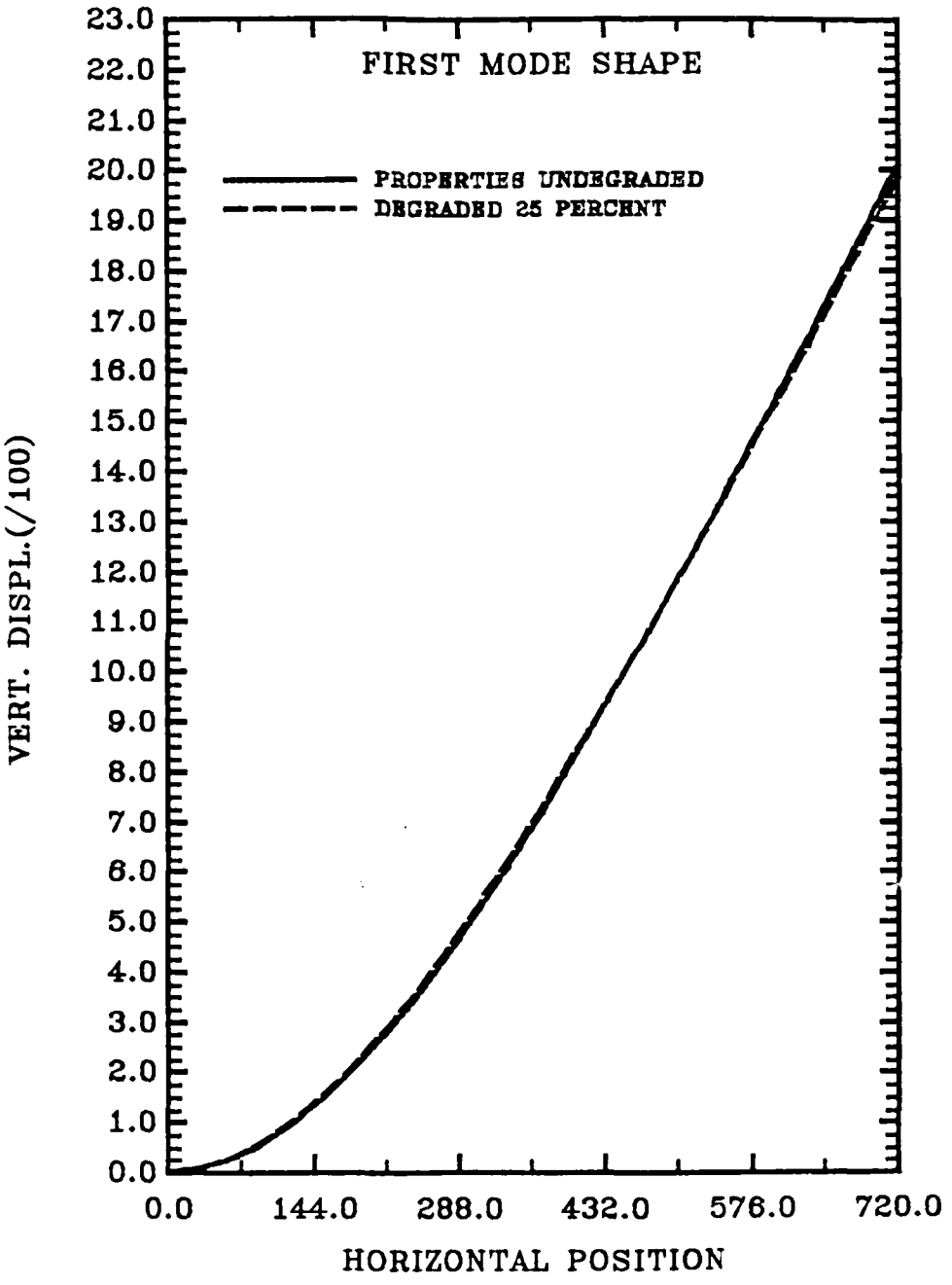
FIRST MODE SHAPE
PROPERTIES UNDEGRADED
DEGRADED 25 PERCENT
VERT. DISPL.(/100)
23.0
22.0
21.0
20.0
19.0
18.0
17.0
16.0
15.0
14.0
13.0
12.0
11.0
10.0
9.0
8.0
7.0
6.0
5.0
4.0
3.0
2.0
1.0
0.0
0.0
144.0
288.0
432.0
576.0
720.0
HORIZONTAL POSITION

FIGURE NO. 5

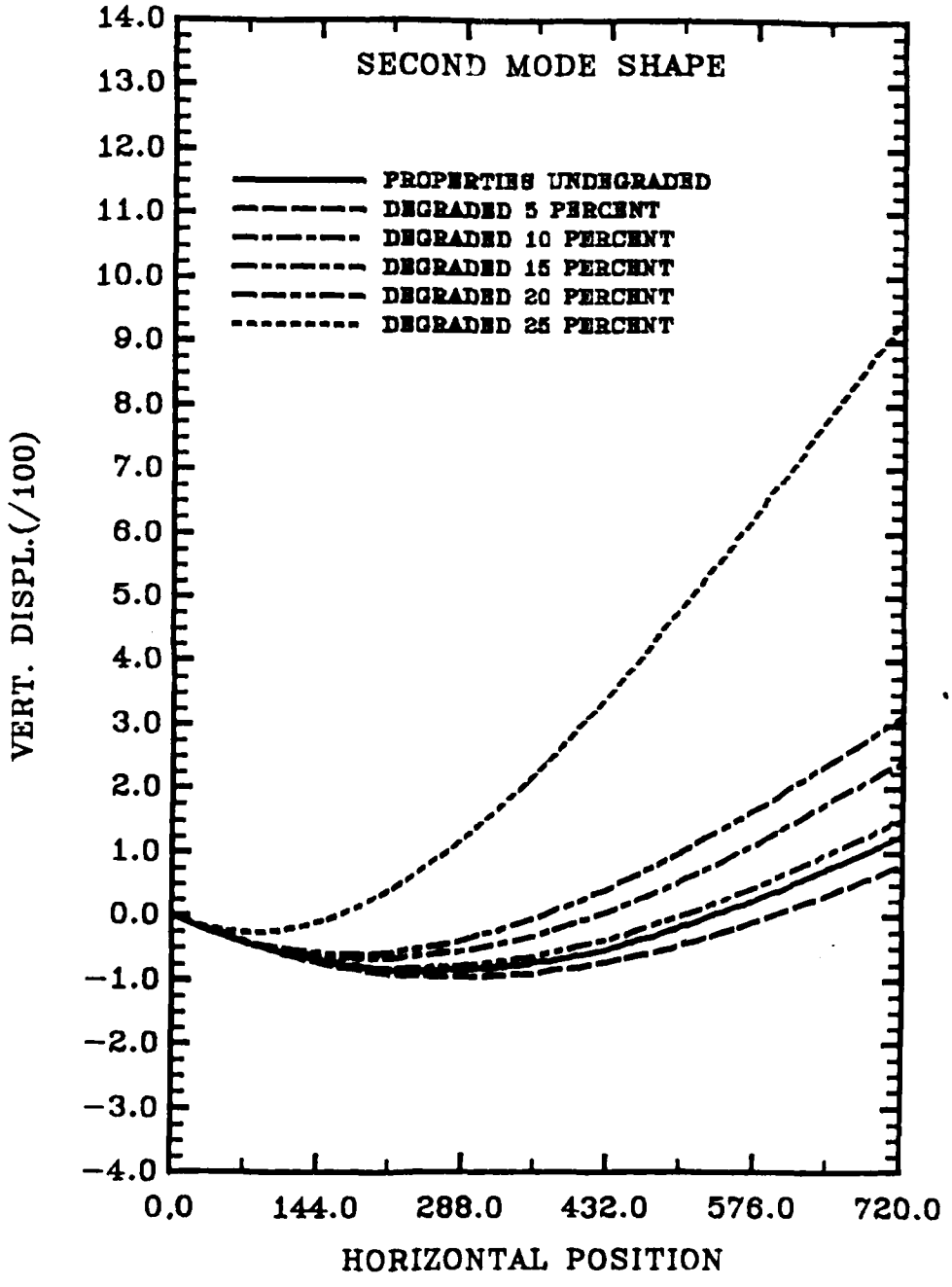
SECOND MODE SHAPE
PROPERTIES UNDEGRADED
DEGRADED 5 PERCENT
DEGRADED 10 PERCENT
DEGRADED 15 PERCENT
DEGRADED 20 PERCENT
DEGRADED 25 PERCENT
VERT. DISPL.(/100)
14.0
13.0
12.0
11.0
10.0
9.0
8.0
7.0
6.0
5.0
4.0
3.0
2.0
1.0
0.0
-1.0
-2.0
-3.0
-4.0
0.0
144.0
288.0
432.0
576.0
720.0
HORIZONTAL POSITION

FIGURE NO. 6

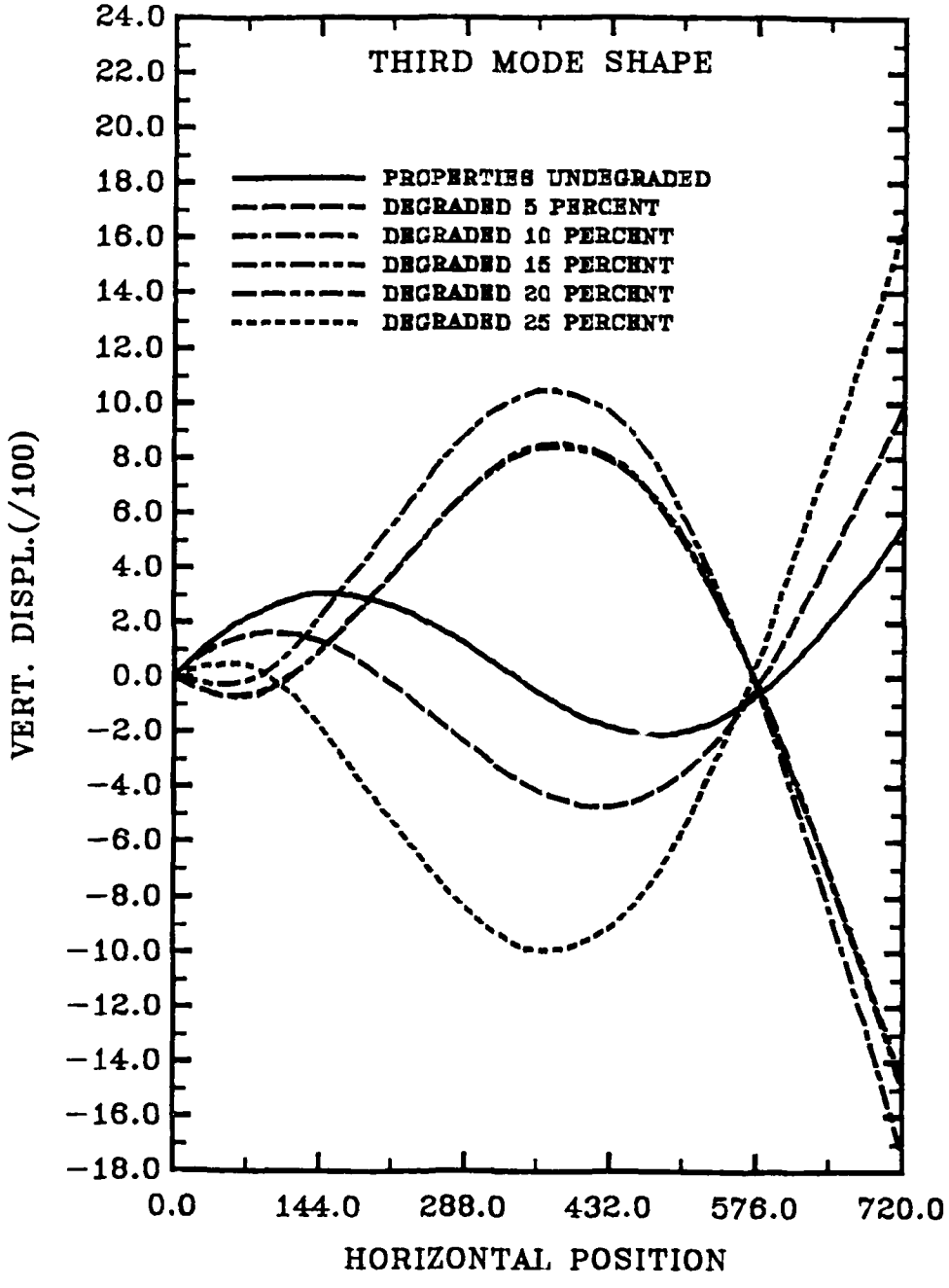
THIRD MODE SHAPE
PROPERTIES UNDEGRADED
DEGRADED 5 PERCENT
DEGRADED 10 PERCENT
DEGRADED 15 PERCENT
DEGRADED 20 PERCENT
DEGRADED 25 PERCENT
VERT. DISPL.(/100)
24.0
22.0
20.0
18.0
16.0
14.0
12.0
10.0
8.0
6.0
4.0
2.0
0.0
-2.0
-4.0
-6.0
-8.0
-10.0
-12.0
-14.0
-16.0
-18.0
0.0
144.0
288.0
432.0
576.0
720.0
HORIZONTAL POSITION

FIGURE NO. 7

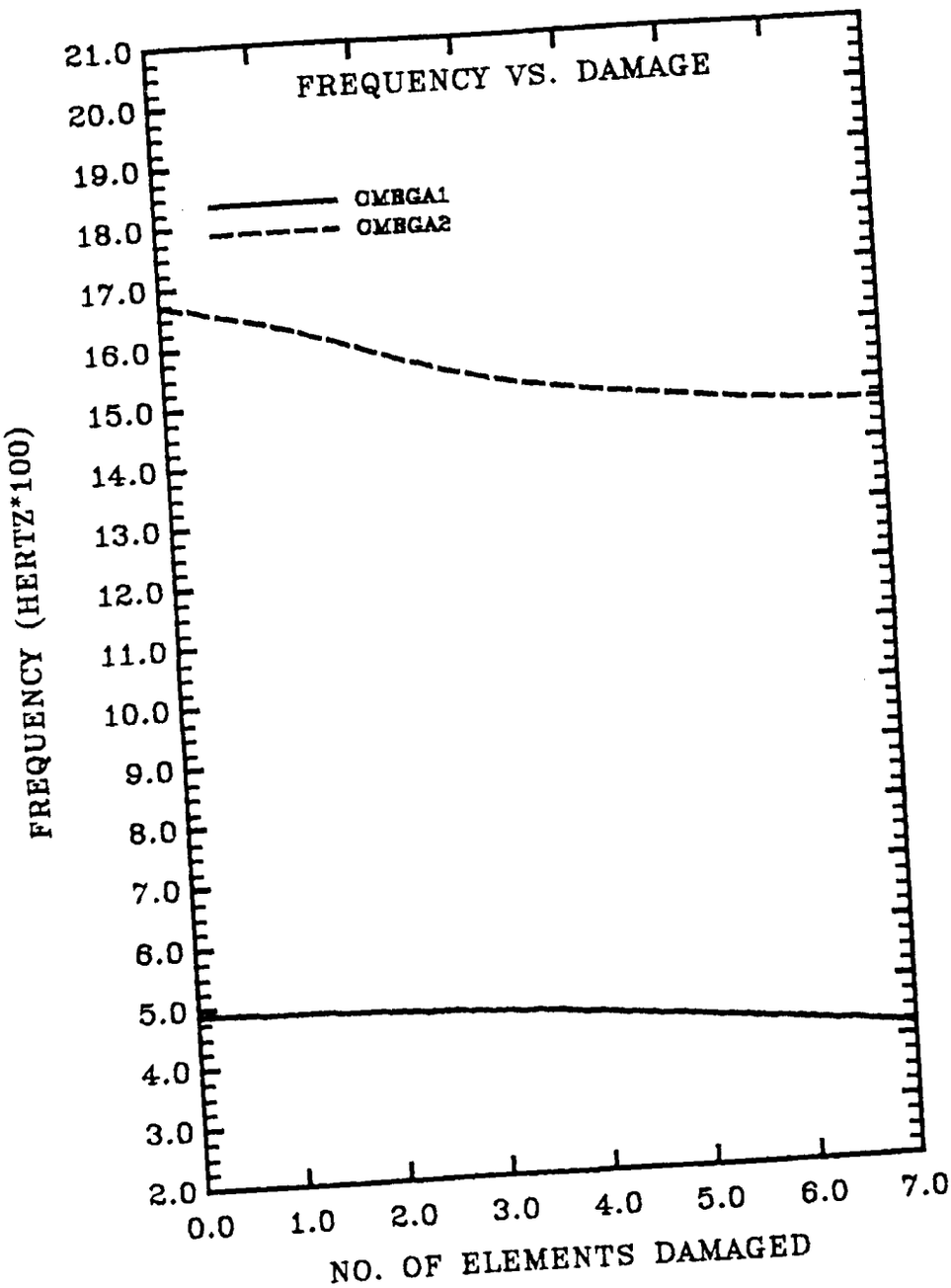
FREQUENCY VS. DAMAGE
OMEGA1
OMEGA2
FREQUENCY (HERTZ*100)
21.0
20.0
19.0
18.0
17.0
16.0
15.0
14.0
13.0
12.0
11.0
10.0
9.0
8.0
7.0
6.0
5.0
4.0
3.0
2.0
0.0
1.0
2.0
3.0
4.0
5.0
6.0
7.0
NO. OF ELEMENTS DAMAGED

FIGURE NO. 8

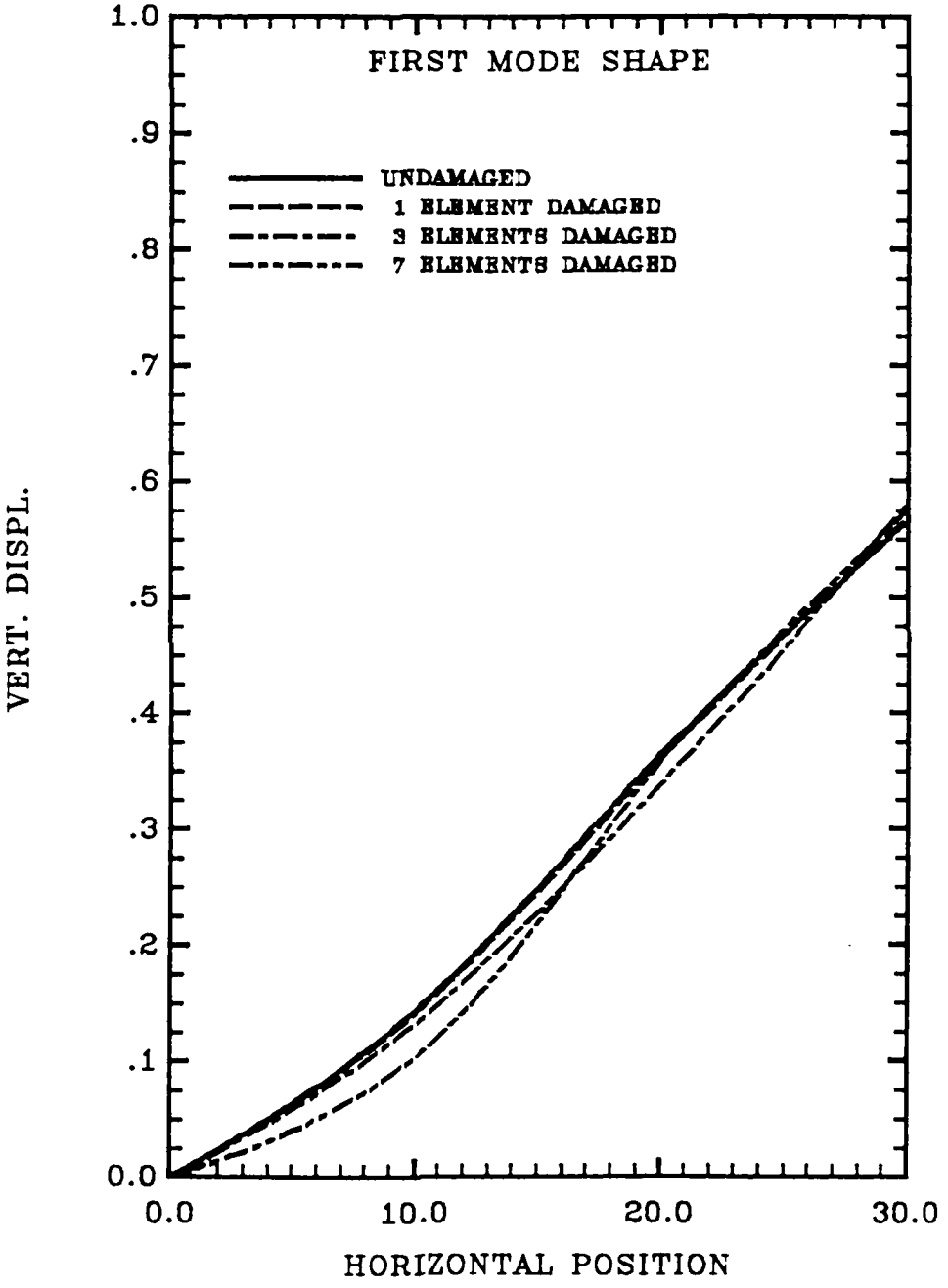
FIRST MODE SHAPE
UNDAMAGED
1 ELEMENT DAMAGED
3 ELEMENTS DAMAGED
7 ELEMENTS DAMAGED
VERT. DISPL.
1.0
.9
.8
.7
.6
.5
.4
.3
.2
.1
0.0
0.0
10.0
20.0
30.0
HORIZONTAL POSITION

FIGURE NO. 9

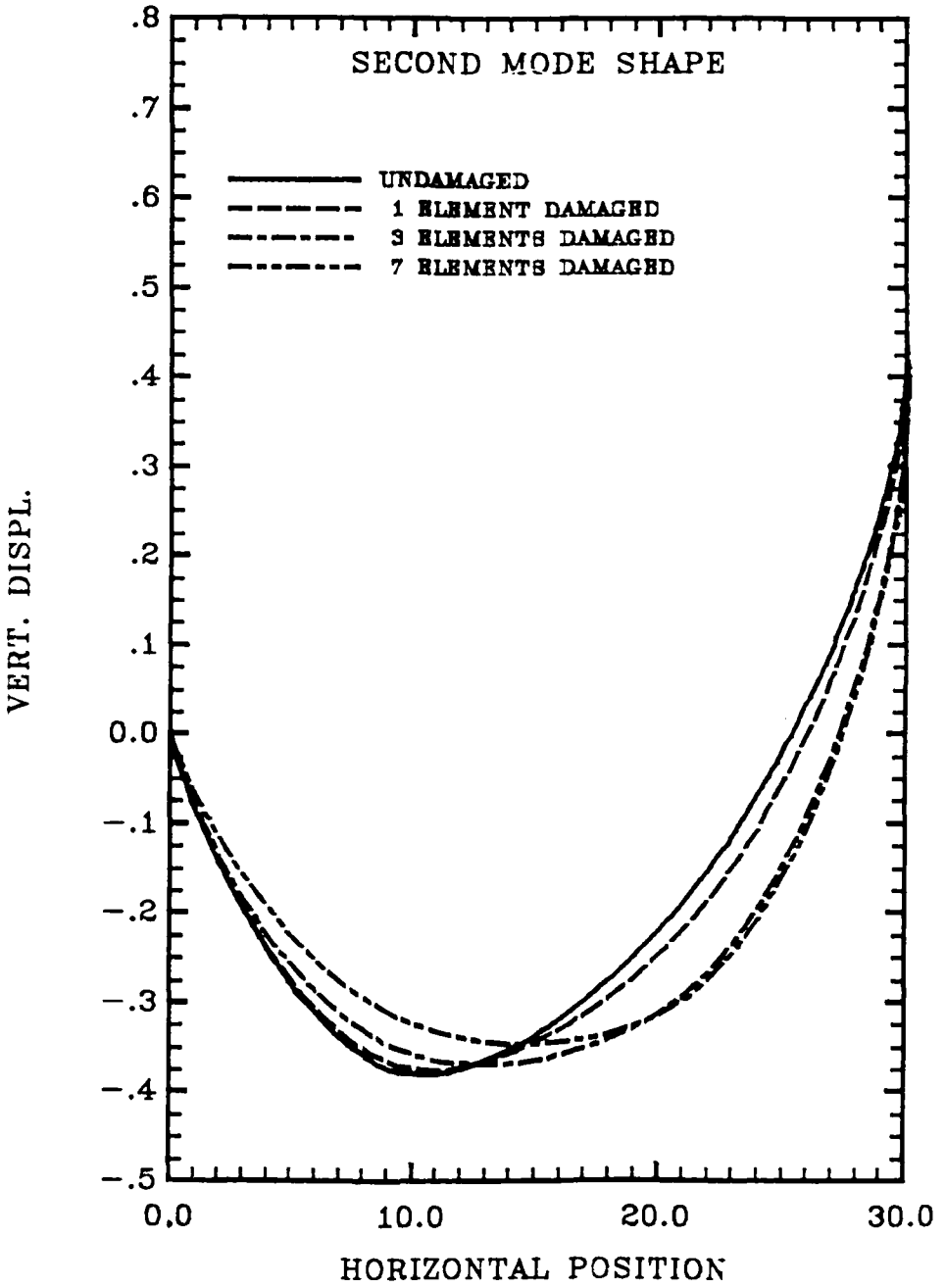
SECOND MODE SHAPE
UNDAMAGED
1 ELEMENT DAMAGED
3 ELEMENTS DAMAGED
7 ELEMENTS DAMAGED
VERT. DISPL.
.8
.7
.6
.5
.4
.3
.2
.1
0.0
-.1
-.2
-.3
-.4
-.5
0.0
10.0
20.0
30.0
HORIZONTAL POSITION

FIGURE NO. 10

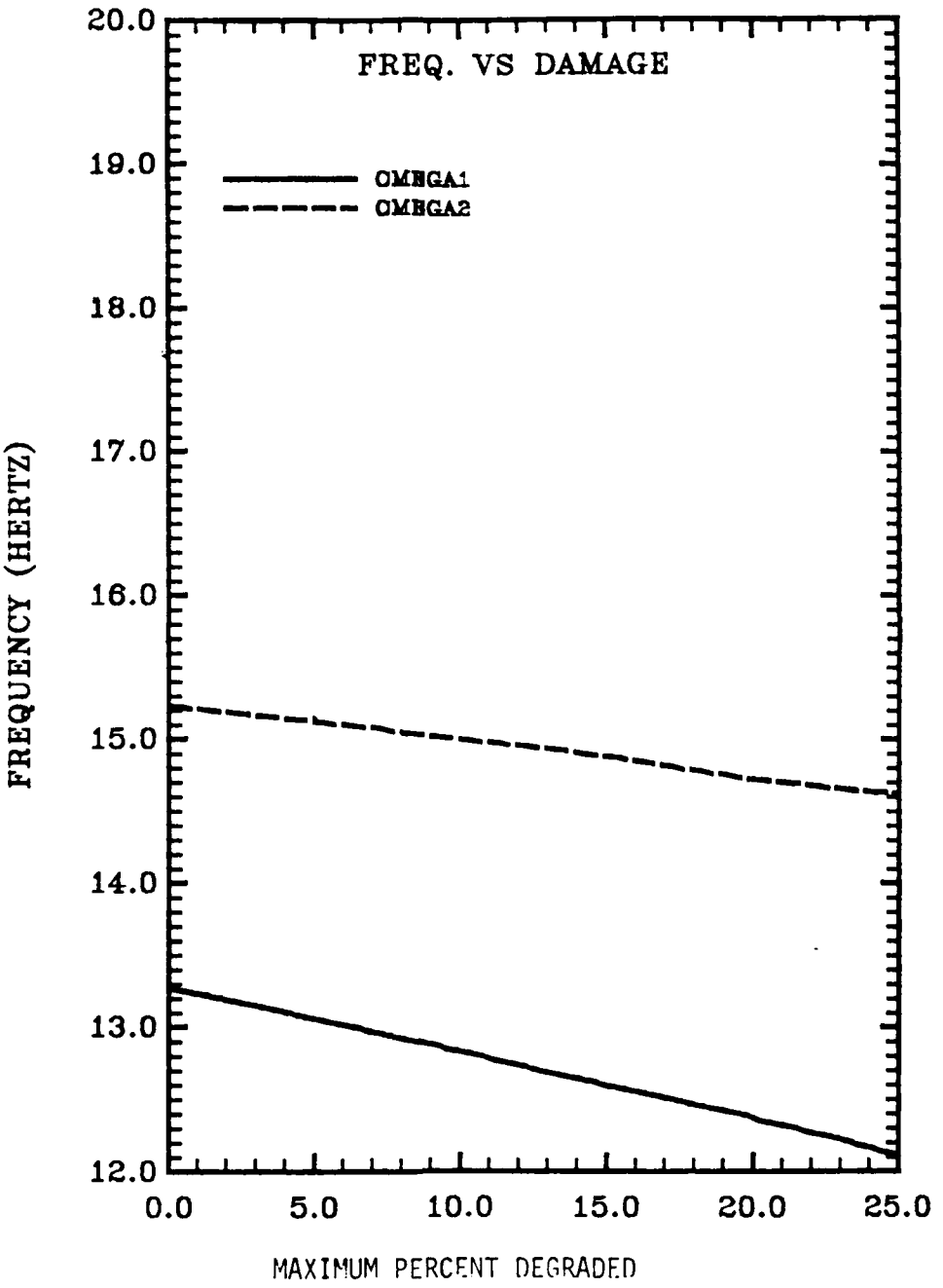
FREQ. VS DAMAGE
OMEGA1
OMEGA2
FREQUENCY (HERTZ)
20.0
19.0
18.0
17.0
16.0
15.0
14.0
13.0
12.0
0.0
5.0
10.0
15.0
20.0
25.0
MAXIMUM PERCENT DEGRADED

FIGURE NO. 11

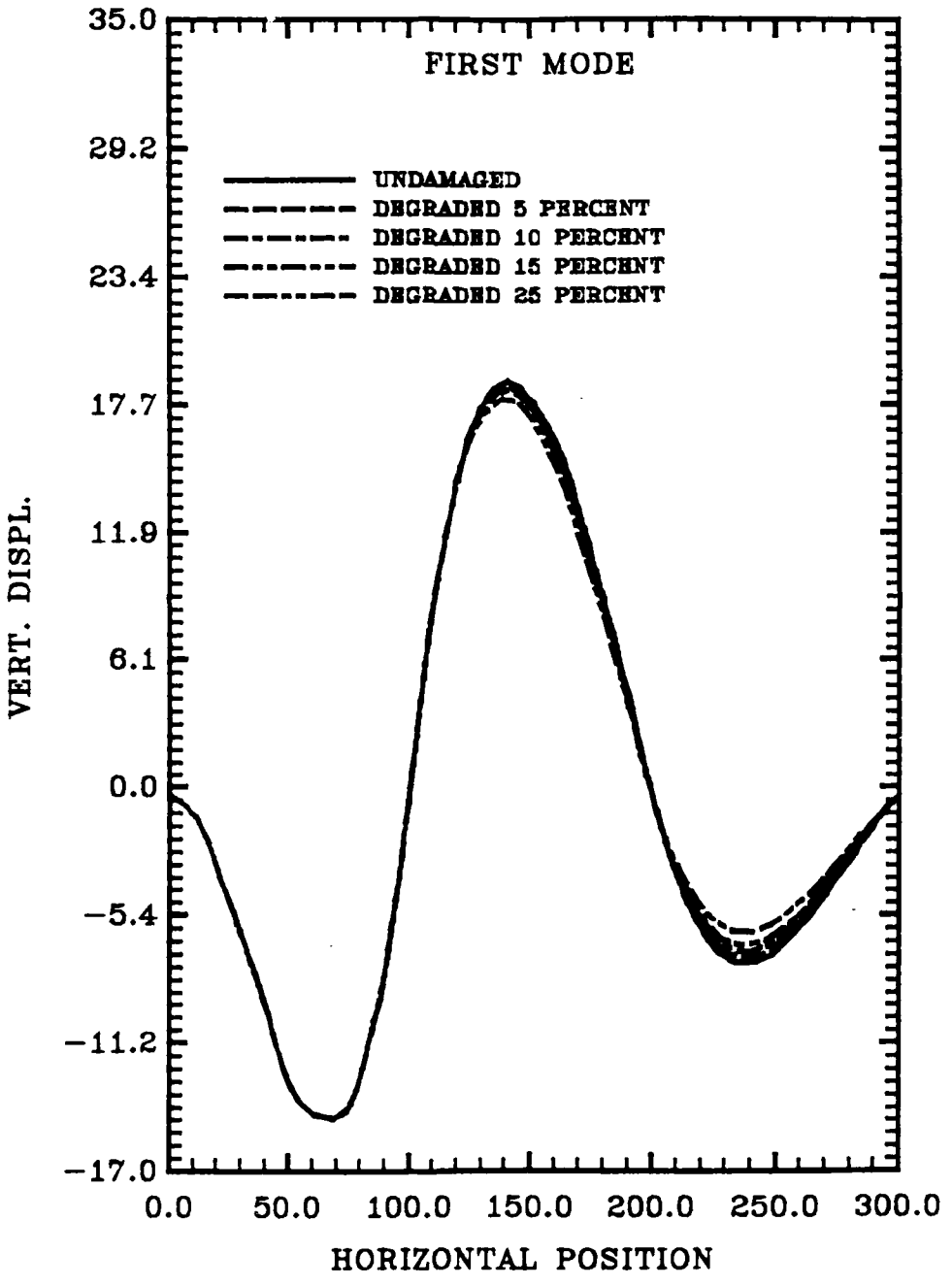
FIRST MODE
UNDAMAGED
DEGRADED 5 PERCENT
DEGRADED 10 PERCENT
DEGRADED 15 PERCENT
DEGRADED 25 PERCENT
35.0
29.2
23.4
17.7
11.9
6.1
0.0
-5.4
-11.2
-17.0
VERT. DISPL.
0.0
50.0
100.0
150.0
200.0
250.0
300.0
HORIZONTAL POSITION

FIGURE NO. 12

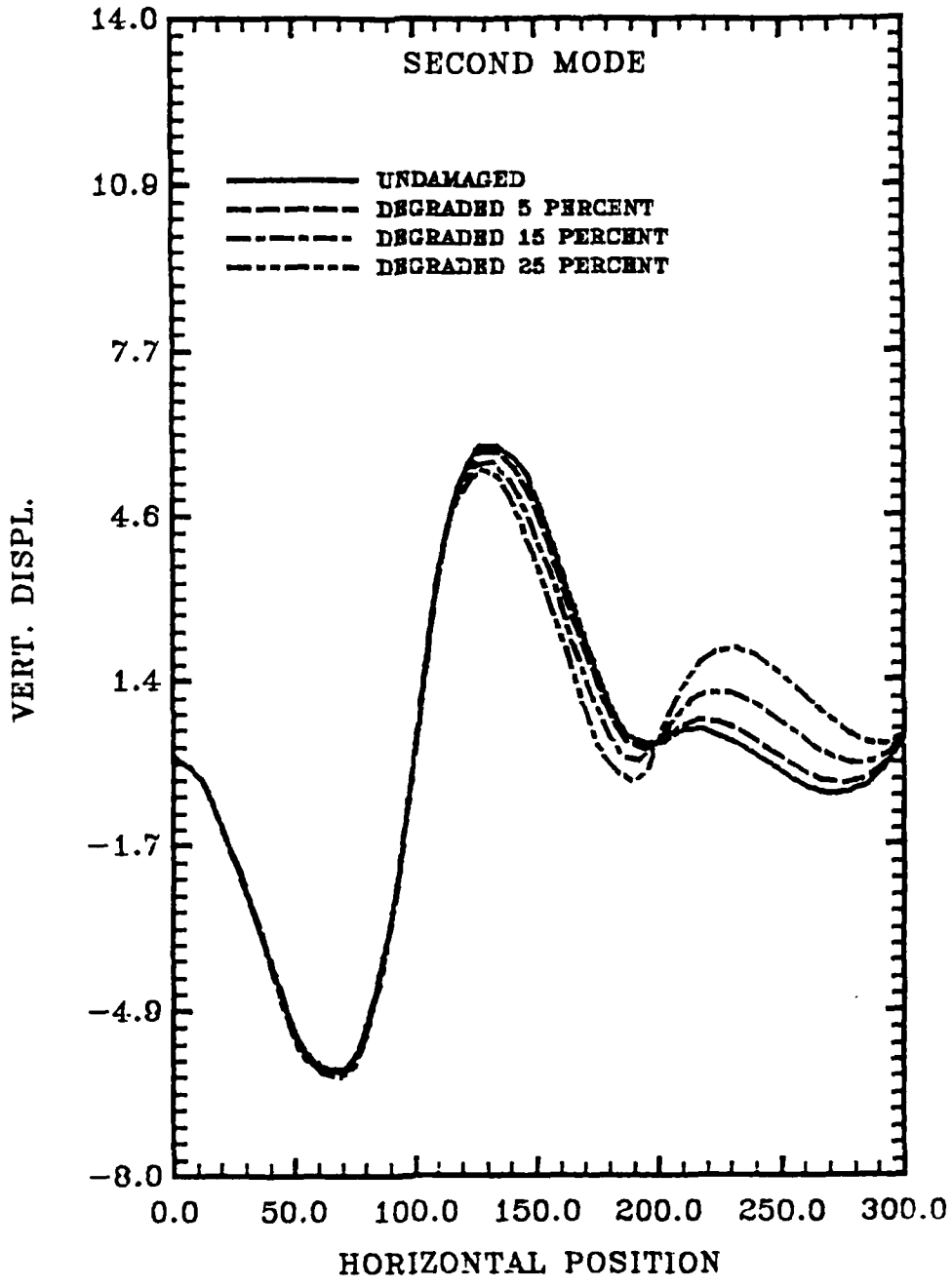
SECOND MODE
UNDAMAGED
DEGRADED 5 PERCENT
DEGRADED 15 PERCENT
DEGRADED 25 PERCENT
VERT. DISPL.
14.0
10.9
7.7
4.6
1.4
-1.7
-4.9
-8.0
0.0
50.0
100.0
150.0
200.0
250.0
300.0
HORIZONTAL POSITION

FIGURE NO. 13

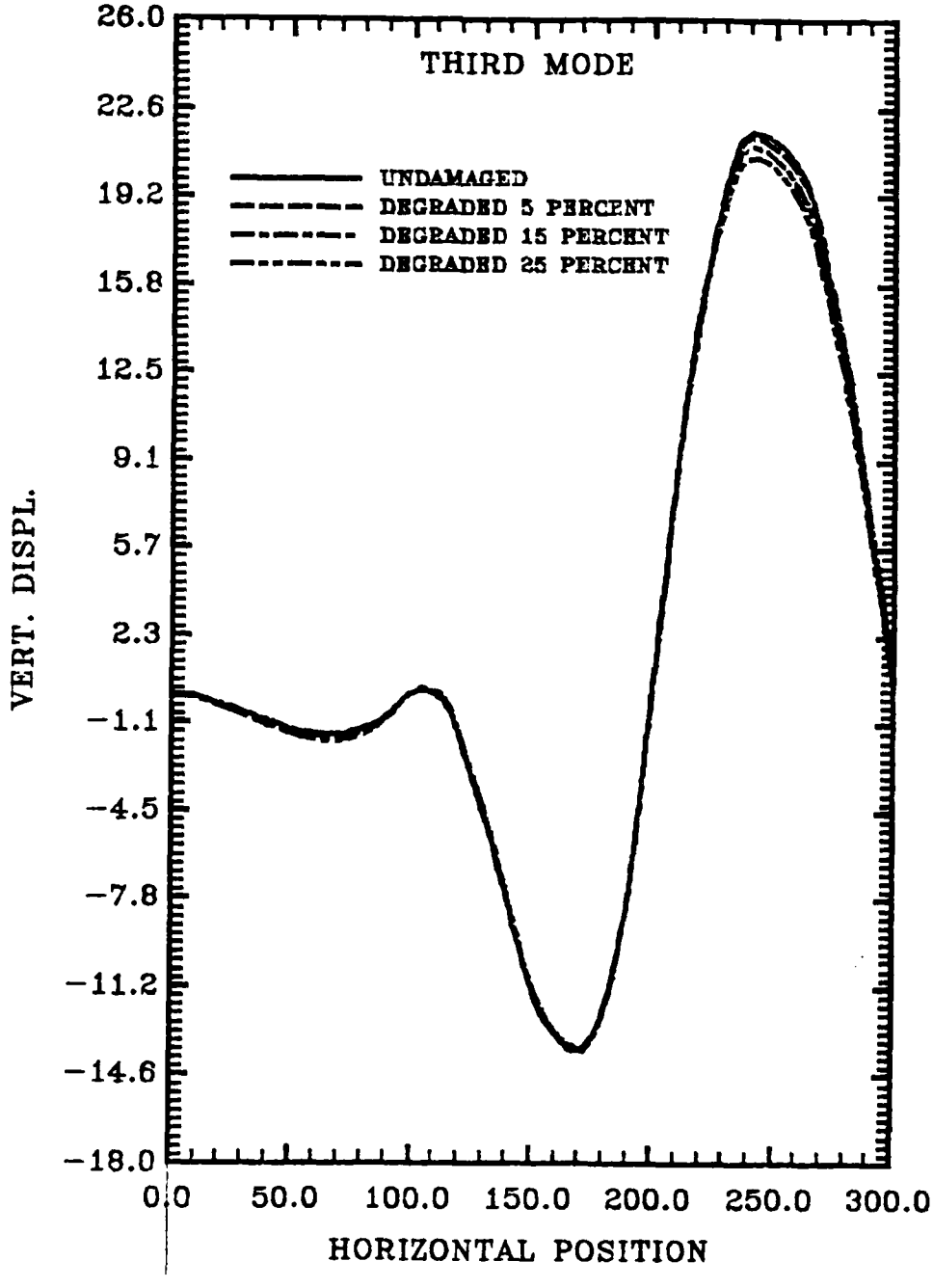
THIRD MODE
UNDAMAGED
DEGRADED 5 PERCENT
DEGRADED 15 PERCENT
DEGRADED 25 PERCENT
VERT. DISPL.
26.0
22.6
19.2
15.8
12.5
9.1
5.7
2.3
-1.1
-4.5
-7.8
-11.2
-14.6
-18.0
0.0
50.0
100.0
150.0
200.0
250.0
300.0
HORIZONTAL POSITION

FIGURE NO. 14

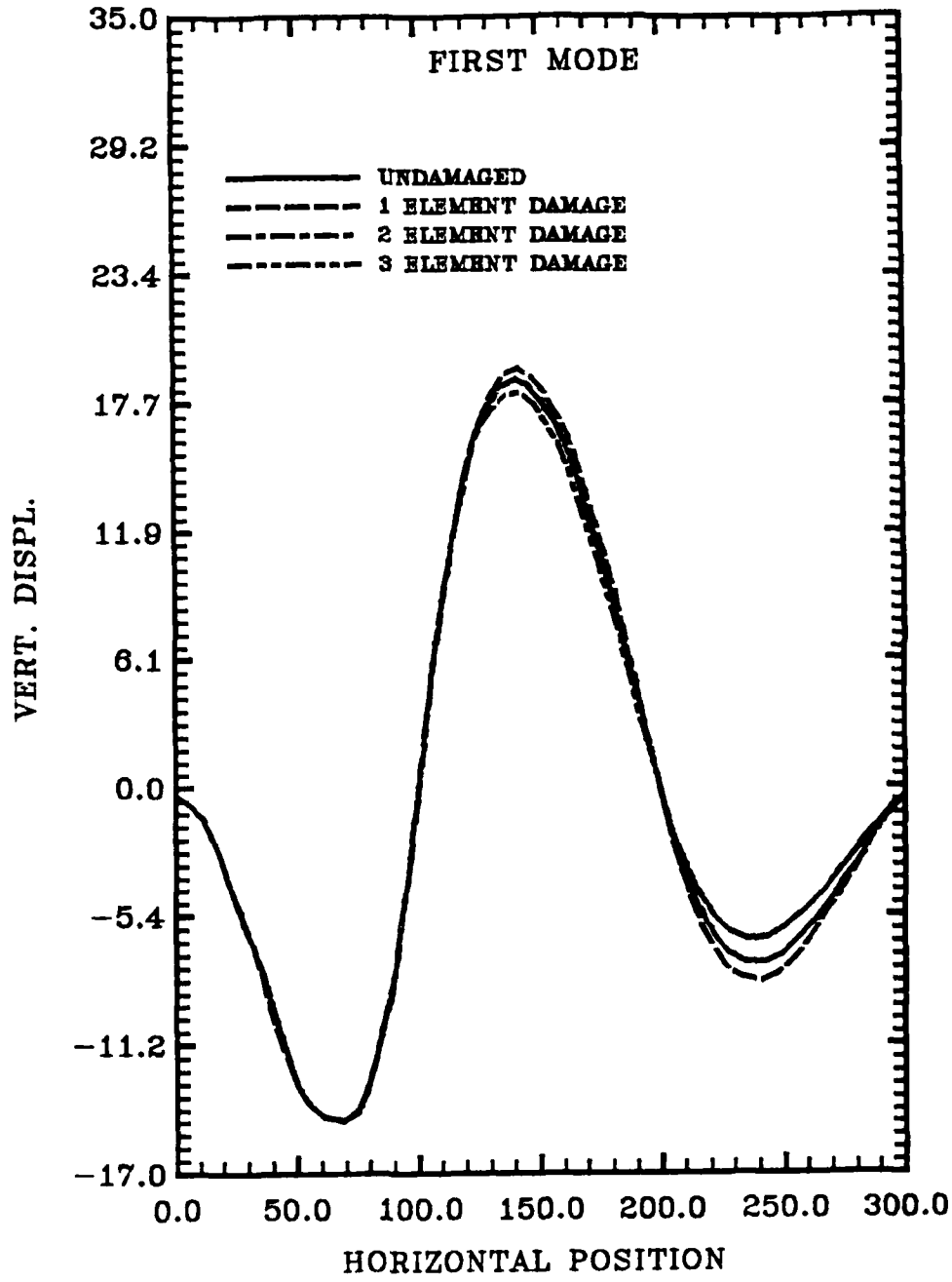
FIRST MODE
UNDAMAGED
1 ELEMENT DAMAGE
2 ELEMENT DAMAGE
3 ELEMENT DAMAGE
35.0
29.2
23.4
17.7
11.9
6.1
0.0
-5.4
-11.2
-17.0
VERT. DISPL.
0.0
50.0
100.0
150.0
200.0
250.0
300.0
HORIZONTAL POSITION

FIGURE NO. 15

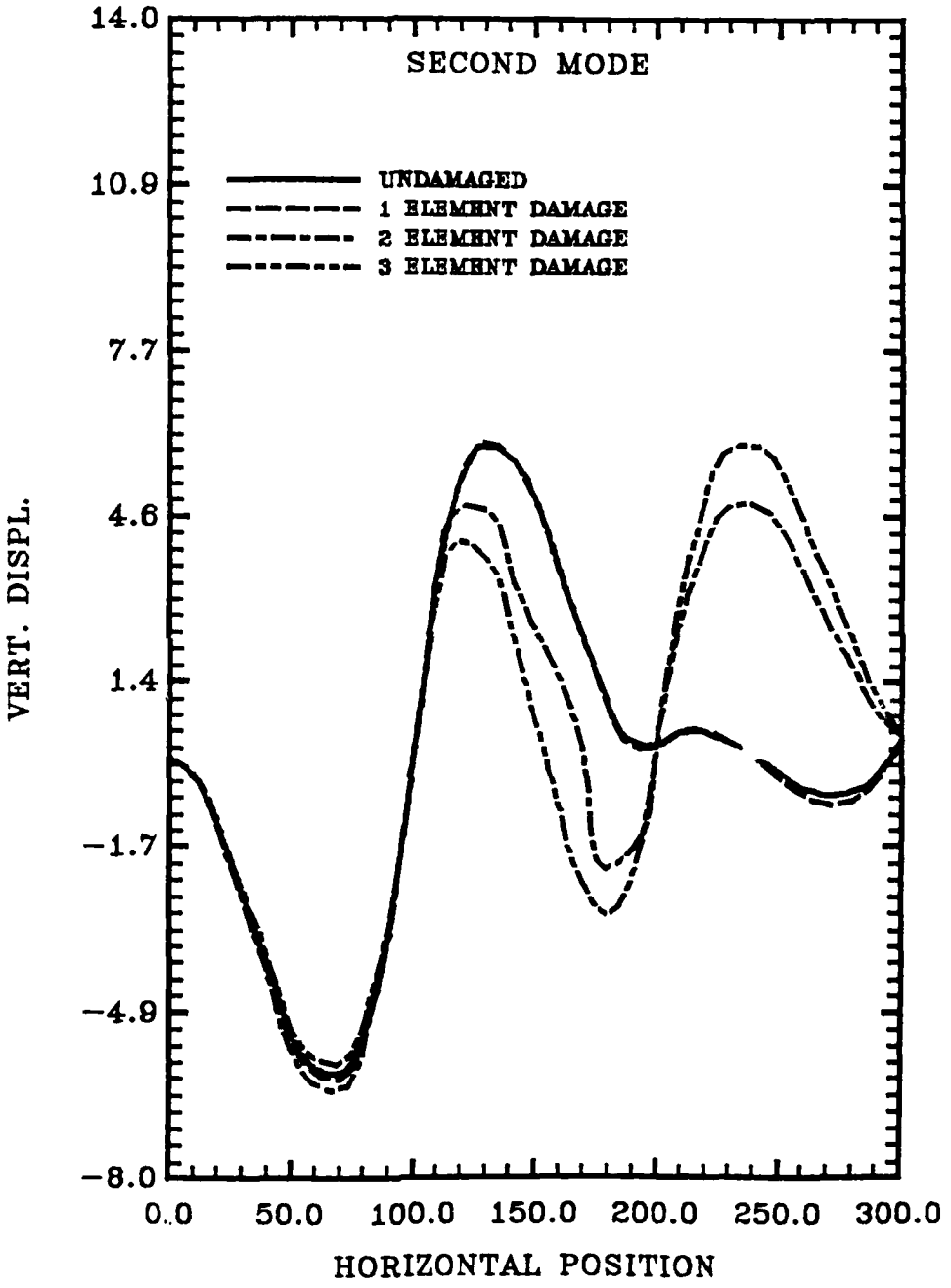
SECOND MODE
UNDAMAGED
1 ELEMENT DAMAGE
2 ELEMENT DAMAGE
3 ELEMENT DAMAGE
VERT. DISPL.
14.0
10.9
7.7
4.6
1.4
-1.7
-4.9
-8.0
0.0
50.0
100.0
150.0
200.0
250.0
300.0
HORIZONTAL POSITION

FIGURE NO. 16

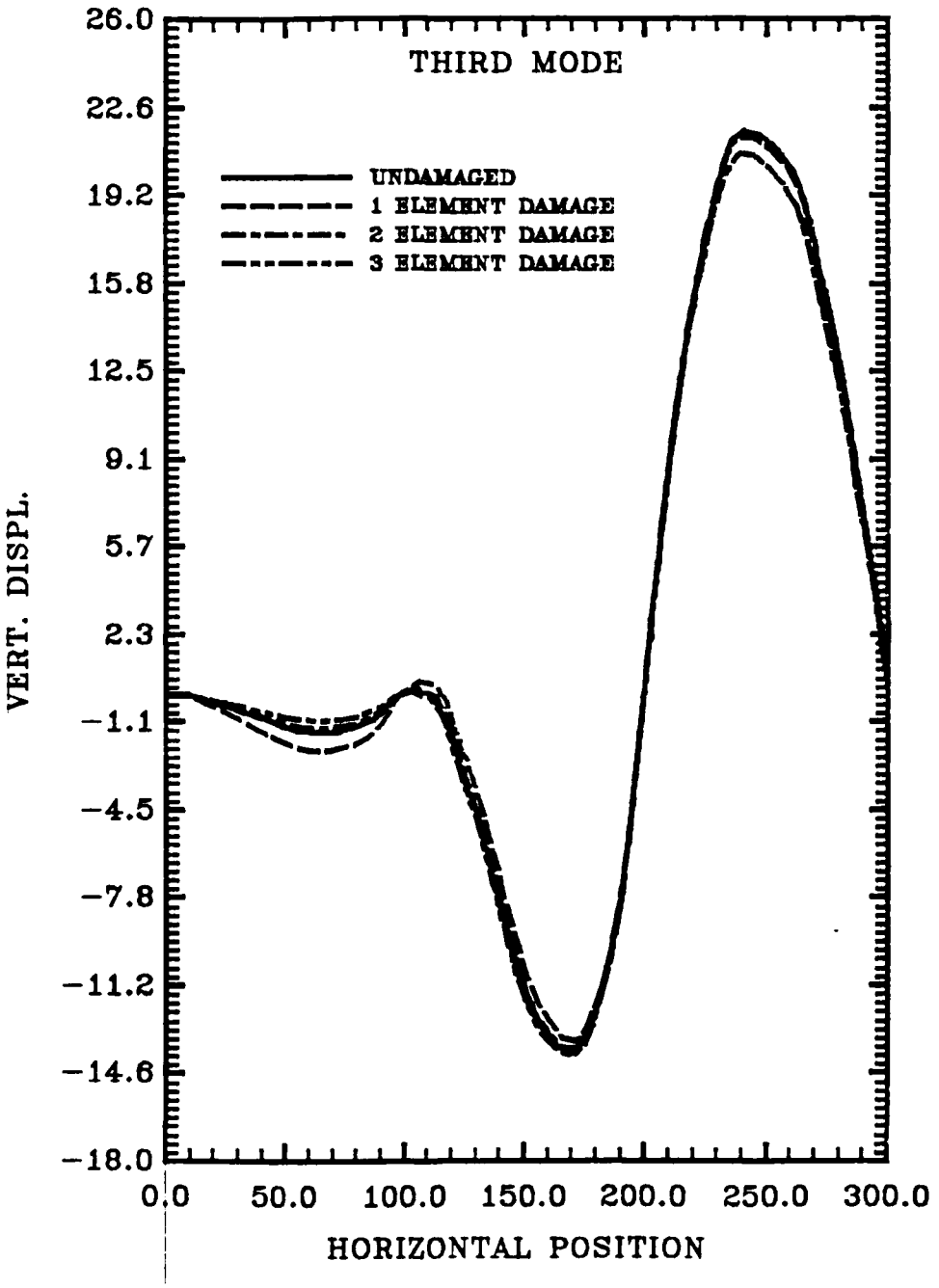
THIRD MODE
UNDAMAGED
1 ELEMENT DAMAGE
2 ELEMENT DAMAGE
3 ELEMENT DAMAGE
VERT. DISPL.
26.0
22.6
19.2
15.8
12.5
9.1
5.7
2.3
-1.1
-4.5
-7.8
-11.2
-14.6
-18.0
0.0
50.0
100.0
150.0
200.0
250.0
300.0
HORIZONTAL POSITION

FIGURE NO. 17

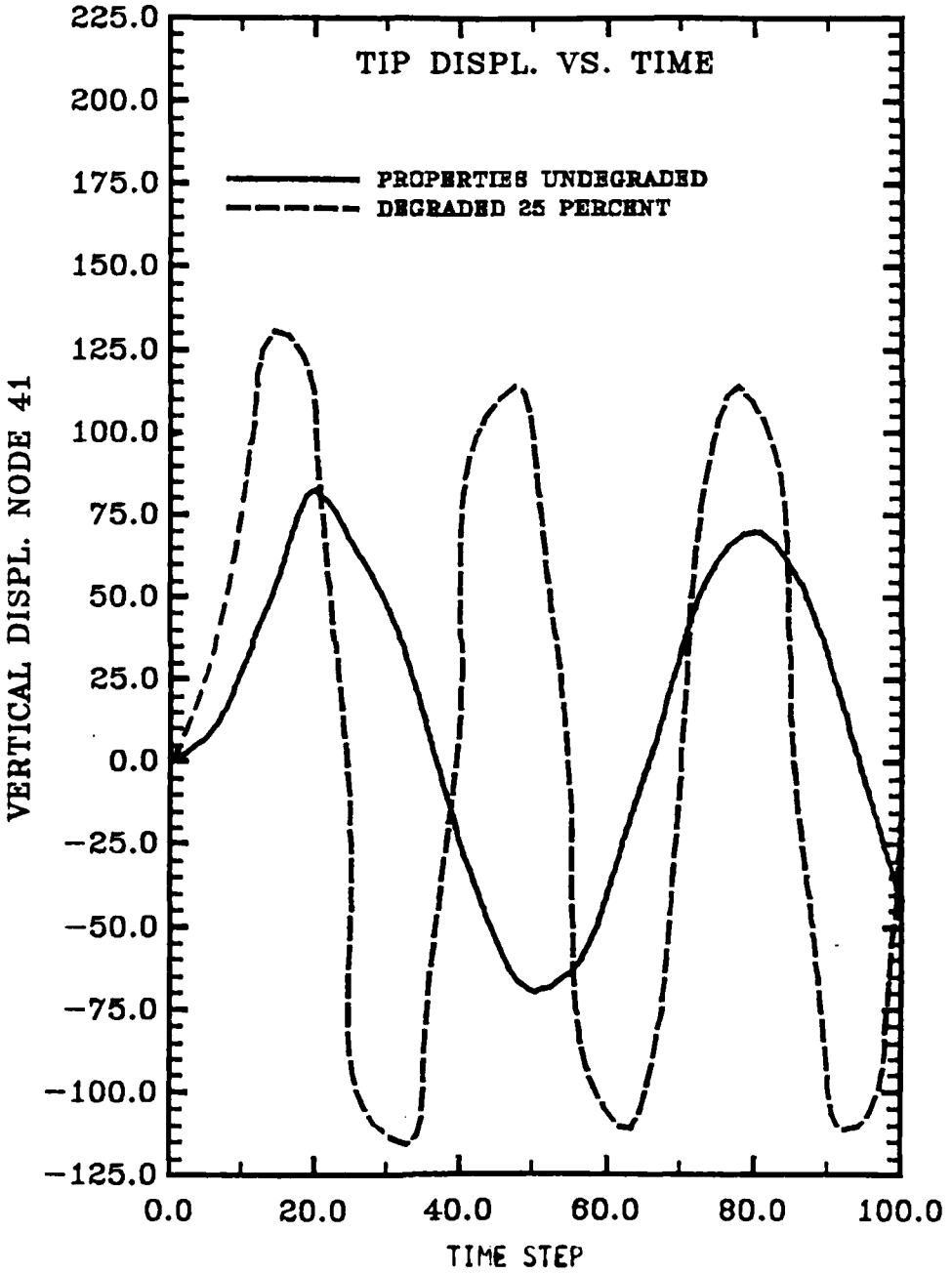
TIP DISPL. VS. TIME
PROPERTIES UNDEGRADED
DEGRADED 25 PERCENT
VERTICAL DISPL. NODE 41
225.0
200.0
175.0
150.0
125.0
100.0
75.0
50.0
25.0
0.0
-25.0
-50.0
-75.0
-100.0
-125.0
0.0
20.0
40.0
60.0
80.0
100.0
TIME STEP

FIGURE NO. 18

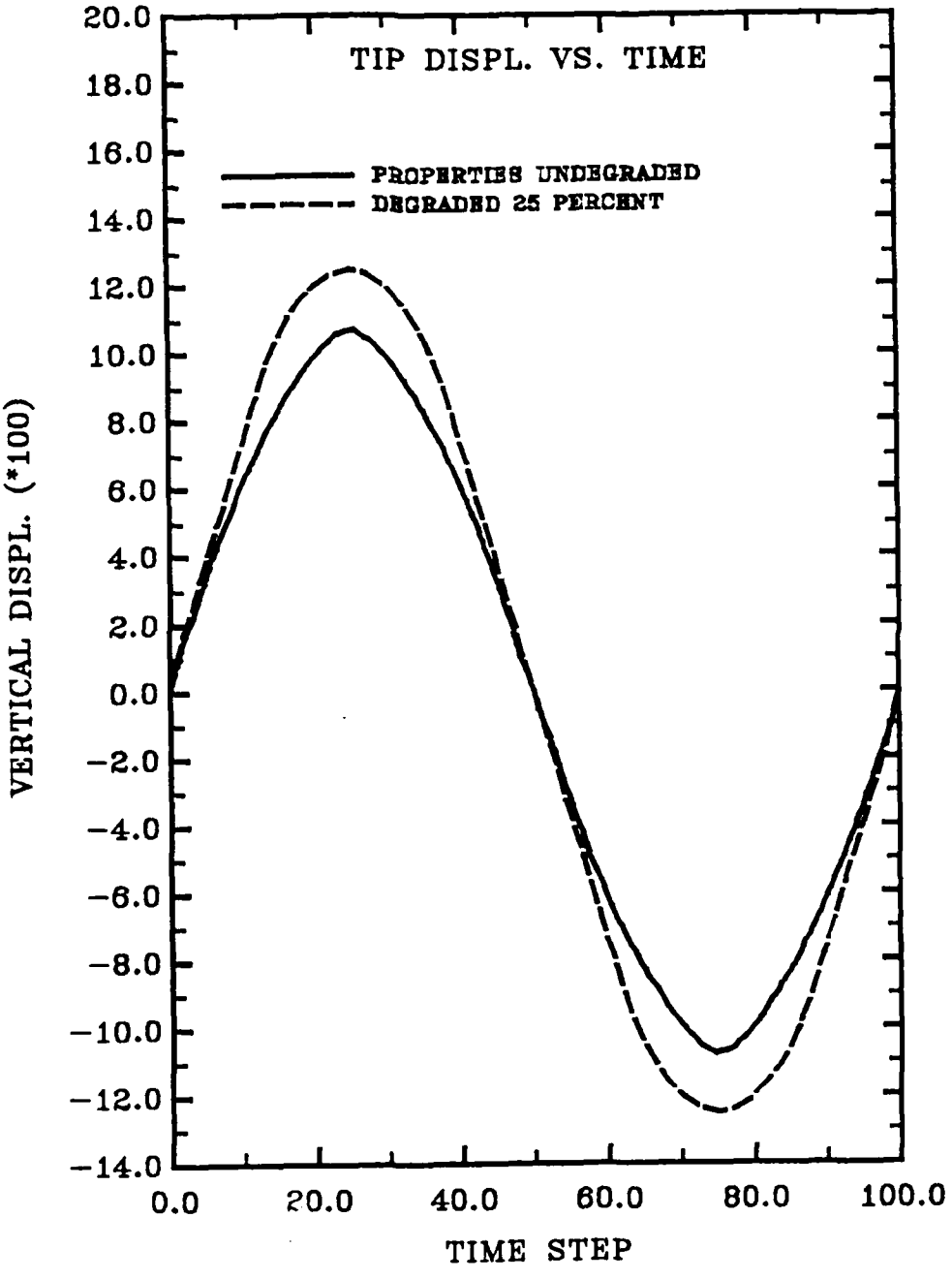
TIP DISPL. VS. TIME
PROPERTIES UNDEGRADED
DEGRADED 25 PERCENT
VERTICAL DISPL. (*100)
TIME STEP
20.0
18.0
16.0
14.0
12.0
10.0
8.0
6.0
4.0
2.0
0.0
-2.0
-4.0
-6.0
-8.0
-10.0
-12.0
-14.0
0.0
20.0
40.0
60.0
80.0
100.0

FIGURE NO. 19

REFERENCES

1. Herzberg R.J., Johansen K.F., and Stroud R.C., "Dynamics and Control of Large Satellites," Astronautics and Aeronautics, Vol. 16, Oct., 1978 pp. 35-39.

2. Skelton R.E., "Algorithm Development for the Control Design of Flexible Structures," NASA-CP-2258, 1982.

3. Skelton, R.E., "Large Space System Control echnology Model Order Reduction Study," NASA-CP-2118, 1979.

4. Hroner, G.C., "Optimum Damper Location for a Free-Free Beam," NASA-CP-2168.

5. Highsmith, A.L., Stinchcomb, W.W., and Reifsnider, K.L., "Stiffness Reduction resulting from Transverse cracking in Fiber-Reinforced Composite Laminates," VPI & SU Report No. VPI-E-81-33, Nov. 1981.

6. Semi-Annual Progress Report No. 3, "Cumulative Damage Model for Advanced Composite Materials," General Dynamics Technical Report FZM-7070, October 1982.

7. Chou, P.C., Wang, A.S.D. and Miller, H., "Cumulative Damage Model for Advanced Composite Materials," Material Laboratory Air Force Wright Aeronautical Laboratories, Report No. AFWAL-TR-82-4089.

8. Schapery R.A., "On Viscoelastic deformation and failure behavior of Composite Materials with Distributed Flaws," Advances in Aerospace Structures and Materials-AD-01, 1981.

9. Allen, D.H., Groves, S.E., and Schapery, R.A., "A Damage Model For Continuous Fiber Composites," in preparation.

10. Allen, D.H., "A Prediction of Heat Generation in a Thermoviscoplastic Unaxial Bar," Texas A&M Mechanics and Materials center, Report No. MM 4875-83-10.

11. Allen, D.H., and Haisler, W.E., "A Theory For Analysics of Thermoplastic Materials," Computers and Structures, Vol. 13, 1981.

12. Bathe, K.J., Wilson, E.L., "Numerical Methods in Finite Element Analysiss," Prentice-Hall Inc., 1976.

13. Zienkiewicz, O.C., "The Finite Element Method," Third Edition McGraw-Hill Book Company, 1978.

14. Meiroviteh, L., "Computational Methods in Structural Dynamics, Sijthoff & Noordhof, 1980.

Appendix 6.5

Mechanics and Materials Center
TEXAS A&M UNIVERSITY
College Station, Texas

PREDICTED AXIAL TEMPERATURE GRADIENT IN A COUPLED THERMOVISCOPLASTIC UNIAXIAL BAR

(WORK IN PROGRESS)

D.H. Allen

MM 4875-84-15

June 1984

SECURITY CLASSIFICATION OF THIS PAGE (When Data Entered)

REPORT DOCUMENTATION PAGE		READ INSTRUCTIONS BEFORE COMPLETING FORM
1. REPORT NUMBER MM 4875-84-15	2. GOVT ACCESSION NO.	3. RECIPIENT'S CATALOG NUMBER
4. TITLE (and Subtitle) Predicted Axial Temperature Gradient in a Coupled Thermoviscoplastic Uniaxial Bar		5. TYPE OF REPORT & PERIOD COVERED Interim 6. PERFORMING ORG. REPORT NUMBER
7. AUTHOR(s) David H. Allen		8. CONTRACT OR GRANT NUMBER(s) F49620-83-C-0067
9. PERFORMING ORGANIZATION NAME AND ADDRESS Aerospace Engineering Department Texas A&M University College Station, Texas 77843		10. PROGRAM ELEMENT, PROJECT, TASK AREA & WORK UNIT NUMBERS
11. CONTROLLING OFFICE NAME AND ADDRESS Air Force Office of Scientific Research Bolling AFB Washington, D. C. 20332		12. REPORT DATE June, 1984 13. NUMBER OF PAGES
14. MONITORING AGENCY NAME & ADDRESS(if different from Controlling Office)		15. SECURITY CLASS. (of this report) Unclassified 15a. DECLASSIFICATION/ DOWNGRADING SCHEDULE

16. DISTRIBUTION STATEMENT (of this Report)

17. DISTRIBUTION STATEMENT (of the abstract entered in Block 20, if different from Report)

18. SUPPLEMENTARY NOTES

19. KEY WORDS (Continue on reverse side if necessary and identify by block number)

thermomechanical coupling
thermoviscoplastic
thermomechanical constitution
finite element method
heat generation

20. ABSTRACT (Continue on reverse side if necessary and identify by block number)

The thermomechanical response of a uniaxial bar with thermoviscoplastic constitution is predicted herein using the finite element method. After a brief review of the governing field equations, variational principles are constructed for the one dimensional conservation of momentum and energy equations. These equations are coupled in that the temperature field affects the displacements and vice versa.

Due to the differing physical nature of the temperature and displacements, first order and second order elements are utilized for these variables, respec-

DD FORM 1 JAN 73 1473 EDITION OF 1 NOV 65 IS OBSOLETE

SECURITY CLASSIFICATION OF THIS PAGE (When Data Entered)

tively. The resulting semi-discretized equations are then discretized in time using finite differencing. This is accomplished by Euler's method, which is utilized due to the stiff nature of the constitutive equations.

The model is utilized in conjunction with stress-strain relations developed by Bodner and Partom to predict the axial temperature field in a bar subjected to cyclic mechanical end displacements and thermal flux boundary conditions. It is found that spacial and time variation of the temperature field is signifi-cnatly affected by the flux boundary conditions.

PREDICTED AXIAL TEMPERATURE GRADIENT IN A COUPLED THERMOVISCOPLASTIC UNIAXIAL BAR

(Work in Progress)

by

D.H. Allen
Assistant Professor
Aerospace Engineering Department
Texas A&M University
College Station, TX 77843

MM 4875-84-15

June 1984

ABSTRACT

The thermomechanical response of a uniaxial bar with thermoviscoplastic constitution is predicted herein using the finite element method. After a brief review of the governing field equations, variational principles are constructed for the one dimensional conservation of momentum and energy equations. These equations are coupled in that the temperature field affects the displacements and vice versa.

Due to the differing physical nature of the temperature and displacements, first order and second order elements are utilized for these variables, respectively. The resulting semi-discretized equations are then discretized in time using finite differencing. This is accomplished by Euler's method, which is utilized due to the stiff nature of the constitutive equations.

The model is utilized in conjunction with stress-strain relations developed by Bodner and Partom to predict the axial temperature field in a bar subjected to cyclic mechanical end displacements and thermal flux boundary conditions. It is found that spacial and time variation of the temperature field is significantly affected by the flux boundary conditions.

TABLE OF SYMBOLS

t - time

P - axial internal resultant force

p_x - axial externally applied force per unit length

x - axial coordinate dimension

σ - axial stress component

A - cross-sectional area

T_x - end traction in units of force per unit area

s - surface area

Table of Symbols (cont.)

S_c - area of the longitudinal surface of the bar

ε - axial strain component

u - axial displacement component

α_1 - internal state variable representing axial inelastic strain

E - Young's modulus in the axial coordinate direction

α - coefficient of thermal expansion in the axial coordinate direction

T - temperature

T_s - reference temperature at which no deformation is observed at zero load

α_2 - internal state variable representing drag stress

q - axial component heat flux

k - coefficient of axial thermal conductivity

C_v - specific heat at constant elastic strain

ρ - mass density

r - internal heat source per unit mass

L - length of the bar

INTRODUCTION

It is well known that mechanical and thermodynamic coupling are significant in metallic solids [1-11]. The author has recently developed a model capable of predicting this coupling effect in thermoviscoplastic metals [12]. In the previous paper a cyclic strain control loading on a sample of IN100 at 1005°K (1350°F) was used to predict a temperature rise of approximately 3.7°K per cycle when the strain amplitude was 2% and the specimen was adiabatically insulated.

The focus of the current research is to consider the effect of thermal flux boundary conditions on this same process. The introduction of these flux

conditions causes the strain and temperature fields to be inhomogeneous even though the stress field is homogeneous if the bar is prismatic. This spacial variation in the field varables causes the process to be difficult to model because the thermomechanical constitutive equations are highly nonlinear stiff differential equations. In this paper the finite element method is utilized to spatially discretize the dependent variables, displacement and temperature, and the finite difference method is employed for timewise discretization. This process results in a set of highly nonlinear algebraic equations.

Since the thrust of this research is to obtain accurate results without regard to numerical efficiency, the results are obtained via the relatively inefficient but accurate method of simply utilizing successively smaller time steps along with refined spatial mesh to obtain a convergent and therefore accurate solution for the temperature and displacement fields both spatially and as a function of time for a cyclically imposed end displacement.

The physical interest in the problem is to determine the effect of various flex boundary conditions on the predicted temperature rise in a bar subjected to cyclic mechanical loading. It is found from the analysis that the introduction of flux boundary conditions causes significant axial temperature gradients. Since flux conditions cannot be avoided in experimental research, it is concluded that experimental tests of this type should be viewed with caution when their purpose is to construct constitutive relations.

PROBLEM SOLUTION

Field Problem Description

The following field equations are given:

a) equilibrium [13],

$$\frac{\partial P}{\partial x} = -p_x(x) \quad , \tag{1}$$

where the axial resultant P is defined by

$$P \equiv \int_A \sigma dA \quad , \qquad \text{and} \quad (2)$$

$$p_x \equiv \oint_{S_c} T_x ds \quad ; \qquad (3)$$

b) strain-displacement relation

$$\varepsilon = \frac{\partial u}{\partial x} \quad ; \qquad (4)$$

c) thermomechanical constitution,

$$\sigma = E[\varepsilon - \alpha_1 - \alpha(T - T_R)] \quad , \qquad (5)$$

$$\frac{\partial \alpha_k}{\partial t} = \Omega_1(\varepsilon, T, \alpha_\ell) \quad , \quad k = 1,z \quad , \qquad \text{and} \quad (6)$$

$$q = -k \frac{\partial T}{\partial x} \quad ; \qquad (7)$$

where z is the total number of internal state variables; and

d) conservation of energy

$$\left[(E\varepsilon - E\alpha_1 + E\alpha T_R) \frac{\partial \alpha_1}{\partial t} + E\alpha^2 T \frac{\partial T}{\partial t}\right] - E\alpha T \frac{\partial \varepsilon}{\partial t} - \rho C_v \frac{\partial T}{\partial t} - \frac{\partial q}{\partial x} + \rho r = 0 \quad . \qquad (8)$$

The conservation of mass is satisfied trivially and the second law of thermodynamics has been previously shown to be satisfied by the above equations [14-16]. It should be noted that equilibrium equation (1) satisfies equilibrium in the axial coordinate direction only in an average sense over the cross-section.

The above 6+k equations (excluding definition (3)) define a nonlinear initial-boundary value problem (together with appropriate thermal and mechanical initial and boundary conditions) in which the following dependent variables are sought as functions of x and t: σ, ε, u, q, T, P, and α_k.

For convenience the domain is defined to be of length L, so that boundary and initial conditions are of the form:

$$\left.\begin{aligned} u(x,0) &\equiv u_0^x = \text{known} \\ T(x,0) &\equiv T_0^x = \text{known} \end{aligned}\right\} \quad \text{initial conditions} \quad ; \tag{9}$$

and

$$\text{essential boundary conditions} \left\{\begin{aligned} &u(0,t) \equiv u_t^0 = \text{known or } P(0,t) \equiv P_t^0 = \text{known} \\ &u(L,t) \equiv u_t^L = \text{known or } P(L,t) \equiv P_t^L = \text{known} \\ &T(0,t) \equiv T_t^0 = \text{known or } q(0,t) \equiv q_t^0 = \text{known} \\ &T(L,t) \equiv T_t^L = \text{known or } q(L,t) \equiv q_t^L = \text{known} \end{aligned}\right\} \quad \text{natural boundary conditions.} \tag{10}$$

It is now assumed that $\sigma = \sigma(x)$ so that equation (2) reduces to

$$P = \sigma A \quad . \tag{11}$$

Therefore, substituting (4) into (5) and this result into (11) gives

$$P = EA\left[\frac{\partial u}{\partial x} - \alpha_1 - \alpha(T - T_R)\right] \quad . \tag{12}$$

The above result is now substituted into (1) to obtain

$$\frac{\partial}{\partial x}\left\{EA\left[\frac{\partial u}{\partial x} - \alpha_1 - \alpha(T - T_R)\right]\right\} = -p_x(x) \quad , \tag{13}$$

which represents the differential equation relating displacements and temperature to the applied load $p_x(x)$.

Equations (4) and (7) are next substituted into energy balance law (8) and this result is integrated over the cross-sectional area A to obtain

$$A\left[\left(E\frac{\partial u}{\partial x} - E\alpha_1 + E\alpha T_R\right)\frac{\partial \alpha_1}{\partial t} + E\alpha^2 T\frac{\partial T}{\partial t}\right] - AE\alpha T\frac{\partial^2 u}{\partial t \partial x} - A\rho C_v\frac{\partial T}{\partial t}$$

$$+ A\frac{\partial}{\partial x}\left(k\frac{\partial T}{\partial x}\right) = -Ar\rho \quad , \tag{14}$$

where it has been assumed that all field variables depend on x and t only.

Now define

$$Q \equiv \int_A q\, dA = -\int_A k\frac{\partial T}{\partial x}\, dA = -k\frac{\partial T}{\partial x}A \quad . \tag{15}$$

Careful inspection of equations (13) and (14) will indicate that these equations, together with internal state variable growth laws (6) and initial and boundary conditions (9) and (10) represent a well-posed boundary value problem in terms of the 2+k dependent variables u, T, and α_k.

Solution Procedure

The field problem is to be solved analytically using the semi-discretized finite element technique with timewise finite differencing. In order to accomplish this, differential equations (13) and (14) must first be written in a suitable variational form.

Variational Equations

Consider first equation (13). This governing equation is integrated against a suitably smooth test function v = v(x) over the domain of some element Ω_e: $x_e < x < x_{e+1}$:

$$\int_{x_e}^{x_{e+1}} v \left[\frac{\partial}{\partial x} \left\{ EA \left[\frac{\partial u}{\partial x} - \alpha_1 - \alpha(T - T_R) \right] \right\} + p_x \right] dx = 0 \quad . \tag{16}$$

Integrating by parts results in

$$- \int_{x_e}^{x_{e+1}} EA \frac{\partial v}{\partial x} \left[\frac{\partial u}{\partial x} - \alpha_1 - \alpha(T - T_R) \right] dx = - \left| v \, EA \left[\frac{\partial u}{\partial x} - \alpha_1 - \alpha(T - T_R) \right] \right|_{x_e}^{x_{e+1}}$$

$$- \int_{x_e}^{x_{e+1}} v \, p_x dx \quad . \tag{17}$$

Substituting equation (12) into the boundary term thus results in

$$- \int_{x_e}^{x_{e+1}} EA \left[\frac{\partial v}{\partial x} \frac{\partial u}{\partial x} - \alpha_1 - \alpha(T - T_R) \right] dx =$$

$$-v(x_{e+1}) \, P(x_{e+1}) + v(x_e) \, P(x_e) - \int_{x_e}^{x_{e+1}} v \, p_x dx \quad . \tag{18}$$

Now consider equation (14). Once again the governing equation is integrated against a suitably smooth test function $w = w(x)$ over the domain of the element Ω_e:

$$\int_{x_e}^{x_{e+1}} w \left\{ A \left[\left(E \frac{\partial u}{\partial x} - E\alpha_1 + E\alpha T_R \right) \frac{\partial \alpha_1}{\partial t} + E\alpha^2 \, T \frac{\partial T}{\partial t} \right] \right.$$

$$\left. -AE\alpha T \frac{\partial^2 u}{\partial t \partial x} - A\rho C_v \frac{\partial T}{\partial t} + A \frac{\partial}{\partial x} \left(k \frac{\partial T}{\partial t} \right) + A \, \rho r \right\} dx = 0 \quad . \tag{19}$$

Integrating the heat flux term by parts results in

$$\int_{x_e}^{x_{e+1}} \left\{ -kA \frac{\partial w}{\partial x} \frac{\partial T}{\partial x} + wA \left[\left(E \frac{\partial u}{\partial x} - E\alpha_1 + E\alpha T_R \right) \frac{\partial \alpha_1}{\partial t} + E\alpha^2 T \frac{\partial T}{\partial t} \right. \right.$$

$$\left. \left. -E\alpha T \frac{\partial^2 u}{\partial t \partial x} \right] \right\} dx = w(x_{e+1})\, Q(x_{e+1}) - w(x_e)\, Q(x_e)$$

$$+ \int_{x_e}^{x_{e+1}} wA \left(\rho C_v \frac{\partial T}{\partial t} - \rho r \right) dx \quad , \tag{20}$$

where equation (15) has been substituted into the boundary terms.

Finite Element Spacial Discretization

Quadratic displacement and linear temperature fields are now chosen within each element:

$$u(x,t) = \sum_{i=1}^{3} u_i^e \psi_i^e \quad , \quad x_e < x < x_{e+1} \quad , \text{ and} \tag{21}$$

$$u(x,t) - \sum_{i=1}^{2} T_i^e \phi_i^e \quad , \quad x_e < x < x_{e+1} \quad , \tag{22}$$

where $u_i^e = u_i^e(t)$ and $T_i^e = T_i^e(t)$ are the nodal displacements and temperatures, respectively, and $\psi_i^e = \psi_i^e(x)$ and $\phi_i^e = \phi_i^e(x)$ are quadratic and linear shape functions, respectively [17].

Appropriately, v and w are endowed with the properties of u and T, respectively, so that

$$v \equiv \psi_i^e \quad i = 1,2,3$$

$$w \equiv \phi_i^e \quad i = 1,2 \quad . \tag{23}$$

Substitution of equations (12) and (21) through (23) into variational principle (18) results in

$$-\int_{x_e}^{x_{e+1}} EA \frac{d\psi_i^e}{dx} \left[\frac{\partial}{\partial x} \left(\sum_{j=1}^{3} u_j^e \psi_j^e \right) - \alpha_1 \right.$$

$$\left. -\alpha \left(\sum_{j=1}^{2} T_j^e \phi_j^e - T_R \right) \right] dx = - \psi_i^e(x_{e+1}) P(x_{e+1}) + \psi_i^e(x_e) P(x_e)$$

$$- \int_{x_e}^{x_{e+1}} \psi_i^e p_x dx \quad , \quad i = 1,2,3 \quad . \tag{24}$$

The above may be written in the following compact form

$$\sum_{j=1}^{3} K_{ij}^e u_j^e + \sum_{j=1}^{2} S_{ij}^e T_j^e = F_i^e \quad , \quad i = 1,2,3, \tag{25}$$

where

$$K_{ij}^e \equiv - \int_{x_e}^{x_{e+1}} EA \frac{d\psi_i^e}{dx} \frac{d\psi_j^e}{dx} dx \qquad i = 1,2,3; \; j = 1,2,3 \quad ; \tag{26}$$

$$S_{ij}^e \equiv \int_{x_e}^{x_{e+1}} EA\alpha \frac{d\psi_i^e}{dx} \phi_j^e dx \qquad i \quad 1,2,3; \; j = 1,2,3 \quad ; \tag{27}$$

$$F_i^e \int_{x_e}^{x_{e+1}} EA \frac{d\psi_i^e}{dx} \quad (-\alpha_1 + \alpha T_R)dx$$

$$-P(x_i) - \int_{x_e}^{x_{e+1}} \psi_i^e \, p_x dx \quad , \qquad i = 1,2,3. \tag{28}$$

Similarly, substitution of equations (21) through (23) into equation (20) results in

$$\int_{x_e}^{x_{e+1}} \left\{ -kA \frac{d\phi_i^e}{dx} \frac{\partial}{\partial x}\left(\sum_{j=1}^{2} T_j^e \phi_j^e \right) + A \, \phi_i^e \left[\left(E \frac{\partial}{\partial x}\left(\sum_{j=1}^{3} u_j^e \psi_j^e \right) - E\alpha_1 \right.\right.\right.$$

$$\left. + E\alpha T_R \right) \frac{\partial \alpha_1}{\partial t} + E\alpha^2 \left(\sum_{j=1}^{2} T_j^e \phi_j^e \right) \frac{\partial}{\partial t}\left(\sum_{m=1}^{2} T_m^e \phi_m^e \right)$$

$$\left.\left.\left. - E\alpha \left(\sum_{j=1}^{2} T_j^e \phi_j^e \right) \frac{\partial^2}{\partial t \partial x}\left(\sum_{m=1}^{3} u_m^e \psi_m^e \right) \right] \right\} dx =$$

$$\phi_i^e(x_{e+1}) \, Q(x_{e+1}) - \phi_i^e(x_e) \, Q(x_e) + \int_{x_e}^{x_{e+1}} \phi_i^e \, A \left[\rho C_v \frac{\partial}{\partial t}\left(\sum_{m}^{2} T_m^e \phi_m^e \right) - \rho r \right] dx,$$

$$i = 1,2. \tag{29}$$

Equations (29) may be written in the following form:

$$\sum_{j=1}^{3} \bar{K}_{ij}^e \, u_j^e + \sum_{j=1}^{2} \bar{S}_{ij}^e \, T_j^e + \int_{x_e}^{x_{e+1}} \phi_i^e \, A \left[E\alpha^2 \left(\sum_{j=1}^{2} T_j^e \, \phi_j^e \right) \left(\sum_{m=1}^{2} \frac{dT_m^e}{dt} \, \phi_m^e \right) \right.$$

$$-E\alpha\left(\sum_{j=1}^{2} T_j^e \phi_j^e\right)\left(\sum_{m=1}^{3} \frac{du_m^e}{dt} \frac{d\psi_m^e}{dx}\right) - \rho C_v\left(\sum_{m=1}^{2} \frac{dT_m^e}{dt} \phi_m^e\right) + \rho r \Bigg] dx$$

$$= - \int_{x_e}^{x_{e+1}} \phi_i^e \, A(-E\alpha_1 + E\alpha T_R) \frac{\partial \alpha_1}{\partial t} + Q(x_i) \quad , \qquad i = 1,2, \tag{30}$$

where

$$\bar{K}_{ij}^e \equiv \int_{x_e}^{x_{e+1}} AE \, \phi_i^e \frac{d\psi_j^e}{dx} \frac{\partial \alpha_1}{\partial t} \, dx \qquad i = 1,2; \; j = 1,2,3; \text{ and} \tag{31}$$

$$\bar{S}_{ij}^e \equiv - \int_{x_e}^{x_{e+1}} kA \frac{d\phi_i^e}{dx} \frac{d\phi_j^e}{dx} \, dx \quad ; \quad 1 = 1,2; \; j = 1,2. \tag{32}$$

Finite Difference Timewise Discretization

Time dependence in equations (6) and (30) is handled via finite differencing. Although higher order approximations may be used, Euler forward difference approximations are now entered for the time rate of change of α_k^e, T_m^e, and u_m^e.

$$\frac{\partial \alpha_k^e}{\partial t}(x,t) \cong [\alpha_k^e(x,t + \Delta t) - \alpha_k^e(x,t)]/\Delta t, \qquad k = 1,z \; , \tag{33}$$

$$\frac{dT_m^e}{dt}(t) \cong [T_m^e(t + \Delta t) - T_m^e(t)]/\Delta t, \qquad m = 1,2 \; , \qquad \text{and} \tag{34}$$

$$\frac{du_m^e}{dt}(t) \cong [u_m^e(t + \Delta t) - u_m^e(t)]/\Delta t, \qquad m = 1,2 \; . \tag{35}$$

Substitution of (33) through (35) into finite element equations (30) gives

$$\sum_{j=1}^{3} \bar{K}_{ij}^{e} u_j^e + \sum_{j=1}^{2} \bar{S}_{ij}^{e} T_j^e$$

$$+ \int_{x_e}^{x_{e+1}} A\phi_i^e \left\{ E\alpha^2 \left[\sum_{j=1}^{2} T_j^e \phi_j^e \right] \left[\sum_{m=1}^{2} \left(\frac{T_m^e(t + \Delta t) - T_m^e(t)}{\Delta t} \right) \phi_m^e \right] \right.$$

$$- E\alpha \left[\sum_{j=1}^{2} T_j^e \phi_j^e \right] \left[\sum_{m=1}^{3} \left(\frac{u_m^e(t + \Delta t) - u_m^e(t)}{\Delta t} \right) \frac{\partial \psi_m^e}{\partial x} \right]$$

$$\left. - \rho C_v \left[\sum_{m=1}^{2} \left(\frac{T_m^e(t + \Delta t) - T_m^e(t)}{\Delta t} \right) \phi_m^e \right] + \rho r \right\} dx$$

$$= - \int_{x_e}^{x_{e+1}} A\phi_i^e \left[-E\alpha_1(t) + E\alpha T_R \right] \frac{\partial \alpha_1}{\partial t}(t)$$

$$+ Q(x_i) \quad , \qquad i = 1,2 \, . \tag{36}$$

The above may be written as follows:

$$\sum_{j=1}^{3} \bar{K}_{ij}^{e} u_j^e + \sum_{j=1}^{2} \bar{S}_{ij}^{e} T_j^e$$

$$+ \sum_{k=1}^{2} \sum_{j=1}^{2} C_{ijk} T_j^e T_k^e + \sum_{j=1}^{2} D_{ij} T_j^e$$

$$+ \sum_{k=1}^{2} \sum_{j=1}^{3} E_{ikj} T_k^e u_j^e + \sum_{j=1}^{2} G_{ij} T_j^e$$

$$+ \sum_{j=1}^{2} H_{ij} T_j^e = \bar{F}_i^e \quad , \qquad i = 1,2, \tag{37}$$

where

$$C_{ijk} \equiv \int_{x_e}^{x_{e+1}} A\phi_i^e \frac{E\alpha^2}{\Delta t} \phi_j^e \phi_k^e \, dx \quad , \qquad i = 1,2;\ j = 1,2;\ k = 1,2 \ , \quad (38)$$

$$D_{i1} \equiv - \int_{x_e}^{x_{e+1}} A\phi_i^e \frac{E\alpha^2}{\Delta t} [T_1^e(t)(\phi_1^e)^2 + T_2^e(t)\ \phi_1^e\phi_2^e] \, dx, \qquad i = 1,2 \ , \quad (39)$$

$$D_{i2} \equiv - \int_{x_e}^{x_{e+1}} A\phi_i^e \frac{E\alpha^2}{\Delta t} [T_1^e(t)\phi_1^e\phi_2^e + T_2^e(t)(\phi_2^e)^2] \, dx, \qquad i = 1,2 \ , \quad (40)$$

$$E_{ikj} \equiv - \int_{x_e}^{x_{e+1}} A\phi_i^e \frac{E\alpha}{\Delta t} \phi_k^e \frac{\partial \psi_j^e}{\partial x} \, dx \quad , \qquad i = 1,2,;\ k = 1,2;\ j = 1,3 \ , \quad (41)$$

$$G_{i1} \equiv \int_{x_e}^{x_{e+1}} A\phi_i^e \frac{E\alpha}{\Delta t} \left[u_1^e(t)\ \phi_1^e \frac{\partial \psi_1^e}{\partial x} + u_2^e(t)\ \phi_1^e \frac{\partial \psi_2^e}{\partial x} + u_3^e(t)\ \phi_1^e \frac{\partial \psi_3^e}{\partial x} \right] dx, \ i = 1,2 \ , \quad (42)$$

$$G_{i2} \equiv \int_{x_e}^{x_{e+1}} A\phi_i^e \frac{E\alpha}{\Delta t} \left[u_1^e(t)\phi_2^e \frac{\partial \psi_1^e}{\partial x} + u_2^e(t)\phi_2^e \frac{\partial \psi_2^e}{\partial x} + u_3^e(t)\phi_2^e \frac{\partial \psi_3^e}{\partial x} \right] dx \ , \ i = 1,2 \ , \quad (43)$$

$$H_{ij} \equiv - \int_{x_e}^{x_{e+1}} A\phi_i^e \frac{\rho C_v}{\Delta t} \phi_j^e \, dx \quad , \qquad i = 1,2;\ j = 1,2; \qquad \text{and} \quad (44)$$

$$\bar{F}_i^e \equiv - \int_{x_e}^{x_{e+1}} A\phi_i^e \left[\frac{\rho C_v}{\Delta t} \left(\sum_{j=1}^{2} T_j^e(t)\phi_j^e \right) + \rho r \right] dx$$

$$- \int_{x_e}^{x_{e+1}} A\phi_i^e \left[-E\alpha_1(t) + E\alpha T_R \right] \frac{\partial \alpha_1}{\partial t}(t) \, dx$$

$$+ O(x_i) \qquad i = 1,2 \ . \quad (45)$$

Equations (37) may be written equivalently as follows:

$$\sum_{j=1}^{3} \bar{\bar{K}}_{ij}^{e} u_j^e + \sum_{j=1}^{2} \bar{\bar{S}}_{ij}^{e} T_j^e = \bar{F}_i^e \quad , \tag{46}$$

where K_{ij}^e and $\bar{F}_i^e$ are as defined previously, and

$$\bar{\bar{K}}_{ij}^{e} = \bar{K}_{ij}^{e} + \sum_{k=1}^{2} E_{ikj} T_k^e \quad , \quad \text{and} \tag{47}$$

$$\bar{\bar{S}}_{ij}^{e} = \bar{S}_{ij}^{e} + \sum_{k=1}^{2} C_{ijk} T_k^e + D_{ij} + G_{ij} + H_{ij} \quad . \tag{48}$$

The above equations may be rejoined with equations (25) to obtain the following set of nonlinear equation for each element.

$$\underbrace{\left[\begin{array}{c|c} K^e & S^e \\ \hline \bar{\bar{K}}^e & \bar{\bar{S}}^e \end{array}\right]}_{\substack{2\times3 \quad 2\times2 \\ 5\times5}} \left\{\begin{array}{c} u^e \\ \hline T^e \end{array}\right\}_{5\times1} = \left\{\begin{array}{c} F^e \\ \hline \bar{F}^e \end{array}\right\}_{5\times1}$$

where all nonlinearity is contained in $[\bar{\bar{S}}]$, $\{F^e\}$, and $\{\bar{F}^e\}$.

Global Assembly and Boundary Conditions

Global assembly is accomplished in the standard way using the Boolean matrix [17]. Interelement continuity is guaranteed by setting

$$p_2^e + p_1^{e+1} = 0 \quad , \quad \text{and} \tag{50}$$

$$\phi_2^e + \phi_1^{e+1} = 0 \quad . \tag{51}$$

Boundary conditions are implemented in the standard way: 1) essential boundary conditions are handled by placing one on the diagonal of the

AD-A162 140 A MODEL FOR PREDICTING THERMOMECHANICAL RESPONSE OF LARGE SPACE STRUCTURE (U) TEXAS A AND M UNIV COLLEGE STATION MECHANICS AND MATERIALS RE D H ALLEN ET AL 3/3

UNCLASSIFIED JUN 84 MM-4875-84-16 AFOSR-TR-85-1080 F/G 11/4 NL

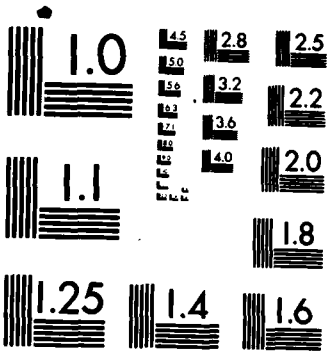

MICROCOPY RESOLUTION TEST CHART
NATIONAL BUREAU OF STANDARDS-1963-A

appropriate row and zeros off diagonal in the stiffness matrix, and the specified value of the essential variable on the right hand side; and 2) natural boundary conditions are implemented directly to the right hand side.

Solution of the Nonlinear Algebraic System

Initial conditions are used for the first time step. The time step Δt is supplied for each load increment and boundary conditions are incremented directly from supplied input functions.

The internal state variable α_1 is handled in equations (23) and (45) by using equations (35). α_1 is initialized as zero. The nonlinear stiffness matrix $[\bar{\bar{S}}]$ is initialized using nodal temperatures and displacements from the previous time step. The displacements and temperatures at time $t + \Delta t$ are then estimated directly and without iteration by utilizing equations (49) for very small time steps.

CONCLUSION

The above algorithm has been implemented into a fortran computer program. The program is currently in the final stage of debugging, with numerical results expected in the near future. It is expected that the inclusion of thermal flux boundary conditions will cause a substantial decrease in the cyclic load induced temperature rise reported in reference 12. These results will be reported as soon as they become available.

Future research will deal with the extension to space structural applications by including coordinate transformation of the truss elements and radiation boundary conditions on element longitudinal surfaces.

ACKNOWLEDGEMENT

The author gratefully acknowledges the support provided for this research by the Air Force Office of Scientific Research under contract no. F49620-83-C-0067.

REFERENCES

[1] J.M.C. Duhamel, Memoire sur le calcul des actions moleculaires developpees par les changements de temperature dan les corps solides. Memoires par divers savans, vol. 5, pp. 440-498, (1838)

[2] F. Neumann, Vorlesungen uber die theorie der elasticitat der festen Korper und des lichtathers. Leipzig, 107-120, (1885)

[3] B.A. Boley and J.H. Weiner, Theory of Thermal Stresses. Wiley, New York, (1960).

[4] O.W. Dillon, Jr., An experimental study of the heat generated during torsional oscillations. J. Mech. Phys. Solids, vol. 10, 235-244 (1962).

[5] O.W. Dillon, Jr., Temperature generated in aluminum rods undergoing torsional oscillations. J. Appl. Mech. 33, vol. 10, 3100-3105 (1962).

[6] O.W. Dillon, Jr., Coupled thermoplasticity. J. Mech. Phys. Solids, vol. 11, 21-33 (1963).

[7] G.R. Halford, Stored Energy of Cold Work Changes Induced by Cyclic Deformation. Ph.D. Thesis, University of ILlinois, Urbana, Illinois (1966).

[8] O.W. Dillon, Jr., The heat generated during the torsional oscillations of copper tubes. Int. J. Solids Structures, vol. 2, 181-204 (1966).

[9] W. Olszak and P. Perzyna, Thermal Effects in Viscoplasticity. IUTAM Symp., East Kilbride, 206-212, Springer-Verlag, New York (1968).

[10] J. Kratochvil and R.J. DeAngelis, Torsion of a titanium elastic viscoplastic shaft. J. Appl. Mech., vol. 42, 1091-1097 (1971).

[11] E.P. Cernocky and E. Krempl, A theory of thermoviscoplasticity based on infinitesimal total strain. Int. J. Solids Structures, vol. 16, 723-741 (1980).

[12] D.H. Allen, A prediction of heat generation in a thermoviscoplastic uniaxial bar. Texas A&M University Mechanics and Materials Center Report no. MM 4875-83-10 (July 1983),(accepted for publication by Int. J. Solids Structures).

[13] D.H. Allen and W.E. Haisler, Introduction to Aerospace Structural Analysis. John Wily (1985), in press.

[14] B.D. Coleman and M.E. Gurtin, Thermodynamics with internal state variables. J. Chem. Phys., vol. 47, 597-613 (1967).

[15] J. Kratochvil and O.W. Dillon, Jr., Thermodynamics of crystalline elastic-visco-plastic materials. J. Appl. Phys., vol. 41, 1470-1479 (1970).

REFERENCES (cont.)

[16] D.H. Allen, Thermodynamic constraints on the constitution of a class of thermoviscoplastic solids. Texas A&M University Mechanics and Materials Center, Report no. MM 12415-82-10, December (1982).

[17] J.N. Reddy, An Introduction to the Finite Element Method. McGraw-Hill, New York (1984).

END

FILMED

1-86

DTIC